MOLECULAR CONTRIBUTIONS OF NOTCH AND HIPPO SIGNALING TO ENDOMETRIAL STROMAL CELL DECIDUALIZATION

By

Genna Elisabeth Moldovan

A DISSERTATION

Submitted to
Michigan State University
in partial fulfillment of the requirements
for the degree of

Cell and Molecular Biology – Doctor of Philosophy

2024

ABSTRACT

Endometrial stromal cell decidualization is required for pregnancy success and defects in this process are associated with infertility. Many of the intricate molecular mechanisms contributing to decidualization remain undefined. Two pathways implicated in endometrial stromal cell decidualization in humans *in vitro*, are the NOTCH and HIPPO signaling pathways. Previously conducted studies showed that NOTCH1, its transcriptional effector, RBPJ, and the effectors of the HIPPO signaling pathway, YAP1 and WWTR1, are required for decidualization initiation. To investigate the *in vivo* contributions of NOTCH and HIPPO signaling in decidualization, we generated genetically engineered mouse models with conditional deletion of *Rbpj* and *Yap1* and *Wwtr1*. Decidual *Rbpj* deletion did not significantly affect female fertility supporting that NOTCH signaling activation is required for the initiation of decidualization but not its maintenance. However, conditional deletion of *Yap1* and *Wwtr1* in the female reproductive tract resulted in subfertility, a compromised decidualization response, partial interruption in embryo transport, blunted endometrial receptivity, delayed implantation and delayed subsequent embryonic development. Transcriptome analysis revealed aberrant maternal remodeling at 7.5 days post coitus and enrichment for terms associated with fertility compromising diseases like pre-eclampsia and endometriosis. Our results indicate that *Yap1* and *Wwtr1* are required for pregnancy establishment, decidualization initiation and maintenance, and pregnancy maintenance. These studies have implications for women's health and support the continued investigation into molecular mechanisms contributing to female fertility.

ACKNOWLEDGEMENTS

The success of a PhD student is not only determined by their own pursuit of knowledge but by the support and training they receive. I would be remiss not to thank my mentor, Dr. Asgerally T. Fazleabas, first. Dr. Asgi has been my mentor for 6 years and counting and has never once lost patience, compassion, or kindness for me. He has been a supportive, knowledgeable, and opportunistic mentor that has pushed me to expand my thinking capabilities, scientific scope, and professional development. In addition, he has supported and fostered many collaborations to allow me to expand my professional network and to ultimately set me up for success for the next stage of my career. Thank you, Dr. Asgi for all you have done to support me and for all that you continue to do.

In addition to my official mentor, there are those unofficial mentors that have made the process of earning a PhD more fruitful. Thank you to Dr. Ripla Arora for all your help and support in mouse studies, reproductive biology, and professional development. Thank you to Dr. Yong Song for being supportive and challenging my thinking in all things reproduction. Thank you to Dr. Emmanuel Paul who has always pushed me to work harder, think smarter, and worked to foster my independence as a blooming scientist. Finally, thank you to Dr. Gregory Burns, my statistics and math hero, bioinformatics support system, uterine physiology expert, and deputy mentor that has helped guide the progress of all the studies outlined in this dissertation and beyond. This dissertation would not have been possible without your support and expertise.

Beyond the support of scientific mentors there are those within the scientific community who supported the scientist within me and the science reported here. Thank

you to Dr. Peggy Petroff, Alaina Burghardt, and the whole MSU CMB community for supporting my progress throughout the PhD and providing me with innumerable professional development opportunities. Thank you to my committee for their guidance, support, and for helping to set me up for success as an independent scientist. Thank you to the impeccable animal care staff at MSU including Mat Rackam and Jackie Keller who provide our mice with the best possible care. Thank you to my right-hand mouse woman, Erin Vegter who has never said no and is always willing to help even when I overschedule! Thank you to our lab Momager, Sam Hrbek for always offering to help and for keeping things running smoothly. Thank you, ladies, for everything you have done for me and for the success of the lab!

In addition, to thank those outside the scientific community who never had any idea what I was talking about but did their best to support my success anyway. Thank you to my parents and brother for their support, unconditional love, and for always being proud of my progress. Thank you to my parents-in-law for their support of what is sometimes a very chaotic lifestyle and for always offering to help. Thank you to my best friend Sam who checked in and made sure I was still alive when I was drowning in science. Thank you to my biggest supporter, presentation screener, science-loving life partner and husband, Tudor, for always listening to me blab and helping me get through the tough times and see the light at the end of the PhD tunnel. Thank you to my canine emotional support duo Dori and Howie for the endless snuggles and for keeping me active.

Finally, a profound thank you and acknowledgement that the majority of the science presented in this dissertation was made possible with the sacrifice of murine life. Thank you to those laboratory animals that made this work and my PhD possible. I hope

that the loss of your lives will help humankind in their pursuit of fertility and continuation of a species.

TABLE OF CONTENTS

CHAPTER I: INTRODUCTION

1.1 A Comparative Overview of Human and Murine Female Reproductive Biology

Female reproductive tract structure

The mammalian uterus comes in many shapes and sizes, but all serve one essential function: to gestate offspring. Humans have a simplex uterus formed during embryonic development by the fusion of the two Mullerian ducts[1]. The fully developed structure has a fundus with two branches at either side called the oviducts or fallopian tubes (Figure 1A). Oviducts terminate in fimbriae that beat around the ovary to capture an ovulated oocyte, facilitate fertilization, and carry an embryo to the uterus. The outermost layer of the uterus is the perimetrium and is continuous with the lining of the peritoneal cavity. Inward is the myometrium, the muscular layer, which serves critical functions in menstruation and parturition. Finally, the innermost layer is termed the endometrium and is the site where implantation and pregnancy occurs. The endometrium consists of two main layers, the functionalis that is shed during menstruation and the

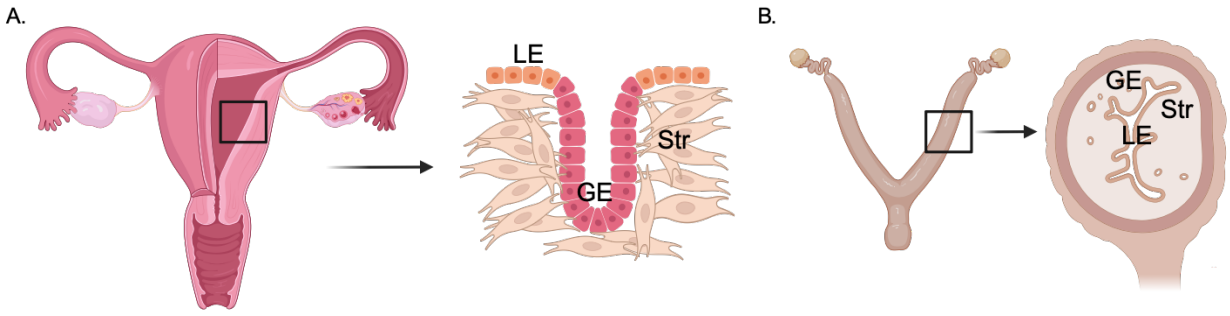

Figure 1. Human and murine uterine morphology. A. Illustration of the anatomy of the human reproductive tract. At right, structural view of the human endometrium including luminal epithelium (LE), glandular epithelium (GE), and stroma (Str). **B.** Illustration of the murine reproductive tract. At right, uterine cross section showing the three major compartments: GE, LE, Str.

basalis that serves as the site of regeneration for the functionalis post-menstruation and post-parturition. These layers include several cell types including the surface luminal

epithelium, branching glandular epithelium, supporting stroma, spiral arteries, and a variety of interspersed immune cells (Figure 1). Each cell within the human uterus serves both distinct and coordinate roles in the intricate processes of pregnancy establishment and maintenance[1].

The murine uterus is comprised of the same layers as the human uterus with some variations in structure but serves the same function. The murine uterus is duplex with two separate cervices, uterine horns, oviducts, and ovaries. These uteri contain two layers of myometrium including an outer longitudinal muscle layer and an inner circular muscle layer[2]. The endometrium is comprised of the same cell types as the human uterus but contains only one layer of endometrium. In addition, murine oviducts are tortuous and end in an infundibulum that meets the ovary and is encircled by a fluid filled bursa. In addition, while humans are monoovulatory, mice are multiovulatory resulting in litters rather than one or two offspring[2]. Despite these structural and functional differences, the higher-order function of these tissues is the same and they respond to steroid hormones in a cyclic manner.

Regulation of female reproductive function

Humans with uteri and ovaries undergo the parallel ovarian and menstrual cycles. Similarly, female mice experience an estrous cycle. Both the estrous and menstrual cycles are regulated by ovarian hormones controlled upstream by the hypothalamic-pituitary-gonadal axis. Within the hypothalamus, kisspeptin neurons secrete kisspeptin that induces secretion of gonadotropin-releasing hormone that acts on the pituitary[1]. The pituitary then releases follicle stimulating hormone (FSH) and luteinizing hormone (LH) that act on the ovary. Locally within ovarian follicles, LH acts to stimulate

steroidogenesis in the theca cells of the ovary. The estradiol precursor androstenedione is released via diffusion to neighboring granulosa cells where it is eventually converted to estradiol by the aromatase enzyme regulated by FSH. Cyclically, FSH and LH are released in a pulsatile fashion, but levels peak to induce ovulation midway through the ovarian cycle, around day 14 in humans or late proestrus in mice[1, 2].

The ovarian cycle begins with the follicular phase when tertiary follicles are maturing into Graafian follicles and finally reach full maturity and ovulate an oocyte. Following ovulation, the remaining granulosa cells undergo luteinization to form the corpus luteum that produces progesterone during the luteal phase and is essential for pregnancy establishment and maintenance. In parallel, the menstrual cycle begins with menstruation, which is initiated by the shedding of the functionalis layer of the endometrium. Following menses the proliferative phase of the menstrual cycle is initiated whereby the endometrium regrows from the basalis under the influence of estradiol. The endometrial basalis likely contains the endometrial stem cell niche that functions to aid regrowth of the endometrium following menses and pregnancy[3]. These mesenchymal stem-like cells are characterized by co-expression of PDGFRβ, CD146, and SUSD2 in humans[3]. The latter half of the menstrual cycle is the secretory phase that is progesterone dominant and encompasses the critical window of implantation. The murine estrous cycle differs slightly but maintains a similar profile. High levels of estradiol induce ovulation during the estrus phase. The corpus luteum then secretes progesterone during metestrus and diestrus. In both humans and mice, the demise of the corpus luteum leads to progesterone withdrawal and resumption of the beginning of the cycle[1, 2].

If fertilization occurs, this disrupts the menstrual and ovarian cycles and then begins pregnancy. In humans, fertilization occurs within the oviducts as it does in mice. In mice, this time is referred to as 0 days post coitus (dpc). Unique to mice compared to humans is a vaginal plug that can be visualized within the vaginal canal of a female that was mated within the previous 8-24 hours. Mice are nocturnal and therefore mating occurs at night and so time of plug visualization is noted as 0.5dpc. Following fertilization, an embryo begins to develop within the oviduct of both mice and humans. In humans, the embryo enters the maternal uterus between days 3-5 but then does not fully implant until days 6-10 post fertilization. In mice, this process is significantly expedited with embryo

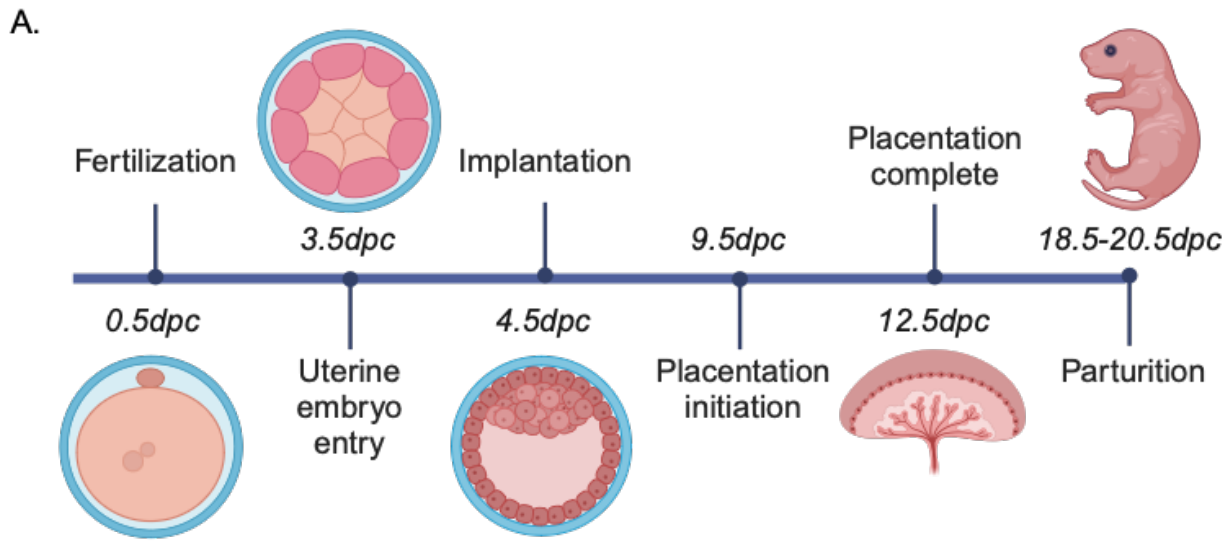

Figure 2. Key timepoints in murine pregnancy. A. Fertilization occurs at 0.5 days post coitus (dpc) with sperm fertilizing an ovulated oocyte. Embryos then mature throughout the oviduct and enter the maternal uterus at 3.5dpc. Implantation follows at 4.5dpc. Placentation begins at 9.5dpc and is complete at 12.5dpc. Finally, parturition occurs between 18.5-20.5dpc.

entry of a blastocyst occurring at 3.5dpc and all embryos implanting at 4.5dpc, just one day past embryo entry. Following implantation, the embryo develops, remodels the maternal endometrium and is eventually expelled from the uterus during parturition (Figure 2). Comparatively, gestation in humans is approximately 40 weeks and in mice is

18-20 days[1, 2]. These differences are significant; however, the utility and ease of the mouse model makes it ideal for pregnancy investigations.

Preparation of the maternal endometrium for pregnancy is a highly coordinated process. As mentioned above, the coordination of hormonal signals is imperative for pregnancy initiation. In humans, this process begins during the secretory phase to prepare the endometrium for the window of receptivity which occurs in the midsecretory phase. In mice, preparation of the endometrium occurs during proestrus and estrus in response to hormones. One route of preparation is decidualization of the endometrial stroma. This is a terminal differentiation process whereby stromal cells transform from mesenchymal fibroblasts to epithelioid-like cells that become secretory in nature rather than providing structural support. Beyond this drastic change in morphology there is a concordant change in function where decidualized stromal cells secrete factors like prolactin, insulin growth factor binding protein 1, and matrix metalloproteases. Functionally, decidual cells are critical to control the level of trophoblast invasion and aberrations in this function can lead to pregnancy complications like placenta accreta or preeclampsia. Indeed, failure of endometrial stromal cells to decidualize compromises fertility and is associated with fertility impairing diseases like endometriosis. Decidualization occurs spontaneously in humans during the midsecretory phase of the menstrual cycles while in mice only occurs with a physical stimulus, like an implanting embryo[1, 2].

Decidualization is critical for pregnancy initiation in mice and preparation for pregnancy in humans and coordinates events to allow embryo implantation. Embryo implantation like decidualization is a highly regulated process. As stated, this occurs at

4.5dpc in mice following embryo entry and hatching of the blastocyst from the zona pellucida. Implantation occurs at the anti-mesometrial side of the uterine horn into a uterine crypt with the inner cell mass oriented toward this anti-mesometrial pole. The embryo will grow and develop in this side of the horn while placentation and vascularization largely occur at the site of uterine vasculature entry, the mesometrial pole. The murine window of receptivity is characterized by a series of highly coordinated hormonal events. During the estrus cycle, estrogen and progesterone levels are high and this serves to prepare the epithelium for receptivity. At the time of embryo entry into the uterus on 3.5dpc the nidatory estrogen surge occurs inducing stromal cell proliferation to prepare for decidualization and increases transcriptional and translational activity within the uterine endometrium. During this preparation window, estradiol acts on estrogen receptors in the epithelium and to induce expression of the progesterone receptor in the stroma. The uterine epithelium will downregulate estrogen receptors, exit the cell cycle and cease proliferation to prepare for implantation. This is required as trophoblasts will begin to differentiate and invade through the luminal epithelium that undergoes spontaneous apoptosis beginning at the anti-mesometrial pole and spreading to the mesometrial pole within implantation sites. In conjunction with this hormonal regulation, prostaglandin E2 aids in the removal of fluid from the uterine lumen, responds to decidualization stimulus and increases vascular permeability in the uterus at implantation sites. The endometrial stroma is primarily affected during pregnancy initiation and in early pregnancy events as it undergoes decidualization, and its vascular networks are significantly remodeled by factors secreted by invading trophoblasts like matrix metalloproteases. This time is also characterized by uterine natural killer cell infiltration

to prevent demise of a semi-allogeneic fetus and to prevent maternal infection[2]. Following these initiating events, a fetus develops, trophoblasts continually differentiate and remodel the maternal endometrium and generate the placenta, and finally parturition is initiated, ending the pregnancy[1, 2]. Beyond these basic mechanisms, there are several important molecular pathways that regulate and crosstalk during endometrial stromal cell decidualization and implantation including the NOTCH and HIPPO signaling pathways.

Both the NOTCH and HIPPO signaling pathways regulate processes that are integral to decidualization and pregnancy success including cell proliferation and differentiation[4, 5]. While the NOTCH signaling pathway is a juxtracrine pathway initiated by cell-cell contact, the HIPPO signaling pathway is mechanosensing and activated when there are changes in extracellular matrix stiffness. These mechanisms of proliferation and increased cell density are essential to pre-decidualization proliferation and can affect activation of both of these highly conserved pathways. In addition, both pathways induce transcriptional activation or inactivation of genes that could contribute to decidualization like cell cycle regulatory genes. Given the canonical roles of both the NOTCH and HIPPO signaling pathways, it is probable that they contribute to the endometrial stromal cell decidualization response.

1.2 NOTCH signaling in reproduction

NOTCH: Regulator of reproduction

The NOTCH signaling pathway is ubiquitous throughout all mammalian species and regulates proliferation, differentiation, cell fate and cell death in many tissues[4]. Briefly, in mammals this pathway consists of four cell surface NOTCH receptors

(NOTCH1-4) which bind Delta-like (DLL1, DLL3, or DLL4) or Serrate-like (JAG1, JAG2) ligands in a juxtracrine manner resulting in the cleavage of the NOTCH receptor and transcriptional activation of target genes[6]. The NOTCH signaling pathway regulates many facets of embryonic, neural, and vascular development, and its dysregulation contributes to a range of cancers and pathologies[7, 8]. The primary focus of this section is the NOTCH signaling pathway's regulation of reproductive physiology[9]. We will outline the diverse roles of NOTCH signaling in female reproductive development and function, show how this pathway contributes to female reproductive pathologies, and suggest future directions of focus to uncover the mechanisms that regulate NOTCH signaling.

Hormonal regulation of NOTCH signaling

Despite the physiological importance of NOTCH signaling, there remain significant gaps in our knowledge regarding its regulation and functional diversity. Major gaps currently include factors upstream of receptor and ligand presentation as well as tissue-specific signaling mechanisms. The governing hormones within the female reproductive tract are 17β-estradiol (E2), progesterone (P4), and human chorionic gonadotropin (hCG). These hormones regulate processes that are integral to fertility maintenance, like ovarian and uterine development, and the ovarian and menstrual cycles. Thus, the NOTCH signaling pathway, which we suggest is an arbiter of reproductive function, could be regulated by these essential hormones. In mice, NOTCH signaling activation mimics P4 levels throughout the estrous cycle indicating that P4 signaling may contribute to cycle specific regulation of NOTCH signaling activation[10]. Transcriptional levels of receptors: *NOTCH1-4,* ligands: *Dll4, Jagged 1* and *2,* and target genes: *Hes1, Hes5,* and *Nrarp*

increase in the mouse uterus throughout the estrous cycle indicating that the NOTCH signaling pathway activity may increase as the estrous cycle progresses[10]. In the Olive baboon, *Papio anubis*, NOTCH1 expression is low in the endometrium during the proliferative phase of the menstrual cycle followed by an increase in glandular expression of NOTCH1 during the secretory phase[11]. In addition, NOTCH1 expression is positively regulated by hCG[11, 12]. Following administration of hCG, NOTCH1 increases in the stromal compartment of the endometrium providing a role for embryonic signal-mediated regulation of NOTCH signaling[11]. Additionally, hCG induces NOTCH1 expression in human stromal cells *in vitro*[11]. In a clinical trial to determine the effect of hCG infusion on the human endometrium during the period of implantation, increased glandular and stromal protein levels of NOTCH1 were noted without observable changes in mRNA expression, suggesting that hCG may induce post-translational modification of NOTCH[13]. To further investigate how hCG regulates NOTCH1 in the endometrial environment, human uterine fibroblasts (HuFs) were treated with P4 and hCG, which resulted in cleavage of NOTCH1 at the primary γ-secretase cleavage site, valine residue 1744, showing that hCG acts to induce NOTCH1 signaling activation in stromal cells[11]. E2 also significantly affects NOTCH signaling in several systems. Treatment of human umbilical vein endothelial cells with E2 leads to increased activation of NOTCH1 and NOTCH4 and decreased NOTCH2 expression showing that E2 modulates NOTCH signaling activation in some cellular contexts[14]. Conversely, in breast cancer cell lines, E2 treatment reduces NOTCH signaling activation by causing accumulations of full-length membrane bound NOTCH1[15]. Additionally, N1ICD can stimulate estrogen receptor α (ER) dependent transcription in the absence of estradiol in breast cancer cells by

recruiting coactivators to ER-responsive elements[16]. E2-regulated NOTCH signaling has also been described in various tissues throughout the reproductive tract. Ishikawa cells, an endometrial carcinoma cell line, exhibited increased availability of NOTCH1 protein and mRNA with E2 administration[17]. In addition, an *in vitro* study of human fallopian tube epithelial cells showed that E2 and P4 induced an increase in mRNA expression of a NOTCH target gene, *Hes1*[18]. These studies collectively indicate that there may be tissue specific and even cell type specific hormonal regulation of NOTCH signaling at multiple levels.

NOTCH signaling in female reproduction

NOTCH signaling is critical for female reproductive function (Figure 3). NOTCH signaling components are expressed throughout the female reproductive tract in rodents, baboons, and humans. In mice, NOTCH signaling components including *NOTCH1-4, Jagged1-2*, and *Dll4* and target genes *Hes1, 2*, and *5* are all expressed in the oviduct and within the mouse uterus[10]. It is thought that the NOTCH signaling pathway contributes to cellular remodeling that occurs throughout the estrous cycle since this pathway functions through cell-to-cell contact and is differentially expressed throughout the estrous cycle[10]. We have shown that NOTCH1 protein expression varies throughout the menstrual cycle suggesting that NOTCH signaling may play distinct roles in primates[11]. Histological analyses of the human endometrium have shown a similar pattern of expression throughout the menstrual cycle[19]. The human endometrial glandular epithelium expresses NOTCH1 and NOTCH4 during the proliferative phase, and the glandular epithelium and stroma express NOTCH1, NOTCH4, and JAG1 during the

secretory phase indicating that the NOTCH signaling pathway is most likely to be active during the secretory phase of the menstrual cycle[19].

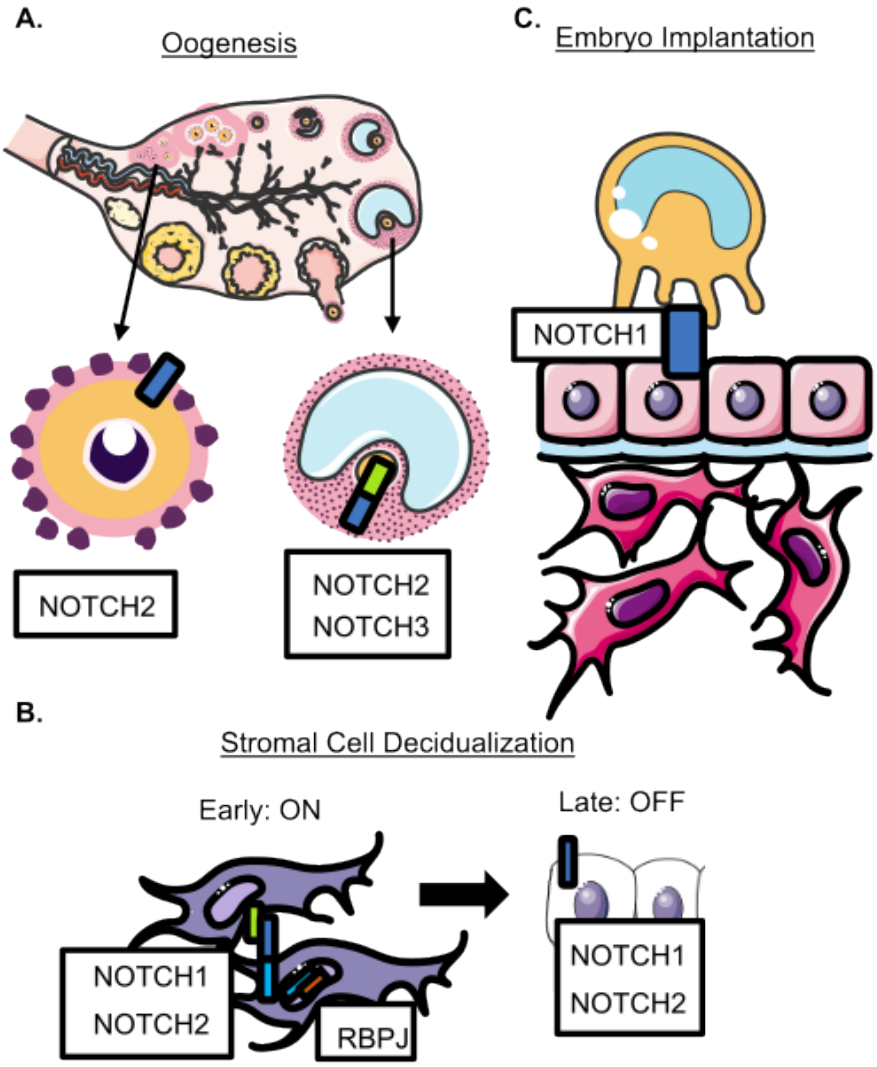

Figure 3. Notch signaling in key reproductive functions. A. During prenatal and early postnatal ovarian development, NOTCH2 is the dominant receptor expressed by the primordial follicles. Later in oogenesis, NOTCH2 and 3 on the surface of granulosa cells interacts with JAG2 ligand expressed by the oocyte. **B.** During the initiation of decidualization, NOTCH1 and 2 receptors are active. During late decidualization, NOTCH1 and 2 are expressed but Notch signaling is inactive. **C.** Notch signaling is active in the endometrium during implantation and decidualization. During the window of implantation, epithelial cells on the surface of the endometrium express NOTCH1.

The NOTCH signaling pathway is clearly active throughout the female reproductive tract but what are its specific roles in these diversely functioning tissues? The ovary contains maturing follicles that are surrounded by granulosa cells, extracellular matrix,

and a layer of theca cells. After ovulation, the remaining granulosa and theca cells transform into the luteal cells of the corpus luteum, which provides hormonal support in early pregnancy[1]. Within the ovarian environment, NOTCH signaling has been shown to play roles in granulosa cell differentiation, luteal cell function, and ovarian steroid hormone production[20]. During embryonic ovarian development, *Jag1*, *Jag2, NOTCH2* and targets *Hes1* and *Hey2* are highly expressed in the prenatal ovary[21]. Our understanding of the roles of NOTCH signaling in the developing murine ovary has evolved from research conducted utilizing conditional knockout mouse lines. Two such models include the $Vasa^{cre/+}$ $Jagged1^{Fl/+}$ mice that contain a conditional deletion of the NOTCH ligand *Jag1* in their germ line, and $Amhr2^{cre/+}$ $NOTCH2^{Fl/+}$, which conditionally deletes *NOTCH2* in the developing ovary[21]. These models are temporally specific and have uncovered the roles of NOTCH signaling in specific cell types at critical developmental timepoints. The ovaries from both transgenic models contain multioocytic follicles indicating a failure to form correct follicle units prenatally[21]. Additionally, the postnatal follicles in these mice display decreased granulosa cell proliferation and increased apoptosis indicating that NOTCH signaling is required for granulosa cell survival[21]. Notably, the *Jag1* knockout mice are subfertile, and both knockout models show premature reproductive aging suggesting that NOTCH signaling in the prenatal ovary is required for proper ovary function[21]. Postnatal studies in the ovary conducted in the presence of hCG resulted in increased *Jag1* and *NOTCH2* expression indicating that NOTCH signaling is hormonally regulated in the ovary[22]. Further studies utilizing DAPT, a γ-secretase inhibitor, in organ-cultured ovaries resulted in degenerating oocytes, decreased primordial follicles which were negative for Ki-67, a marker of proliferation,

signifying that NOTCH signaling is integral to oocyte survival and proliferation[23]. Although NOTCH signaling is most likely an important pathway in the ovary, the γ-secretase complex cleaves many proteins that regulate proliferation. Therefore, these results may also indicate a role for other pathways that promote oocyte survival and proliferation[24]. More recently, evidence of lateral crosstalk of the NOTCH signaling pathway amongst multiple cell types in the ovary has been reported[25]. In this study the authors determined that JAG1 in the oocyte activates NOTCH2 or NOTCH3 in granulosa cells showing that different cell types communicate via NOTCH signaling[25]. These studies support the concept that the NOTCH signaling pathway is integral to maintaining fertility at the level of the ovary through developmental regulation and granulosa cell function.

The endometrium is the primary site of embryo development and cyclically responds to ovarian hormones and the presence of an embryo, ultimately providing a hospitable and nourishing environment for an embryo and fetus. The endometrium is composed of four major cell types, the epithelium that forms the lumen and branching glands, stromal cells that provide support in the endometrium, various immune cells that regulate maternal-fetal interactions and repair within the endometrium, and endothelial cells that line the spiral arteries, which serve to support the embryo during implantation and in utero development[9]. The cells that make up the endometrium participate in significant crosstalk to encourage reproductive success. The cyclical changes of the menstrual cycle, decidualization, implantation, and uterine repair are all processes that are in part regulated by NOTCH signaling.

Decidualization is the terminal differentiation of endometrial stromal cells that begins during the latter part of the menstrual cycle in humans and non-human primates, and at the time of implantation in mice. Decidualization is an important process for the success of pregnancy. Decidualized stromal cells function throughout pregnancy in the maternal decidua, a tissue which forms as the maternal side of the placenta. NOTCH1 regulates decidualization in mice, nonhuman primates, and humans[11, 26, 27]. Extensive studies from our laboratory provide a role for NOTCH signaling in endometrial stromal cell decidualization. In HuF cells, knockdown of the NOTCH1 receptor compromises the decidualization response when these cells are treated with decidualization stimuli: E2, the progesterone analogue medroxyprogesterone acetate (MPA), and cAMP (EPC)[11]. In a conditional NOTCH1 knockout mouse model in the uterus ($Pgr^{cre/+}$ $NOTCH1^{Fl/Fl}$), we noted a decreased decidualization response as measured by uterine wet weight and mRNA expression of decidualization markers *Bmp2* and *Wnt4*[26] and a smaller litter size in the first pregnancy[28]. While these data suggest that NOTCH1 is required for an appropriate decidualization response both *in vitro* and *in vivo*, we sought to investigate the specific mechanisms of these interactions. We generated a uterine N1ICD overexpression mouse model ($Pgr^{cre/+}$ $Rosa26^{N1ICD/+}$) to ascertain whether constitutive activation of the NOTCH1 signaling pathway would affect the decidualization response. We observed that constitutive activation of the NOTCH1 signaling pathway through *N1icd* overexpression compromises decidualization and implantation[29]. We also sought to determine if *Rbpj*, the transcriptional effector for all four NOTCH receptors, plays an independent role in the uterus. In an *Rbpj* conditional knockout mouse model in the uterus ($Pgr^{cre/+}$ $Rbpj^{Fl/Fl}$), we observed a severely

compromised decidualization response, as measured by uterine wet weight and mRNA levels of *Bmp2* and *Wnt4*, and compromised uterine repair that resulted in a recurrent pregnancy loss phenotype[30]. In this model, we determined that the decidualization failure occurred as a result of decreased progesterone receptor expression and signaling as well as reduced *Slc2a1* expression, a glucose transporter important for stromal cell differentiation[30]. We further characterized the roles of NOTCH signaling *in vitro* through NOTCH1 knockdown in HuF cells followed by EPC treatment to induce decidualization[27]. These data indicate that NOTCH1 knockdown prior to the initiation of decidualization compromises the decidualization response, but if the decidualization reaction has already begun, NOTCH1 knockdown has no effect[27]. These studies indicate that NOTCH1 is an early regulator of decidualization in endometrial stromal cells. Another NOTCH receptor is also implicated in endometrial stromal cell decidualization. In primary human decidual stromal cells (HDSCs) of early pregnancy, NOTCH2 is the most abundant receptor as determined by immunofluorescence of decidual tissue[31]. The authors then treated isolated HDSCs *in vitro* with cAMP, E2 and P4; and EPC treatment. There were no alterations in NOTCH2 protein or mRNA expression after 3 and 6 days of treatment but increases in ligands *DLL1* and *DLL4* were induced with cAMP and EPC treatment showing that NOTCH ligand availability is decidualization dependent[31]. Furthermore, inhibition of NOTCH2 expression or activation treatment of HDSCs with subsequent EPC treatment compromised decidualization suggesting that NOTCH2 expression and signaling activation are required for decidualization in HDSCs[31]. While we and others have established a clear role for NOTCH signaling in the decidualization process, the question that remains is what regulates NOTCH signaling during

decidualization and how is NOTCH signaling mediating the decidualization response? This remains an open area of research, but one study shows that post-translational modification of the NOTCH1 receptor may be one mechanism. Fucosylation of NOTCH1 by poFUT1 increased receptor-ligand binding since we know from previous studies that NOTCH receptors contain EGF repeats that are glycosylated to promote receptor-ligand interactions[32]. This mechanism permits increased NOTCH1 signaling activation in endometrial stromal cells, but when poFUT1 is inhibited, fucosylation of NOTCH1 is decreased leading to a compromised decidualization response[32]. This suggests that fucosylation is an active mechanism of NOTCH1 signaling regulation in decidualizing endometrial stromal cells[32]. Future directions for the field include discerning mechanisms, either hormonal or otherwise, that are regulating the NOTCH signaling pathway during the decidualization process and how the NOTCH signaling mediates the decidualization response.

Implantation is the process whereby a developing embryo enters the uterine cavity and attaches to the endometrium following fertilization. NOTCH signaling and target gene expression play a role throughout the implantation process. During the peri-implantation period, NOTCH signaling is active in the endothelial cells of the uterus[33]. Endothelial cells within the uterus typically form the vasculature and are critical for nutrient delivery through the uterus to the fetus. In addition, decidualization, implantation, placental development and pregnancy maintenance are all dependent on angiogenesis or the formation of new blood vessels[33]. NOTCH and vascular endothelial growth factor signaling are well known players in angiogenesis but have only recently been associated with decidual angiogenesis[33]. NOTCH1, 2, and 4 as well as ligands Dll4 and Jag1 are

expressed in murine endothelial cells during the peri-implantation period and there is limited expression of NOTCH3 and Jag1 in pericytes, vascular peripheral cells, prior to implantation[33]. In addition, NOTCH1, 4, Dll4 and Jag1 are expressed in decidual endothelial cells after implantation suggesting a role for NOTCH signaling in pre- and post-implantation angiogenesis[33]. An endothelial post-implantation, pre-placentation *Jag1* deletion mouse model exhibits increased NOTCH1 signaling and increased Dll4 expression, suggesting that *Jag1* is not an essential NOTCH ligand in post-implantation, pre-placentation angiogenesis[34]. Early studies focused on identifying expression of NOTCH signaling member expression in angiogenesis, therefore functional analyses of NOTCH signaling in post-implantation angiogenesis are lacking. NOTCH signaling also plays direct roles in the endometrium during the implantation process. NOTCH1 receptor and ligands, DLL4 and Jagged1, are expressed on the apical surface of luminal epithelial cells of the mid-secretory endometrium indicating that NOTCH signaling may aid in blastocyst implantation[35]. Cuman et al reported that blastocyst-conditioned media influences NOTCH1 and Jag1 expression in epithelial cells *in vitro* suggesting that blastocysts may modulate uterine receptivity and implantation through mechanisms that alter NOTCH signaling[36]. In the peri-implantation uterus, *Rbpj* is expressed in stromal cells in the primary and secondary decidual zones[37]. In an Rbpj uterine conditional deletion mouse model ($Pgr^{cre/+}$ $Rbpj^{Fl/Fl}$), deletion of Rbpj results in altered embryo implantation orientation producing a high rate of miscarriage as evident by many resorbing implantation sites[37]. The deletion of Rbpj also results in increased E2 responsiveness in the endometrial stroma and increased epithelial cell proliferation[37]. The authors noted that Rbpj directly interacts with estrogen receptor α (ER) in a NOTCH

independent manner suggesting that Rbpj may act to regulate E2 signaling in the endometrium[37]. These studies show expression and function of NOTCH signaling components within the processes of implantation, implantation associated angiogenesis, and maternal-fetal crosstalk of endometrial receptivity.

In addition to the NOTCH signaling pathway's role in the uterus throughout the menstrual cycle and in the establishment of pregnancy, the NOTCH signaling pathway is implicated in placentation[38]. During the initiation of decidualization, NOTCH signaling is active in endothelial cells of the decidua and in nonvascular decidual cells at embryonic day 8.5 in a mouse model[38]. In the mature murine placenta on embryonic day 12.5, NOTCH receptors and ligands are expressed in the decidua, junctional zone, and labyrinth in multiple cell types indicating that the NOTCH signaling components are available during placental development and function[38]. NOTCH1 signaling is active in proximal cell column trophoblasts and promotes proliferation and cell survival in the mature placenta[39]. In conjunction, NOTCH2 is the active receptor in the distal cell column of placental villi and functions to promote endovascular invasion and remodeling[39]. Another functional study established the role of Rbpj, the primary NOTCH signaling transcriptional effector, in placental morphogenesis[40]. Lu et al generated several Rbpj systemic, and conditional knockout mouse models that revealed that RBPJ deletion in the placenta compromises chorioallantoic branching and trophoblast differentiation in the ectoplacental zone[40]. These results combined with their other observations indicate that allantoic Rbpj expression targets *Vcam1* to aid chorioallantoic fusion which is critical for fetal vessel development in the chorion. In addition, Rbpj is essential for specification of trophoblast cells as it functions with Mash2 to induce

trophoblast specific protein α expression[40]. These diverse roles of Rbpj show the ubiquitous importance of NOTCH signaling and independent action of Rbpj as drivers of placental structure and function.

NOTCH signaling in gynecological pathologies

Polycystic ovary syndrome (PCOS) affects approximately 10-20% of reproductive aged women and is characterized by hormonal dysregulation accompanied by enlarged ovaries with an accumulation of ovarian follicles creating a cyst-like appearance on the surface of the ovary[41]. NOTCH receptor and ligand expression is aberrant in patients with PCOS including decreased *NOTCH1, JAG1, JAG2*, and increased *NOTCH3* mRNA expression during the window of implantation in endometrial samples (Figure 4) [42]. Protein expression of JAG1 and JAG2 is also decreased in the endometrium of PCOS patients[42]. In addition to altered endometrial expression, NOTCH signaling is enriched in granulosa cells of patients with PCOS as identified by microarray analysis, and members of this pathway have been suggested as potential biomarkers of PCOS[43]. Together these data suggest that NOTCH signaling may contribute to PCOS pathology and could be utilized to identify patients with PCOS.

Endometriosis is an E2 dependent disease characterized by endometrial-like tissue found at ectopic sites, most commonly in the peritoneal cavity[44]. This disease is associated with idiopathic infertility and is a major cause of pelvic pain in women of reproductive age[44]. We have shown that *NOTCH1* expression as well as ligands *JAG2* and *DLL4* and NOTCH1 gene targets *NOTCH4*, *HES5*, and *HEY1* are significantly

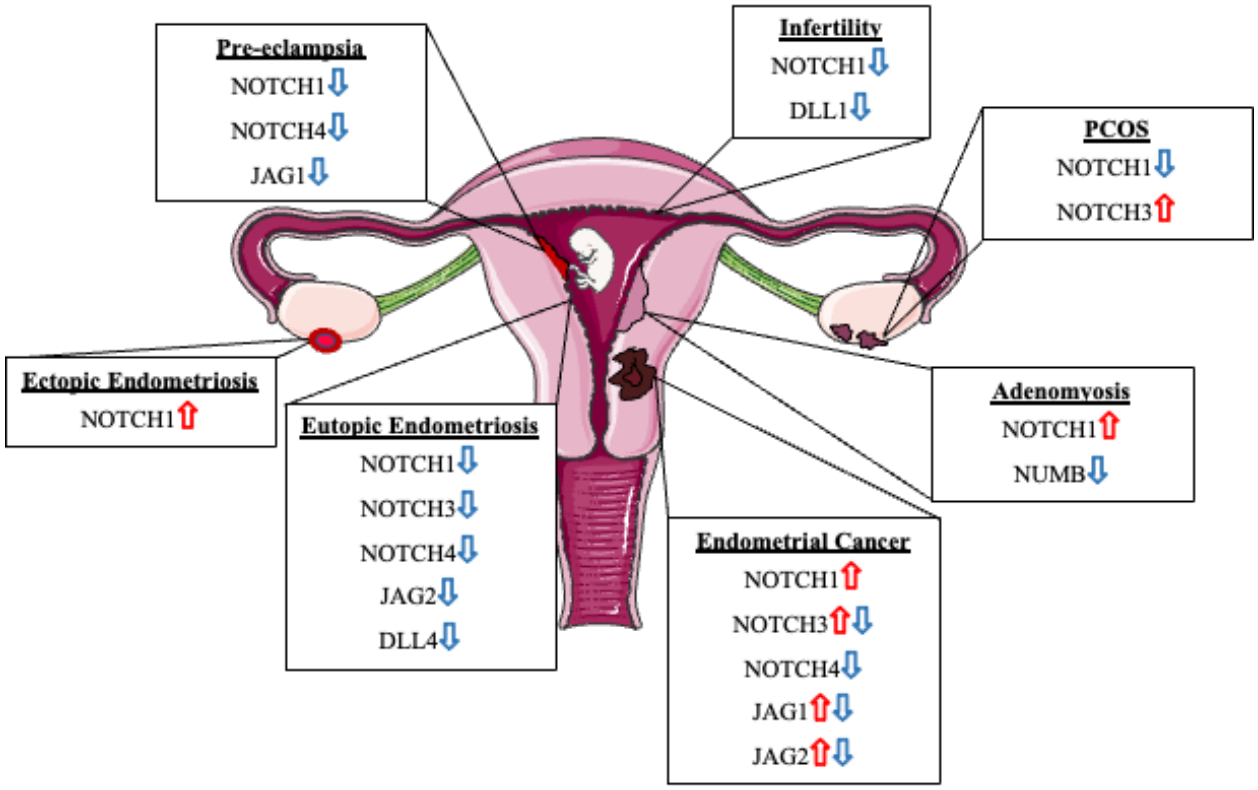

Figure 4. Notch receptor and ligand expression aberrations in gynecological pathologies. Notch receptors and ligand expression are dysregulated in a myriad of gynecological pathologies including pre-eclampsia, infertility, PCOS, adenomyosis, endometrial cancer, and eutopic and ectopic endometriosis in comparisons to disease-free controls. These alterations in expression contribute to infertility and disease pathology by compromising decidualization and hormone signaling, inducing recurrent pregnancy loss, increasing epithelial to mesenchymal transition, and contributing to placental defects.

decreased in the eutopic endometrium (EuE) of women with endometriosis[27]. In addition, stromal cells isolated from women with endometriosis have reduced *NOTCH1* and ligand expression as well as a reduced decidualization response *in vitro*[27]. We hypothesized based on gene expression profiling, that the reduced NOTCH1 signaling contributes to a decidualization defect in women with endometriosis by downregulating *FOXO1*, a molecule that is critical for many reproductive functions including decidualization[27, 45-48]. Another study has corroborated the decrease in *NOTCH1* and ligand expression in the EuE of women with endometriosis[42]. In addition, during the

window of receptivity the endometrium from women with endometriosis exhibits reduced NOTCH3 expression[42]. Additional histological studies determined the localization of NOTCH receptors and ligands in the endometrium of women with and without endometriosis and identified lower staining intensity for NOTCH1 in the epithelium of infertile patients with endometriosis during the midsecretory phase compared to patients without endometriosis[49]. In addition to the EuE, the NOTCH signaling pathway is integral in endometriotic lesion pathogenesis. Angiogenesis or establishing a blood supply for growth is essential to ectopic lesions and NOTCH signaling plays a major role in this process in other contexts. Korbel et al found that the γ-secretase inhibitor DAPT increased angiogenic sprouts in lesions[50]. They postulated this increase could lead to a reduction in lesion size and decreased function based on similar results in tumor studies[50]. Significant differences in NOTCH1 expression and activation have been identified in ectopic (Ec) and EuE, including increased N1ICD expression that is associated with increased proliferation measured by Ki-67 expression, ER expression, and decreased PR expression in EcE[51]. Given these data, the authors suggest that increased NOTCH1 signaling in Ec may contribute to P4 resistance since inhibition of NOTCH signaling with DAPT helped to sensitize immortalized uterine fibroblasts, HESCs, to P4[51]. Additionally, NOTCH signaling is linked with oxidative stress and severity of disease in endometriosis. A study of peritoneal fluid and stromal cells isolated from eutopic and ectopic endometrium from women with deep infiltrating endometriosis showed higher ADAM17 expression and activity, higher NOTCH signaling activation, and that these changes are associated with increased oxidative stress and lesion fibrosis[52]. NOTCH signaling is also activated by immune modulation in many other contexts, as well

as in EcE. In our study of ectopic tissue, we identified increased NOTCH1 expression in humans and in our baboon model of endometriosis[53]. In addition to these alterations in expression, we elucidated a potential mechanism of NOTCH1 signaling regulation in the epithelium of lesions where IL-6 regulates P38/MAPK signaling to induce *NOTCH1* promoter occupancy of E2A/HEB[53]. NOTCH signaling is altered in Ec and EuE of women with endometriosis providing potential therapeutic targets for future studies to identify to combat this pathology.

Adenomyosis is a disease characterized by endometrial tissue found within the myometrium resulting in dysmenorrhea, dyspareunia, abnormal uterine bleeding, and infertility[54]. A histological study performed on endometria from fertile women and women with adenomyosis revealed increased NOTCH1 expression in ectopic endometria of women with adenomyosis[55]. Expression of an inhibitory regulator of NOTCH signaling, NUMB, is decreased in adenomyosis lesions within the myometrium[55]. Decreased NUMB expression may explain the increased NOTCH1 expression noted in adenomyosis lesions. Functional analyses revealed that adenomyosis lesions exhibit increased Slug and Snail, known markers of epithelial to mesenchymal transition (EMT), transcriptional expression that is mediated by NOTCH1 signaling activation thereby inducing EMT that contributes to the pathogenesis of adenomyosis[55]. The etiology and pathophysiology of adenomyosis remain significant areas of study, but these results suggest that the NOTCH signaling pathway may be an important contributor to this disease warranting future investigation of the role of NOTCH signaling in adenomyosis.

Pre-eclampsia is a pregnancy disorder that is characterized by hypertension and proteinuria in the mother. This disease affects 3-5% of pregnancies and can result in

significant health risks for both mother and fetus including death[56]. NOTCH1 and NOTCH4 are decreased in pre-eclamptic placentas compared to normal control placentas suggesting that defective NOTCH signaling may contribute to the etiology of this disease[57]. A study performed *in vitro* indicates that inhibition of NOTCH signaling resulted in reduced trophoblast invasion suggesting a role for NOTCH signaling in placental invasion[58]. In addition, the authors also noted that NOTCH2 deletion resulted in placental development defects, which resulted in offspring lethality[58]. The study also suggests that decreased JAG1 expression combined with the role of NOTCH signaling in vascular development could contribute to pre-eclampsia[58].

Several studies provide a role for NOTCH signaling in infertility and uterine repair. We utilized a murine model to constitutively activate NOTCH1 signaling through overexpression of the NOTCH1 intracellular domain ($Pgr^{cre/+}$ $Rosa26^{N1ICD/+}$)[29]. This constitutive activation of NOTCH1 signaling resulted in a glandless phenotype that resulted in infertility suggesting that NOTCH1 signaling is critical for glandular development in mice[29]. In addition to being infertile, these mice fail to respond to decidualization stimuli and display decreased P4 responsiveness highlighting the importance of NOTCH signaling in regulating and responding to hormonal signals[29]. Further investigation uncovered that N1ICD overexpression results in hypermethylation of the progesterone receptor through activation of a PU.1/Dnmt3b complex and this reduction allowed for an increase in estrogen signaling compromising decidualization and implantation[29]. We also generated $Pgr^{cre/+}$ $Rbpj^{Fl/Fl}$ mice to conditionally delete all NOTCH signaling in the mouse uterus[59]. These mice display a recurrent pregnancy loss (RPL) phenotype where mice give birth to a normal sized first litter, but subsequent

litters decrease in size, and these mice show a reduced decidualization response compared to controls[59]. We noted postpartum nodules following parturition in these mice that did not regress normally and an abnormal inflammatory environment that compromised implantation in future pregnancies[59]. Furthermore, in this study we found that women with recurrent pregnancy loss also exhibited reduced RBPJ expression suggesting that women exhibiting recurrent pregnancy loss may have dysregulated uterine repair mechanisms contributing to their pathology[59]. In addition, endometria from infertile women exhibit decreased NOTCH1 and DLL1 expression and increased NUMB expression by histological analysis[49]. These results indicate that NOTCH signaling as well as the NOTCH transcriptional effector, Rbpj may significantly contribute to infertility.

Endometrial cancer encompasses two subtypes of endometrial carcinoma: Type I endometroid endometrial cancer (EEC) and Type II serous endometrial cancer (SEC). EEC is the more common type of endometrial cancer where the endometrium is hyperplastic, and tumors are ER and PR positive. In SEC, the endometrium is atrophic and tumors are ER independent[60]. Alterations in NOTCH receptor, ligand, and target gene expression are associated with the endometrium of endometrial carcinoma patients. A decrease in NOTCH4 was originally identified in endometrial cancer cells and later validated by immunohistochemical analysis in endometrial carcinoma tissue [19, 61]. Conversely, NOTCH1 expression is increased in endometrial cancer and is associated with a poor prognosis[60]. Mixed data also indicate both increases and decreases in JAG1, JAG2, and NOTCH3, while data for other NOTCH receptor and ligand expression is currently lacking[60]. Aberrations in NOTCH signaling component expression are

present in both non-malignant and malignant gynecologic disorders, suggesting diverse roles for this pathway in reproductive tract abnormalities (Figure 4).

Concluding remarks and future perspectives

Regulation of NOTCH signaling is an underexplored area of research in the context of reproduction. Due to the importance of this signaling pathway in reproductive tract development, function, and disease, it warrants increased investigation. Current areas of investigation include hormonal regulation of NOTCH signaling by hCG, E2, and P4, but these mechanisms and interactions are not well understood. It is possible that these hormones may be regulating NOTCH signaling at the level of ligand presentation, receptor activation, cleavage enzyme activation, or by interacting with the NOTCH transcriptional activator RBPJ. Other evidence also suggests that NOTCH may interact with epigenetic modifiers, such as members of the SWI/SNF family, to alter chromatin accessibility, but this has not been thoroughly investigated in the context of reproductive physiology[29, 62]. In addition, dysregulation of NOTCH signaling has been shown to play a role in developmental defects, reproductive diseases, and cancer. The NOTCH signaling pathway may be an integral pathway in many different disease etiologies, especially in pathologies of the reproductive tract such as endometriosis, PCOS, pre-eclampsia, adenomyosis, and infertility. Targeting NOTCH signaling could also provide novel and beneficial therapeutics to advance patient treatment for reproductive pathologies and infertility. Therefore, there are multiple avenues open for further investigation and evidence suggests that NOTCH signaling, and regulation may differ within the different organs of the reproductive tract.

1.3 HIPPO signaling in reproductive function

HIPPO signaling pathway overview

The HIPPO signaling pathway is another ubiquitous pathway present in mammalian tissues governing tissue size, organ growth, and differentiation of tissues. The HIPPO signaling pathway was first identified in *Drosophila melanogaster* and was so named because loss of the key kinases induced significant overgrowth[5]. The HIPPO signaling pathway is a mechanosensing kinase cascade. It begins with extracellular signals like changes in cell density or extracellular matrix stiffness being transduced into cells through cell surface receptors which initiate the kinase cascade beginning with the Ste-like kinases STK3/4 (mouse) or MST1/2 (human). MST1/2 then phosphorylates its own binding partner, SAV1, and sequentially phosphorylates the next kinases LATS1/2 and its partner MOB1[5]. The active phosphorylation cascade terminates at the homologs YAP and WWTR1 (formerly known as TAZ) rendering these factors inactive and inducing either degradation or cytoplasmic sequestration by the 14-3-3 family of proteins. Alternatively, if the HIPPO signaling kinase cascade is inactive when the extracellular environment is stiffer in nature, YAP/WWTR1 actively serve their function as transcriptional cofactors to the TEAD family of transcription factors[63]. YAP and WWTR1 share very similar structure and binding capacity with YAP containing two double tryptophan repeats while WWTR1 only contains one double tryptophan repeat[64]. YAP/WWTR1-TEAD complexes affect transcription by binding to promoter regions or more commonly binding to distal enhancers then to promoter regions[63]. In addition, these complexes frequently bind with cis-regulatory elements like the AP-1 complex, N1ICD/RBPJ, E2F, MYC, etc and most often induce activation of target genes through

these cooperative complexes[63]. Specific targets of YAP/WWTR1-TEAD complexes include genes involved in cell cycle regulation like cyclins, polymerases, kinesins, and aurora kinases whereby they affect activation of DNA replication, mitosis, and replication checkpoints[63]. In addition to these targets, two canonical targets most often utilized as readouts of YAP/WWTR1-TEAD activity are cellular communication network factor 1 (CCN1, previously known at CYR61) and CCN2 (previously known as CTGF), two proteins that are secreted, participate in extracellular matrix structure, and affect proliferation, chemotaxis and cell adhesion[65]. As stated, the HIPPO signaling pathway is highly conserved and participates ubiquitously throughout the human and murine bodies therefore it is no surprise that notable roles have been assigned to this pathway in the context of pregnancy and throughout the female reproductive tract. It is important to note that a significant gap in the field of HIPPO biology is the assumption that both YAP and WWTR1 serve redundant functions in all tissues. This led to a predisposition for investigators to focus solely on YAP and infer function of WWTR1 based on the roles of YAP. Indeed, the bias of the literature toward investigating YAP is evident and creates a significant gap for the investigation of the roles of WWTR1 in a variety of tissues.

The contributions of YAP and WWTR1 to reproductive function

The role of the HIPPO signaling effector, YAP, has been well characterized in the ovary. Several mouse models have been utilized to elucidate these roles with the conclusion that YAP expression is required in granulosa cells. One study utilized two complementary tissue specific Cre recombinase models to investigate the role of *Yap* in granulosa cells, *Foxl2 Cre-ERT2*, and luteinized granulosa cells, *Cyp19 Cre*[66]. Utilizing a floxed *Yap* mouse[67] crossed to either of the Cre models resulted in significant

recombination and loss of *Yap* expression. Further investigation into the granulosa cell conditional knockout indicated loss of YAP in granulosa cells of growing follicles and resulted in smaller ovaries, fewer corpora lutea, and more atretic follicles compared to controls. In addition to these measures, the *Foxl2 Cre-ERT2 Yap f/f* mice produced significantly fewer pups across a 5-month breeding trial and significantly smaller litters. The loss of YAP in growing follicles compromised follicular development evidenced by decreased AKT1 staining, a marker of follicular proliferation, and increased Cleaved Caspase 3, a marker of apoptosis which explained the increased follicular atresia and decreased fertility in these mice[66]. The authors also generated *Cyp19 Cre Yap f/f* mice to investigate whether YAP is also required in luteinized granulosa cells responsible for hormonal production that is critical for pregnancy initiation and early maintenance. This model again showed significant recombination, but the ovaries of these mice did not show any overt morphological or qualitative alterations in reproductive tract morphology or function, respectively. A complimentary study from Derek Boerboom's group connected *in vivo* and *in vitro* studies of luteinizing hormone (LH) dependent activation of the Hippo signaling pathway concluding that YAP acts as a transcriptional cofactor for amphiregulin, a factor secreted by granulosa cells in response to the LH surge during ovulation[68]. Mechanistically, these results support a transcriptional activation role for YAP in granulosa cells to initiate ovulation and therefore a required role in ovarian function. Beyond the role of YAP, *Lats1* has also been implicated in ovarian function[69]. The authors generated whole body knockouts of *Lats1* and investigated ovarian effects. Principally, they noted higher rates of germ cell apoptosis in newborn ovaries concordant with decreased primordial and activated follicle quantities in culture. In addition, these

ovaries developed cystic structures *in vitro* suggesting abnormal follicular development and maintenance with the loss of *Lats1[69]*. The role of *Yap1* and appropriate activation of the HIPPO signaling pathway in follicular development and maturation is evident in these studies.

YAP is also required for appropriate oviductal development and function as evidenced in another genetically engineered mouse model. Derek Boerboom's group generated *Anti-Mullerian hormone receptor type II Cre* (*Amhr2* Cre) crossed to *Yap f/f Wwtr1 f/f* mice to generate a double *Yap/Wwtr1* knockout in all Mullerian derived tissues which includes the Mullerian duct mesenchyme of the murine reproductive tract of course excluding the oviductal and uterine epitheliums[70, 71]. They noted significant recombination in oviductal myosalpinx but not within granulosa cells of antral follicles nor within the uterus. The *Amhr2 Cre* is expected to be active in granulosa cells, muscular and stromal layers of the oviduct, within both muscular layers of the uterus, and within the endometrial stroma. The resulting phenotypes in female mice included subfertility, a progressive loss in fertility as the mice aged that was ultimately caused by degeneration of the isthmus myosalpinx through an undiscovered molecular mechanism. This degeneration and lack of muscular structure led to bleb like formations within the oviduct, trapping ovulated oocytes but not inhibiting fertilization. This delay in embryonic transport compromised pregnancy success. Interestingly, there were no aberrations in ovarian function as measured by serum hormonal levels and ovulation rates nor were there uterine abnormalities. The lack of phenotype in these tissues can be attributed to the lack of recombination in ovaries and uteri [68]. Ultimately, this work suggests that YAP/WWTR1 are required for postnatal oviductal muscular development of the murine

oviduct. In conjunction with this study, the same group investigated *Amhr2 Cre Lats1 f/f Lats2 f/f* double and individual knockouts[72]. The individual knockouts, *Amhr2 Cre Lats1 f/f* and *Amhr2 Cre Lats2 f/f* did not produce any significant phenotypes. The result of the combinatory loss of *Lats1/2* in the Mullerian duct mesenchyme was much more impactful. The double knockout females were infertile, exhibited thickened Mullerian duct at embryonic day 17.5, thickened tortuous uterine horns at birth, ovaries but no oviductal structures in adult mice, and a lack of uterine glands in adult uteri[72]. The structure of the female reproductive tract was overrun with myofibroblasts suggesting a lack of multipotency in mesenchymal cells. These significant phenotypes suggest that temporal activation of HIPPO signaling initiating suppression of YAP/WWTR1 is required for normal Mullerian mesenchymal cell fate developmentally while the previous study showed the importance of YAP/WWTR1 in postnatal Mullerian duct mesenchyme development.

In the uterus, the HIPPO signaling pathway also plays integral roles with evidence for YAP and WWTR1 activation in specific functional contexts. The nonpregnant cycling murine uterus expresses high levels of *Yap* during estrous and diestrus stages of the estrous cycle[73]. Protein expression of YAP and p-YAP are highest in estrous and diestrus with much lower intensity levels in proestrus and metestrus. Importantly, nuclear expression of YAP appears highest in stromal cells during estrus and diestrus while cytoplasmic YAP expression appears highest in the luminal and glandular epithelium during these stages. These expression levels suggest a potential regulation of YAP activity and expression concordant with estrogen levels during the estrous cycle. Indeed, the authors show that with 17β-estradiol (E2) administration YAP expression significantly increased with coordinating increases of p-YAP in the endometrial epithelial layers. The

authors also showed that independent of nascent ovarian hormones the uterine epithelium similarly upregulated YAP and p-YAP[73]. The presence and estrogenic effects on YAP expression suggest a role for YAP during the estrous cycle. To identify the role of YAP during pregnancy, another group investigated YAP expression during the peri-implantation period compared to estrus staged uteri[74]. Specifically, nuclear YAP expression was evident in the luminal epithelium at day 1 of pregnancy and subsequently in the inter-implantation sites at day 5 of pregnancy. Glandular epithelial YAP expression was highest on the 1st day of pregnancy but then declined as pregnancy progressed. Conversely, the stroma exhibited nuclear YAP expression that increased as pregnancy progressed with highest expression being exhibited at days 5 and 6 of pregnancy[74]. The expression pattern of YAP suggests roles in uterine preparation for pregnancy and particularly during the integral process of decidualization.

The HIPPO targets, YAP and WWTR1 have independently been shown to be involved in endometrial stromal cell decidualization. *In vitro* decidualization can be induced with the administration of a progesterone analog that is stable in culture, medroxyprogesterone acetate (MPA), and dibutyryl cyclic adenosine monophosphate (cAMP) for up to 8 days. To identify whether YAP was required for endometrial stromal cell decidualization, one group treated primary endometrial stromal cells with MPA and cAMP for 4 days and investigated the expression of YAP[75]. They found that in the early stages of *in vitro* decidualization, YAP protein and *YAP* mRNA increases steadily up to 48 hours then begins to decline by 96 hours post-treatment. Since these data suggest an initiating role for YAP in decidualization, the authors treated endometrial stromal cells with a siRNA targeting YAP prior to the administration of MPA and cAMP. The loss of YAP

prior to decidualization treatment resulted in a blunted response evidenced by decreased IGFBP1 and decidual prolactin mRNA and protein levels, two canonical markers of decidualization, compared to controls[75]. These results concluded that YAP is required for the *in vitro* decidualization response. Another study investigated the independent role of WWTR1 in *in vitro* decidualization[76]. The authors showed that relative WWTR1 levels remained stable throughout decidualization, but that nuclear expression of WWTR1 was induced with cAMP plus MPA and E2 after 13 days of treatment. Another unpublished study by the same group utilized siRNA targeting WWTR1 prior to the decidualization administration. The authors showed that loss of WWTR1 compromised prolactin expression levels but not IGFBP1 when treated with E2, MPA, and cAMP to induce decidualization (K Morris et al, unpublished data). Together these studies indicate

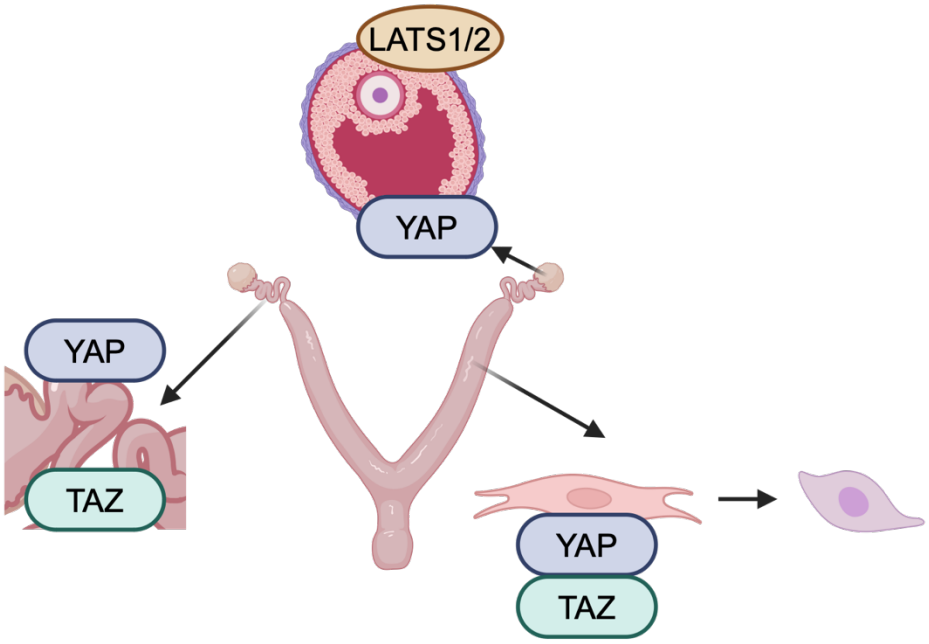

Figure 5. HIPPO signaling contributes to ovarian, oviductal, and uterine reproductive function. YAP and LAST1/2 expression is required for granulosa cell function. YAP and WWTR1 are required for proper oviductal development pre- and postnatally. YAP and WWTR1 are required for endometrial stromal cell decidualization.

independent but confirmatory roles for YAP and WWTR1 in endometrial stromal cell decidualization (Figure 5).

The NOTCH and HIPPO signaling pathways greatly contribute to female reproductive function and specifically to endometrial stromal cell decidualization. These two classical pathways coordinate in other systems like in the liver and kidney, but their crosstalk within female reproductive function has yet to be explored. In addition, many questions remain such as how, when, and where the NOTCH and HIPPO signaling pathways function during the decidualization response. The premise of this dissertation is to elucidate the specific independent roles of the NOTCH and HIPPO signaling pathways in endometrial stromal cell decidualization *in vivo* utilizing conditional knockout mouse models.

CHAPTER II: RBPJ IS REQUIRED FOR THE INITIATION OF ENDOMETRIAL STROMAL CELL DECIDUALIZATION

2.1 Introduction

The endometrium is an essential site for female reproductive function. This innermost layer of the uterus is comprised of several cell types, most notably the epithelial and stromal cells that facilitate implantation and support and maintain pregnancy. Specifically, the luminal epithelial cells at the surface of the endometrium coordinate embryo attachment and apposition while the branching glandular epithelium secretes factors to support implantation. These populations of uterine epithelial cells crosstalk with the adjacent differentiating stromal cells, known as decidual cells, that also help facilitate implantation while also supporting endometrial remodeling[2, 77].

Endometrial stromal cell decidualization is critical for reproductive success in species that undergo interstitial implantation[78]. Stromal cell decidualization is the terminal differentiation process of stromal cells regulated by increased progesterone (P) and cyclic adenosine monophosphate (cAMP) signaling and low levels of estrogen (E)[79]. In humans, decidualization begins spontaneously in the latter half of the secretory phase of the menstrual cycle while in mice decidualization is initiated in response to an implanting embryo[2, 78]. Studies surrounding implantation and decidualization *in vivo* in humans are limited due to obvious ethical concerns while studies in the non-human primate and mouse have identified some of the critical molecular mechanisms responsible for successful implantation and decidualization such as those mediated by steroidal and embryonic signals[79]. Although the central mechanisms regulating decidualization have been identified, many pathways interact in this incredibly complex

differentiation process[78]. Furthermore, the specific mechanisms by which these pathways affect the decidualization response have yet to be uncovered indicating a significant need to investigate the precise mechanisms at play in decidualization.

The Notch signaling pathway is a ubiquitous juxtracrine signaling pathway that plays key roles in cell proliferation, cell fate, differentiation, and death[4, 80]. The Notch signaling pathway consists of four transmembrane Notch receptors and five transmembrane Delta-like and Jagged ligands[81]. Initial proteolysis of the Notch receptor is initiated by ligand binding leading to activation and release of the extracellular domain. Proteolytic cleavage of the transmembrane portion of the Notch receptor releases the Notch intracellular domain that translocates to the nucleus to interact with the Notch signaling pathway transcriptional effector, Rbpj, and its cofactors to induce transcription of target genes such as the *Hes* and *Hey* family of genes[80]. The Notch signaling pathway regulates processes that are critical in decidualization like differentiation, cell fate and cell death indicating a potential role in the decidualization response. Indeed, the Notch signaling pathway plays significant roles in female reproduction including regulation of decidualization, implantation, and uterine repair[11, 26, 29, 30, 37, 59].

Notch signaling activation is required for successful implantation, decidualization, and uterine repair following parturition[82]. Our laboratory has extensively studied the specific roles of the Notch signaling pathway in female reproduction[11, 26, 27, 29, 30, 59]. Utilizing a *progesterone* driven *Cre recombinase* mouse model, we conditionally deleted *Notch1, Rbpj*, and overexpressed the *Notch1 intracellular domain* (*N1ICD*) all of which resulted in impaired decidualization[26, 29, 30, 59]. We first determined that Notch1 is critical for endometrial stromal cell decidualization utilizing a $Pgr^{cre/+}Notch1^{Fl/Fl}$

conditional deletion mouse model[26]. These mice exhibit an impaired decidualization response, decreased stromal cell proliferation, and increased decidual cell apoptosis indicating that Notch1 signaling is an important mediator of stromal cell proliferation and cell fate[26]. A $Pgr^{cre/+}Rbpj^{Fl/Fl}$ conditional deletion mouse model exhibits a decreased decidualization response compared to wild-type controls caused by decreased progesterone receptor expression and signaling and reduced glucose transporter, *Slc2a1*, expression both of which are important for stromal cell differentiation[30]. Importantly, these mice also exhibit compromised implantation orientation leading to embryonic death highlighting the importance of *Rbp*j in maternal-fetal communication at the initiation of pregnancy[37]. Additional studies on the importance of the Notch signaling pathway demonstrated that overexpression of *N1ICD* in the uterus resulted in a glandless phenotype and a completely impaired decidualization response[29]. Functional analyses revealed that overexpression of the *N1ICD* in conjunction with *Rbpj* knockout induces hypermethylation of the progesterone receptor through the PU.1-Dnmt3b complex compromising P4 signaling and enhancing E2 signaling[29]. Importantly, these data indicate that epithelial and stromal compartmentalization and cross-compartment Notch signaling and hormone signaling have profound effects on the decidualization response. Furthermore, these conditional deletion and overexpression mouse models provide significant evidence for the role of Notch1 signaling in endometrial stromal cell decidualization. To further elucidate these mechanisms, we induced decidualization artificially *in vitro* in human uterine fibroblasts[83] utilizing 17b-estradiol (E2), medroxyprogesterone acetate (MPA), and dibutyryl cyclic AMP (cAMP) with *NOTCH1* knockdown by shRNA before and after the initiation of decidualization. *NOTCH1* inhibition

prior to decidualization stimulus inhibits the decidualization response while *NOTCH1* inhibition following the decidualization stimulus has no effect on the decidualization response[27]. These *in vitro* data combined with our extensive *in vivo* data suggest important roles for Notch signaling in both the epithelial and stromal compartments of the endometrium during early pregnancy events and specifically at the initiation of decidualization.

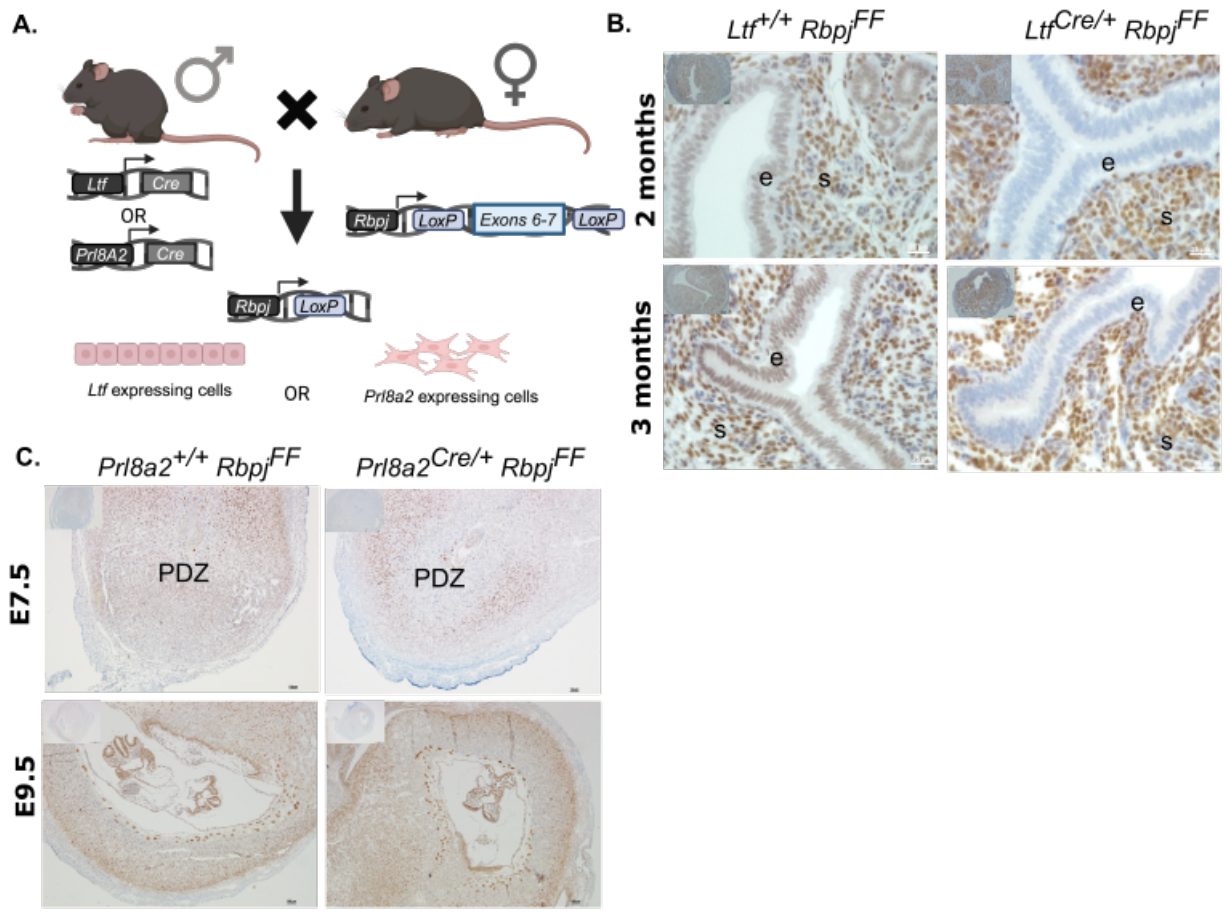

Figure 6. Conditional deletion of *Rbpj* in epithelial and decidual cells was successful. A. *Ltf*^{cre} or *Prl8A2*^{cre} mice were crossed with *Rbpj*$^{Fl/Fl}$ mice to generate epithelial (e-KO) or decidual stromal (ds-KO) specific deletion of *Rbpj* in mature female uteri. **B.** RBPJ expression in e-KO females at 2 and 3 months of age. e: epitheliium, s: stroma **D.** ds-KO of *Rbpj* shown at E7.5 in the primary decidual zone (PDZ) and return of Rbpj expression at E9.5. Negative controls shown in upper left corner of micrographs.

Given the importance of the Notch signaling pathway and its transcriptional effector, RBPJ in female reproductive function in both the epithelial and stromal compartments and its significant roles in decidualization, we sought to investigate the compartment specific roles of *Rbpj* in uterine epithelial cells and separately in decidual stromal cells utilizing transgenic mouse models. We generated an epithelial conditional knockout mouse model of *Rbpj* (*Ltf*$^{cre/+}$ *Rbpj*$^{Fl/Fl}$, e-KO) and a decidual stromal conditional knockout mouse model of *Rbpj* (*Prl8A2*$^{cre/+}$ *Rbpj*$^{Fl/Fl}$, ds-KO) to selectively inhibit all Notch signaling in each of these compartments (Figure 6). We hypothesized that given the severe phenotypes in the *Pgr*$^{cre/+}$ *Rbpj*$^{Fl/Fl}$ and *Pgr*$^{cre/+}$ *Rosa26*$^{N1ICD/+}$ mouse models, we would see infertility phenotypes resulting from decidualization failure or lack of uterine repair in the compartmental specific knockouts. Surprisingly, we observed a normal decidualization response and fertility in both models suggesting a role for Notch signaling in early decidualization, in line with our previous *in vivo* and *in vitro* data[11, 26, 27, 29, 30].

2.2 Materials and Methods

Animal Models

Ltf$^{iCre/+}$[84], *Prl8A2*$^{iCre+/}$[85], and *Rbpj*$^{Flox/Flox}$ [86] mice were housed and maintained in a designated animal care facility at Michigan State University or South China Agricultural University on a 12 hour light/dark cycle with free access to food and water. *Ltf*$^{iCre/+}$ mice were crossed with *Rbpj*$^{Flox/Flox}$ mice to produce uterine epithelial deletion of Rbpj in mature female mice (Figure 6A)[84]. *Prl8A2*$^{iCre/+}$ mice were crossed with *Rbpj*$^{Flox/Flox}$ mice to produce mice containing a deletion of *Rbpj* in decidualized stromal cells (Figure 6A)[87]. Females were placed with proven fertile males in the evening for

timed mating experiments. Seminal plugs were checked each morning with day of plug designated as embryonic day (E) 0.5. All animal procedures were approved by the Institutional Animal Care and Use Committee of Michigan State University and South China Agricultural University.

Immunohistochemistry

Tissues were fixed in 4% paraformaldehyde, dehydrated in ethanol and xylene and embedded in paraffin. Sections (6μm) were deparaffinized and rehydrated in a graded alcohol series followed by antigen retrieval (Vector Laboratories, Burlingame, CA) and hydrogen peroxide treatment. Next, sections were blocked and incubated with antibodies against Rbpj, Esr1, p-Esr1, or Ki67 overnight at 4°C (Table A1). On the following day, sections were incubated with biotinylated secondary antibodies followed by incubation with horseradish peroxidase conjugated streptavidin. Immunoreactivity was detected using the DAB substrate kit (Vector Laboratories) and visualized as brown staining by light microscopy. Incubation with secondary antibody only served as a negative control. Alternatively, after dehydration, slides were stained with hematoxylin and eosin (H&E) followed by rehydration in a graded ethanol series then cover slipped and visualized by light microscopy. ImageJ image analysis software (NIH, v1.52s), was utilized to determine a digital HSCORE for staining intensity.

RNA Isolation and Real-time Quantitative PCR

Total RNA was isolated from frozen mouse tissue using TRIzol reagent (Invitrogen, Waltham, MA). One μg of RNA was reverse transcribed to cDNA using a High-Capacity cDNA Reverse Transcription Kit according to the manufacturer's instructions (Applied Biosystems, Foster City, CA). Quantitative real time PCR (qPCR) was performed with

SYBR Green PCR Master Mix (Applied Biosystems) using the ViiA7 qPCR system (Applied Biosystems). Primer sequences utilized are listed in Table A2.

Statistical Analysis

Data are expressed as mean ± SEM. Data were analyzed utilizing Student's t-Test and one-way ANOVA followed by Tukey's posthoc multiple-range test. Values were considered significant if $p<0.05$. All statistical analyses were performed by GraphPad Prism (Graphpad Software, v9.0).

2.3 Results

Uterine epithelial and decidual stromal cell knockouts are fertile

We confirmed epithelial knockout of Rbpj by immunohistochemistry (IHC) in uterine cross-sections from sexually mature mice at 2 and 3 months of age (Figure 7B). No positive staining wa s observed in the luminal and glandular epithelium of the e-KO mice while controls expressed positive Rbpj stain in both the luminal and glandular epithelium (Figure 7B). Knockout of Rbpj in stromal cells in the primary decidual zone at E7.5 in ds-KO mice was observed but we noted perfuse staining by E9.5 throughout the stromal compartment in the ds-KO and controls (Figure 7C). Rbpj e-KO mice exhibited Rbpj deletion after sexual maturity as expected, while the ds-KO mice showed transient deletion in decidual stromal cells post-implantation and a return to normal expression at the time of placentation, E9.5.

Next, we performed a 6-month breeding trial to assess fertility in these knockout models. Both the e-KO and ds-KO mice exhibited normal litter sizes compared to controls during a six-month breeding trial (Tables 1 and 2). The e-KO mice had significantly less litters per mouse compared to the controls (Table 1). Unlike in the $Pgr^{cre/+}$ $Rbpj^{Fl/Fl}$ model

in which Rbpj was conditionally deleted in both epithelial and stromal cells postnatally[59], the e-KO and ds-KO mice maintained litter sizes consistent with controls in subsequent litters (Figure 7A and 7B). Both the e-KO and ds-KO mice had normal implantation site

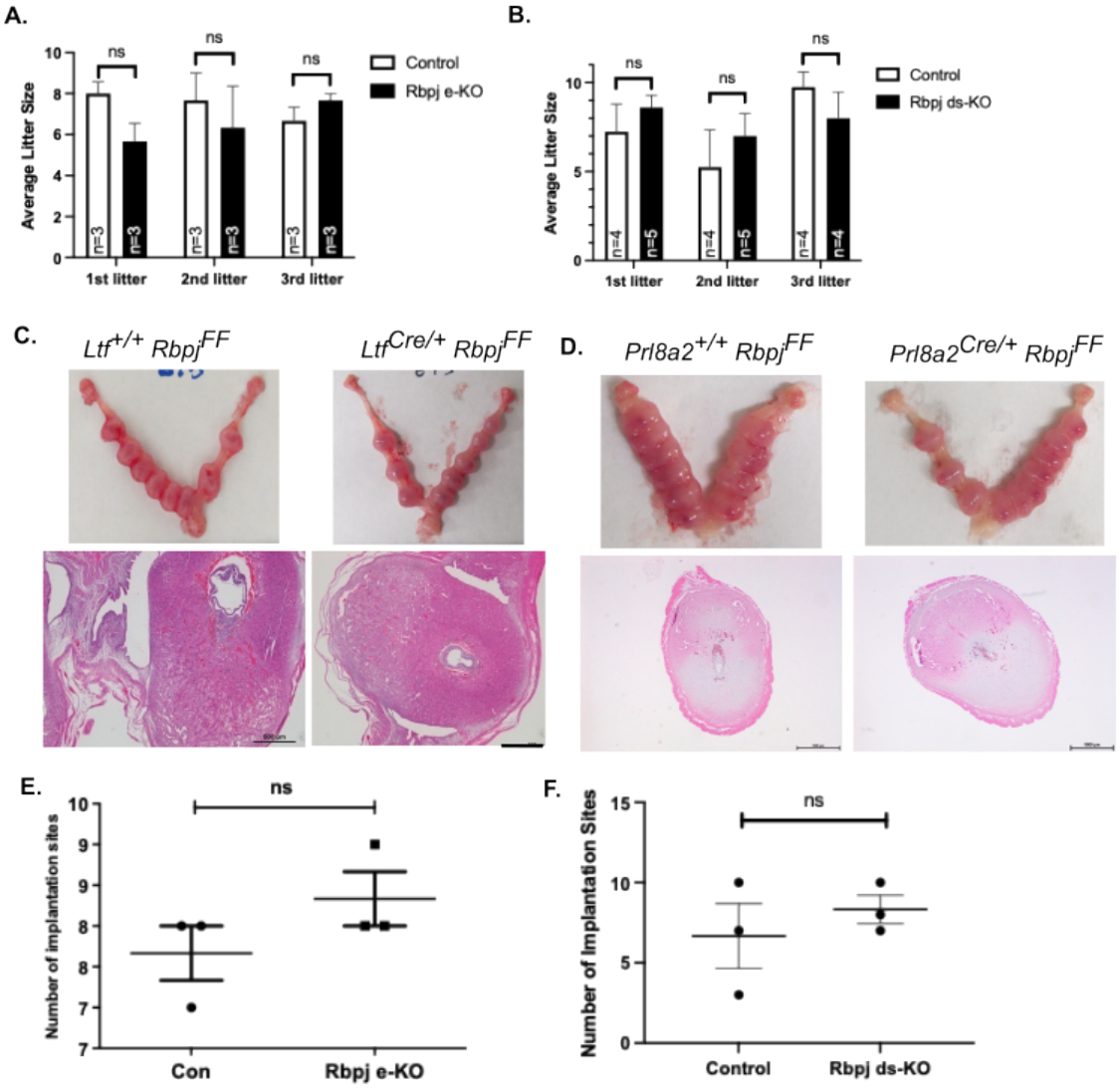

Figure 7. Rbpj epithelial and decidual stromal cell knockout mice are fertile. A. e-KO of *Rbpj* does not affect fertility evidenced by litter sizes consistent with controls. **B.** ds-KO of *Rbpj* does not affect litter size compared to controls. Error bars represent standard error of the mean. **C.** Normal implantation sites at E7.5 in control and e-KO mice shown by gross morphology and H&E staining. **D.** Normal implantation sites at E7.5 in control and ds-KO mice shown by gross morphology and H&E staining. **E.** e-KO mice implantation site quantity is not significantly different from controls at E7.5. **F.** ds-KO mice do not have a difference in implantation site number compared to controls at E7.5.

morphology at E7.5 both grossly and in H&E-stained uterine cross-sections (Figure 7C and 7D). The number of implantation sites at E7.5 was also consistent with controls (Figure 7E and 7F). These data indicated that the *Rbpj* e-KO and ds-KO mice are fertile and do not display aberrations in early pregnancy.

Table 1. Epithelial *Rbpj* knockout fertility trial assessment.

Genotype	n	Total number of litters	Total number of pups	Mean number of pups per litter	Mean number of litters per mouse
$Ltf^{+/+}$ $Rbpj^{Fl/Fl}$	7	37	280	7.6±0.41	5.29±0.42
$Ltf^{cre/+}$ $Rbpj^{Fl/Fl}$	9	27	204	7.6±0.52	3±0.47*

Table 2. Decidual stromal *Rbpj* knockout fertility trial assessment.

Genotype	n	Total number of litters	Total number of pups	Mean number of pups per litter	Mean number of litters per mouse
$Prl8A2^{+/+}$ $RBPj^{fl/fl}$	4	14	102	7.3±0.9	3.5±0.6
$Prl8A2^{cre/+}$ $RBPj^{fl/fl}$	5	20	141	7.1±0.6	4±0.5

Epithelial Rbpj knockout mice exhibit increased E2 signaling and increased stromal proliferation

Esr1 expression in the e-KO mice at E3.5 was consistent with controls, but p-Esr1, indicative of active estrogen signaling, was increased in both the luminal epithelium and stroma (Figure 8A). In addition, Esr1 targets *Muc1* and *C3* were increased in the e-KO mice (Figure 8B). Finally, we observed increased Ki67 expression in the stroma of e-KO mice indicative of increased stromal proliferation (Figure 8A). These results suggest that a lack of *Rbpj* expression encourages activation of E signaling and increased stromal proliferation. Limited fetal resorption sites, between one and three (n=3), were present in the in the e-KO mice at E15.5, however this did not compromise the average number of pups per litter (Figure 8C lower panel). There were not differences in the quantity of

normal implantation sites between the e-KO and control mice despite the presence of resorption sites (Figure 8D). The number of abnormal implantation sites in the e-KO mice was significant compared to controls with at least one resorption site per e-KO mouse (n=3, Figure 8E). These results suggest that Rbpj e-KO induces fetal resorption but does not compromise the fecundity of these mice.

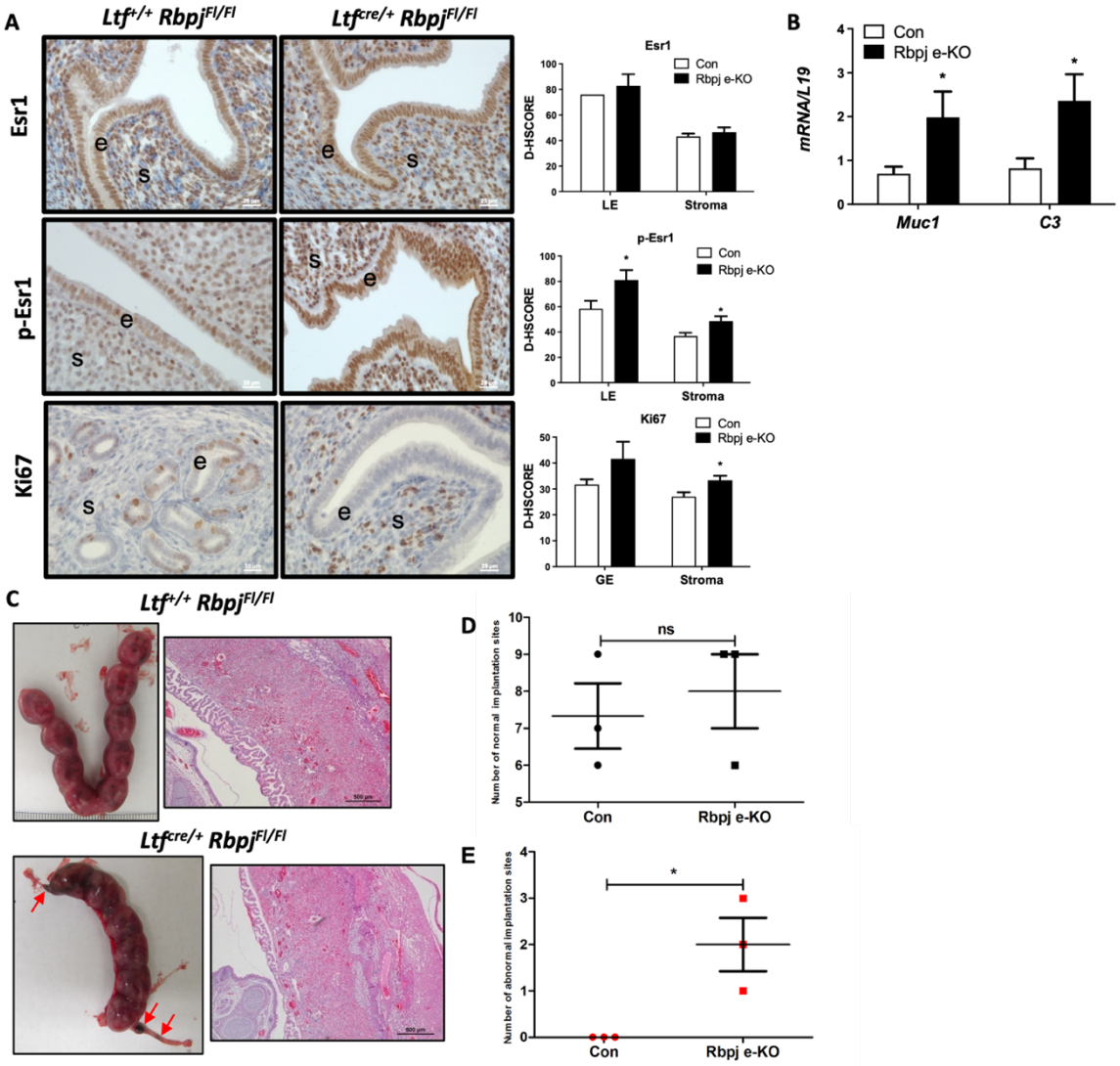

Figure 8. Epithelial Rbpj KO mice exhibit increased estrogen signaling at E3.5 and abnormal implantation sites at E15.5. A. IHC staining of e-KO mouse uteri for ESR1, P-ESR1, and Ki67 at E3.5. **B.** qPCR results for estrogen target genes *Muc1* and *C3* in eKO uteri at E3.5. **C.** Gross morphology and H&E staining of e-KO uteri at E15.5. Red arrows indicate resorption sites **D.** Total normal implantation site number in e-KOs and controls at E15. **E**. Total abnormal implantation site number in e-KOs and controls at E15.5. e: epithelium s: stroma

2.4 Discussion

Endometrial stromal cell decidualization is an early critical reproductive event that involves the coordinated transformation of endometrial stromal cells into decidual cells[78]. This process is regulated by P and cAMP signaling, but many pathways integrate to coordinate the success of decidualization. Previously, the Notch signaling pathway was implicated in this process and considered significant for the decidualization response[11, 26, 27, 29, 30]. The current study shows that neither epithelial nor decidual stromal deletion of *Rbp*j has detrimental effects on the decidualization process, nor on reproductive success. First, this suggests that the Notch signaling pathway has compartment specific roles in the uterus. Since epithelial deletion lead to increased resorption sites, this shows that Rbpj signaling may play a specific role in implantation and post-implantation development although the sample size in this collection was small indicating a potential limitation. Indeed, Rbpj expression is required for appropriate embryo orientation during implantation[37]. Furthermore, deletion of Rbpj in stromal cells that have already decidualized has no effect on fertility which solidifies the importance of Notch-dependent Rbpj signaling during the initiation of decidualization but not decidualization maintenance.

The decidualization process is a terminal differentiation of stromal cells that involves a coordinated change in morphology and function to prepare for and to support pregnancy. The Notch signaling pathway is known to regulate proliferation and indeed proliferation of endometrial stromal cells[81]. We have previously shown that Notch1 is required for the initiation of decidualization *in vitro* to induce proliferation of endometrial stromal cells and must be downregulated for differentiation to occur or cells undergo

apoptosis[26, 27]. Utilizing *in vitro* decidualization studies we determined that the NOTCH1 receptor is cleaved and therefore active until day 6 but is inactive after that[88]. The temporal requirement of Notch1 expression during pregnancy initiation *in vivo* was not identified until this study. Our previous studies indicate that active NOTCH signaling through RBPJ is most important during the initiation of decidualization. *Prl8a2 Cre* was most efficient at deleting *Rbpj* in the primary decidualization zone at E7.5 but did not affect expression or have phenotypic repercussions immediately post-implantation at E5.5 indicating that only cells that are already decidualized express Prl8a2[89]. These results support the idea that once decidualization has already begun and the initial stromal cell proliferation events have occurred, inhibiting Notch signaling by deleting Rbpj expression has no effect. This confirms that Notch signaling is not important in the differentiation process of decidualization but is required for early proliferative initiation events.

Notch signaling has previously been shown to interact with steroid hormone receptor signaling in many contexts[82]. Epithelial knockout of Rbpj resulted in increased p-Esr1 expression and increased esr1 target gene expression resulting in increased proliferation, particularly in the stromal compartment. These results mimic those seen in the N1ICD overexpression model suggesting that regulated activation of the Notch signaling pathway is important for estrogen signaling in the uterus[29]. Indeed, total uterine deletion of Rbpj also resulted in significant decreases in *Pgr* and target gene expression during artificial decidualization indicating that Rbpj expression is important for P responsiveness in the uterine environment[30]. Our studies show that canonical Notch signaling through Rbpj leads to overactivation of estrogen signaling and inhibition of progesterone signaling in a coordinated manner between the epithelium and stroma[29].

This e-KO further supports these findings given that epithelial deletion of Rbpj increases p-Esr1 expression and proliferation in the stromal compartment. Other studies have also shown the importance of epithelial-stromal crosstalk in hormone signaling during epithelial proliferation, implantation and decidualization (summarized in [90]). This further supports our previous findings that the Notch signaling pathway indirectly coordinates hormone signaling in the uterine environment through epithelial-stromal crosstalk.

In summary, we have shown that epithelial deletion of *Rbpj* does not compromise fertility, suggesting that Notch signaling in the epithelium is not required for the establishment of pregnancy but is required for pregnancy maintenance given the increased resorption sites noted in these mice. Complementary to this, deletion of *Rbpj* after decidualization has already been initiated has no effect on pregnancy success confirming that canonical *Notch* signaling activation in the stroma is required at the initiation of decidualization but is not required to maintain the decidualization response. Future studies will investigate the precise role of Notch dependent and independent RBPJ signaling in stromal cells prior to and at the beginning of the establishment of pregnancy and the compartmental specific roles of this pathway throughout pregnancy.

CHAPTER III: CONDITIONAL LOSS OF YAP1 OR WWTR1 CONTRIBUTES TO SUBFERTILITY

3.1 Introduction

Infertility affects 20% of reproductive aged persons world-wide (WHO). This is approximated as 50% of contribution from either the male or female partner amongst heterosexual couples. Patients experiencing infertility must undergo extensive financial, emotional, and physical hurdles to conceive. Despite the growing need for fertility sparing treatments, research remains underfunded, and many causes of infertility remain unknown or untreatable. One critical process that is associated with infertility is decidualization failure. Defective decidualization is associated with miscarriage, recurrent pregnancy loss, pre-eclampsia, and fertility impairing diseases like endometriosis[44]. Decidualization is one of many hormonally regulated processes required for pregnancy initiation and is characterized as the terminal differentiation of endometrial stromal cells under the regulation of ovarian hormones. This terminal differentiation is required for appropriate trophoblast invasion and preparation of the maternal endometrium for an implanting embryo. Two factors that are implicated in decidualization are YAP and WWTR1 (WWTR1). *In vitro* investigations indicated independent requirements for YAP and WWTR1 in endometrial stromal cell decidualization (Morris et al, unpublished) [75, 76]. However, its mechanisms and roles *in vivo* remain uninvestigated.

HIPPO signaling is mediated by changes in extracellular matrix stiffness, growth hormone availability, and cell-cell contact[5]. This kinase cascade is activated when lower tension is present externally such as when cell density is high, extracellular matrix stiffness is low, and cellular/tissue growth is highly active. The principal kinases, MST1/2

in humans or STK3/4 in mice, phosphorylate their own cofactor SAV1, they then phosphorylate LATS1/2 that then phosphorylates YAP and its homolog WWTR1 (WWTR1)[5]. This final phosphorylation of YAP and WWTR1 leads to their inactivation followed by either cytoplasmic sequestration by the 14-3-3 family of proteins or degradation. Alternatively, when cell density is low and extracellular and intracellular stiffness is high, YAP and WWTR1 are not phosphorylated and are free to translocate to the nucleus where they act as transcriptional cofactors with the TEAD family of transcription factors. YAP/WWTR1-TEAD complexes bind to distal enhancers or directly to promoters to affect gene transcription of known target genes. We hypothesized that given this pathway's roles in mechanical transduction, and previous data indicating a requirement for YAP and WWTR1 expression in *in vitro* decidualization, that YAP and WWTR1 would be required for endometrial stromal decidualization *in vivo*. To address this hypothesis, we generated *Progesterone Cre* mediated individual knockouts to investigate the independent roles of *Yap* and *Wwtr1* in murine pregnancy initiation and maintenance.

3.2 Materials and Methods

Animal Models

Pgr$^{Cre/+}$[91] mice were crossed to *Yap*$^{fl/fl}$ or *Wwtr1*$^{fl/fl}$[67, 92] to generate *Pgr*$^{Cre/+}$ *Yap*$^{fl/+}$ (YKO) or *Pgr*$^{Cre/+}$ *Wwtr1*$^{fl/fl}$ (TKO) conditional knockouts. The *Pgr*$^{Cre/+}$ mice are a mixed background of 129Sv × C57BL/6, the *Yap*$^{fl/fl}$ and *Wwtr1*$^{fl/fl}$ mice are 129SvEv. Animals were housed and maintained in a designated animal care facility at Michigan State University on a 12-hour light/dark cycle with free access to food and water. All

animal procedures were approved by the Institutional Animal Care and Use Committee of Michigan State University.

Fertility Evaluation

Sexually mature females 8-weeks of age or older were co-housed with proven fertile wild-type males for a 6-month breeding trial. Males were rotated in or out of cages if females did not produce a live born litter within one-month from time of set up. For timed mating experiments, proven fertile wild-type males were placed in female cages in the evening. Seminal plugs were checked each morning with day of plug designated at 0.5 days post coitus (dpc). Tail vein injection with Chicago blue dye served as a positive identifier for implantation sites at all time points. Following blue dye injection, female mice were sacrificed for collection at 5.5 and 12.5dpc. Body weight, uterine wet weight, ovarian wet weight, implantation site number, and gross morphology were catalogued. Uterine, oviductal, and ovarian tissues were divided and flash frozen or stored in RNAlater for downstream RNA and protein analyses or fixed in 4% paraformaldehyde for histological analysis.

Artificial Decidualization

Sexually mature, 8-weeks or older, female mice were ovariectomized followed by two weeks of rest. Animals were treated with three daily subcutaneous injections of 100ng 17β-estradiol diluted in sesame oil followed by two days of rest then three daily injections of 1mg progesterone plus 6.7ng 17β-estradiol diluted in sesame oil. Six hours following injection on the third day, an intraluminal scratch was performed surgically on the anti-mesometrial side of the endometrium of one uterine horn utilizing a blunted 25G needle. The unscratched uterine horn served as an unstimulated hormonal control.

Decidualization reaction was maintained with daily subcutaneous injection of 1mg progesterone plus 6.7ng 17β-estradiol for a total of 5 days followed euthanasia (n=5/genotype). Uterine tissues were collected as described above. Decidual reaction was measured by uterine wet weight ratio of stimulated/unstimulated horn and molecular markers *Wnt4* and *Bmp2* by qPCR of stimulated uterine horn compared to unstimulated horn from the same animal.

Immunohistochemistry

Tissues were fixed in 4% paraformaldehyde, dehydrated in ethanol and xylene, and embedded in paraffin. Sections (6 μm) were deparaffinized and rehydrated in a graded alcohol series followed by antigen retrieval (Vector Laboratories, Burlingame, CA) and hydrogen peroxide treatment. Next, sections were blocked and incubated with antibodies against YAP, WWTR1, ER-alpha, PGR, or Ki67 overnight at 4◦C (see Table A1 for complete antibody information). On the following day, sections were incubated with biotinylated secondary antibodies followed by incubation with horseradish peroxidase conjugated streptavidin. Immunoreactivity was detected using the DAB substrate kit (Vector Laboratories) and visualized as brown staining by light microscopy. Incubation with secondary antibody only served as a negative control. ImageJ image analysis software (NIH, v2.14.0), was utilized to determine a digital HSCORE for staining intensity of luminal epithelium, glandular epithelium, and stromal compartments of each uterine section.

RNA isolation and real-time quantitative PCR

Total RNA was isolated from frozen mouse uterine tissue using TRIzol reagent (Invitrogen, Waltham, MA). About 1μg of RNA was reverse transcribed to cDNA using a

High-Capacity cDNA Reverse Transcription kit according to the manufacturer's instructions (Applied Biosystems, Foster City, CA). Quantitative real-time PCR (qPCR) was performed with SYBR Green PCR Master Mix (Applied Biosystems) using the BioRad CFX Opus 384 qPCR system utilizing primers targeting genes of interest (Table A2). Expression was normalized to the average of *36b4* and *18s* per sample and fold change determined compared to time matched floxed controls ($Pgr^{+/+}$ $Yap^{fl/fl}$ or $Pgr^{+/+}$ $Wwtr1^{fl/fl}$).

Statistical analysis

qPCR data were tested for normality then log transformed in the case of non-normal data and analyzed by one-way ANOVA. Data that were not normal were analyzed utilizing Kruskal-Wallis nonparametric tests. Statistical analyses were performed utilizing GraphPad Prism 10 (GraphPad Software) and values were considered significant if $p<0.05$.

3.3 Results

Progesterone Receptor Cre conditional deletion of Yap1 and Wwtr1 was partially successful

To determine if effective recombination occurred in either the YKO or the TKO females, mRNA and protein expression for YAP, WWTR1, and key target genes were assessed (Figure 9). YAP was not differentially expressed in any of the three endometrial compartments, glandular epithelium (GE), luminal epithelium (LE), and stroma (St), nor in YKOs compared to controls (Figure 9A). In TKOS, WWTR1 expression was not differentially expressed in TKOs compared to controls however compartmental specific expression was evident (Figure 9B). WWTR1 was most highly expressed in the GE and

lowest in the LE and St within genotypes (Figure 9B). *Yap* and one target gene, *Ccn1*,

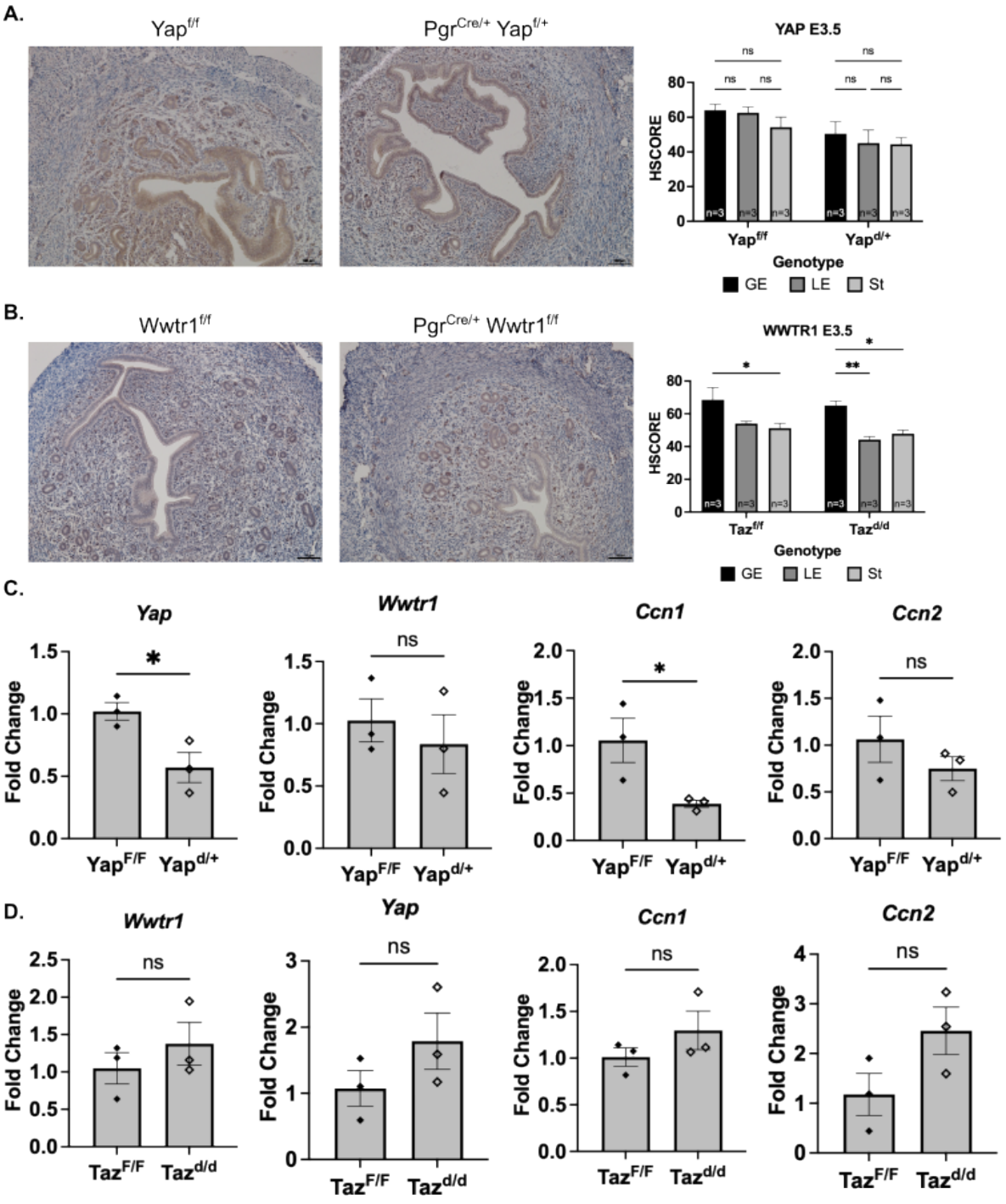

Figure 9. Recombination efficiency in individual *Yap* and *Wwtr1* Knockouts. A. YAP expression via immunohistochemistry and semi-quantitative H-SCORE at right in uterine cross-sections at 3.5dpc. **B.** WWTR1 expression via immunohistochemistry and semi-quantitative H-SCORE at right in uterine cross-sections at 3.5dpc. **C.** and **D.** YAP/WWTR1 target gene expression in YKO, TKO, and floxed control whole uteri at 3.5dpc.

was significantly decreased in YKOs compared to controls (Figure 9C). However, TKOs did not differentially express either *Yap* or *Wwtr1* nor their canonical target genes (Figure 9D).

Independent loss of Yap1 and Wwtr1 in the female reproductive tract induces subfertility

YKO and TKO females were subfertile compared to controls in a 6-month breeding trial (Tables A3 and A4). Partial knockout of Yap1 had a less severe effect on fertility

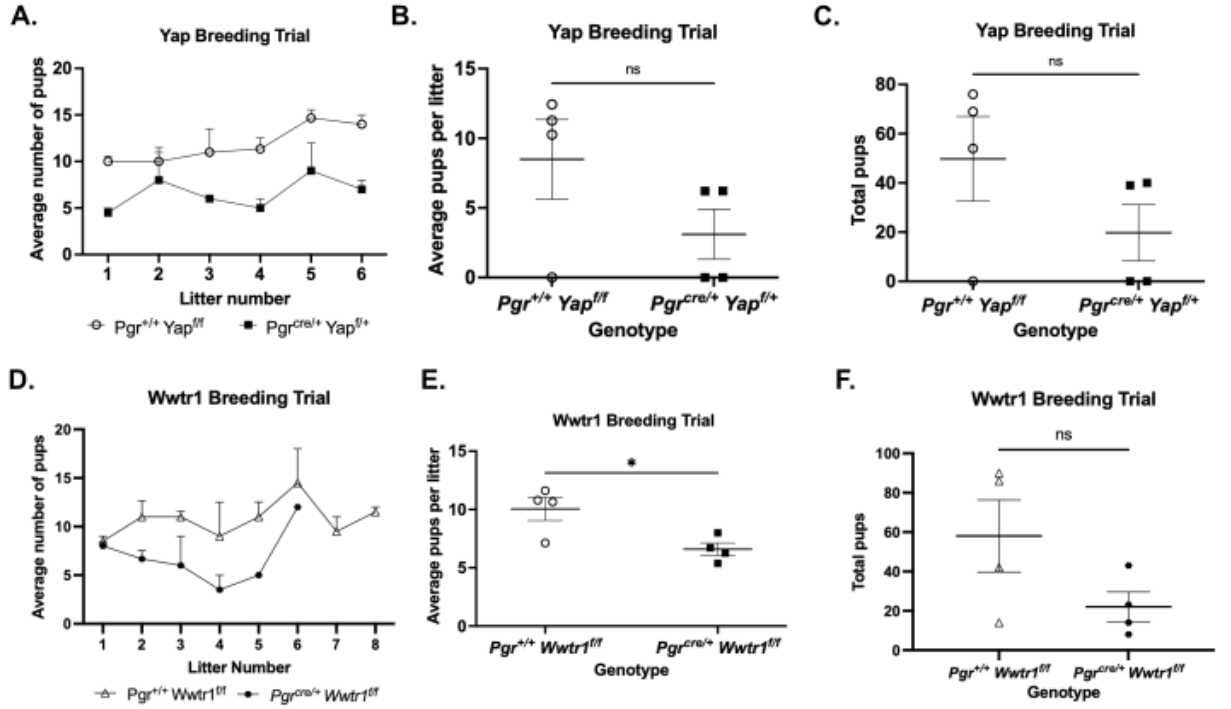

Figure 10. Heterozygous deletion of *Yap* and heterozygous deletion of *Wwtr1* induces female subfertility. A. Average pups per genotype across 6-month breeding trial for YKOs. **B.** Average pups per litter for YKO breeding trial. **C.** Total pups across 6-month breeding trial for YKOs. **D.** Average pups per genotype across 6-month breeding trial for TKOs. **E.** Average pups per litter for TKO breeding trial. **F.** Total pups across 6-month breeding trial for TKOs.

evidenced by no significant differences amongst average litter sizes and the total number of pups produced (Figure 10B and C). However, a wholistic view indicates that the average number of pups per individual was decreased in YKOs compared to controls (Figure 10A). Across the 6-month breeding period, TKO females produced significantly

fewer pups per litter and fewer litters, but not fewer total pups compared to controls (n=4/genotype, Figure 10D-F).

YKO and TKO females display normal uterine receptivity

Uterine receptivity was assessed in YKO and TKO females utilizing hormone receptor expression and proliferative marker, Ki67. YKOs expressed patterns of ER, PR, and Ki67 consistent with controls at embryonic day 3.5 (Figure 11A-C). Similarly, TKO

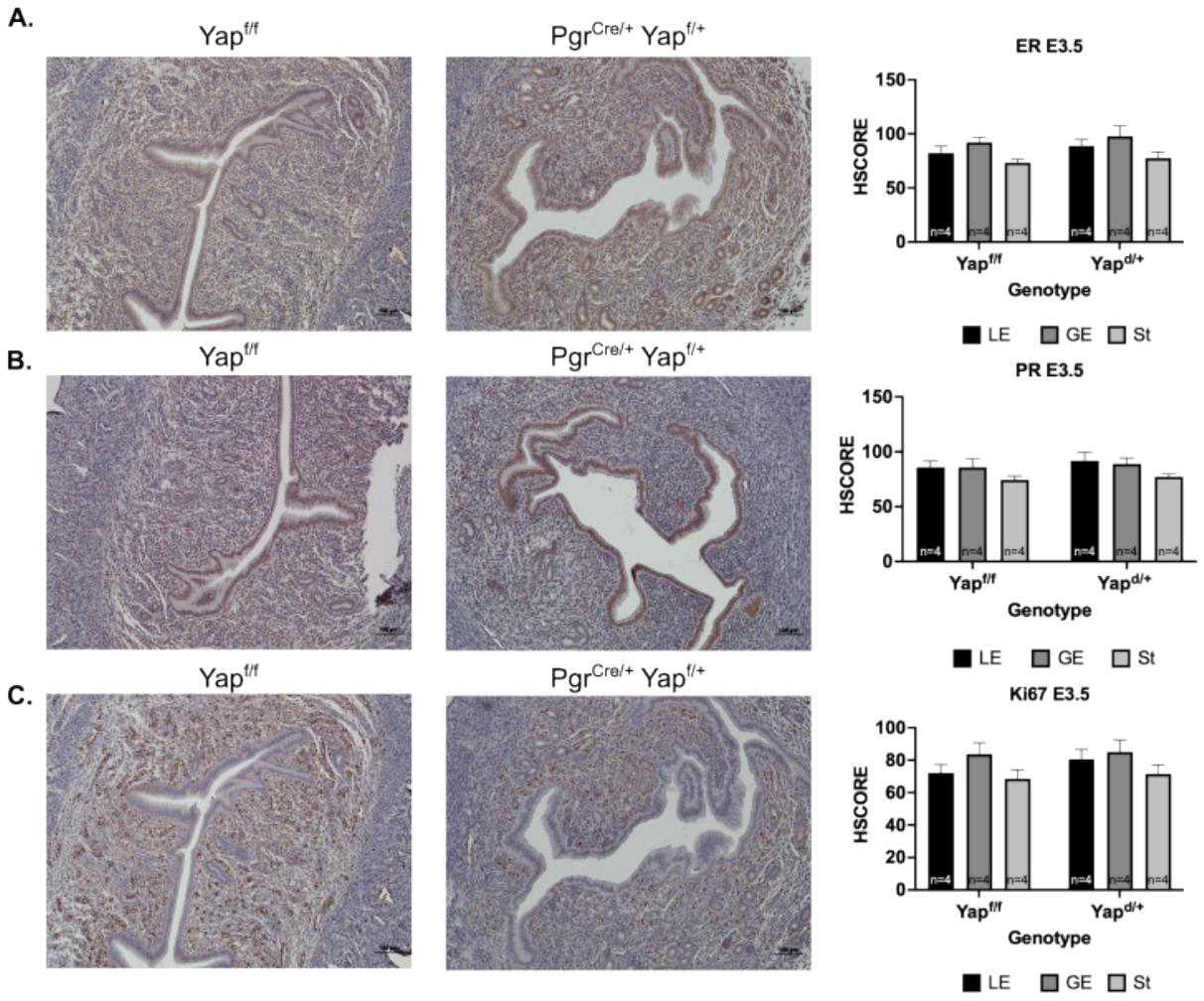

Figure 11. YKO and TKO females exhibit normal uterine receptivity. A. Immunohistochemistry staining and semi-quantitative H-SCORE analysis of uterine cross-sections at E3.5 for estrogen receptor (ER), **B.** Progesterone receptor (PR) and **C.** Ki67 in YKO females. **D.** Immunohistochemistry staining and semi-quantitative H-SCORE analysis of uterine cross-sections at E3.5 for estrogen receptor (ER), **E.** Progesterone receptor (PR) and **F.** Ki67 in TKO females.

Figure 11 (cont'd)

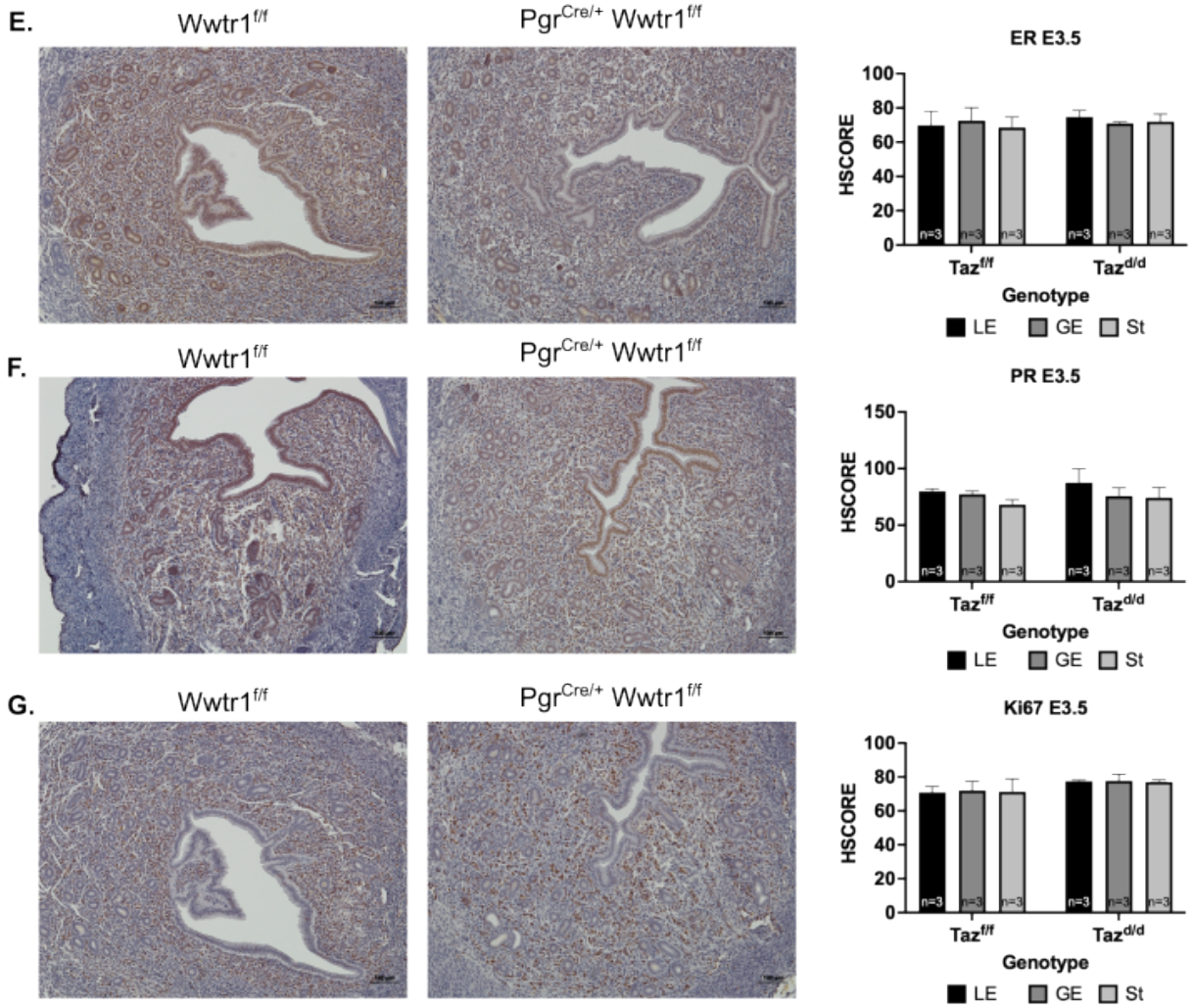

females expressed hormone receptor and proliferative marker Ki67 in compartment specific levels comparable to controls (Figure 11D-F).

TKO but not YKO females exhibit decreased decidualization response

Artificial decidualization response was measured by uterine wet weight ration and molecular markers Wnt4 and Bmp2 in stimulated and unstimulated horns after 5 days of stimulus (Figure 12). Neither YKOs nor TKOs exhibited aberrant gross morphological response to decidualization scratch (Figure 12 A and D). However, the uterine wet weight ratio of TKO uteri was significantly decreased compared to controls (Figure 12E). Despite

this qualitative measure, molecular markers of decidualization *Wnt4* and *Bmp2* indicated appropriate response to stimulus compared to controls.

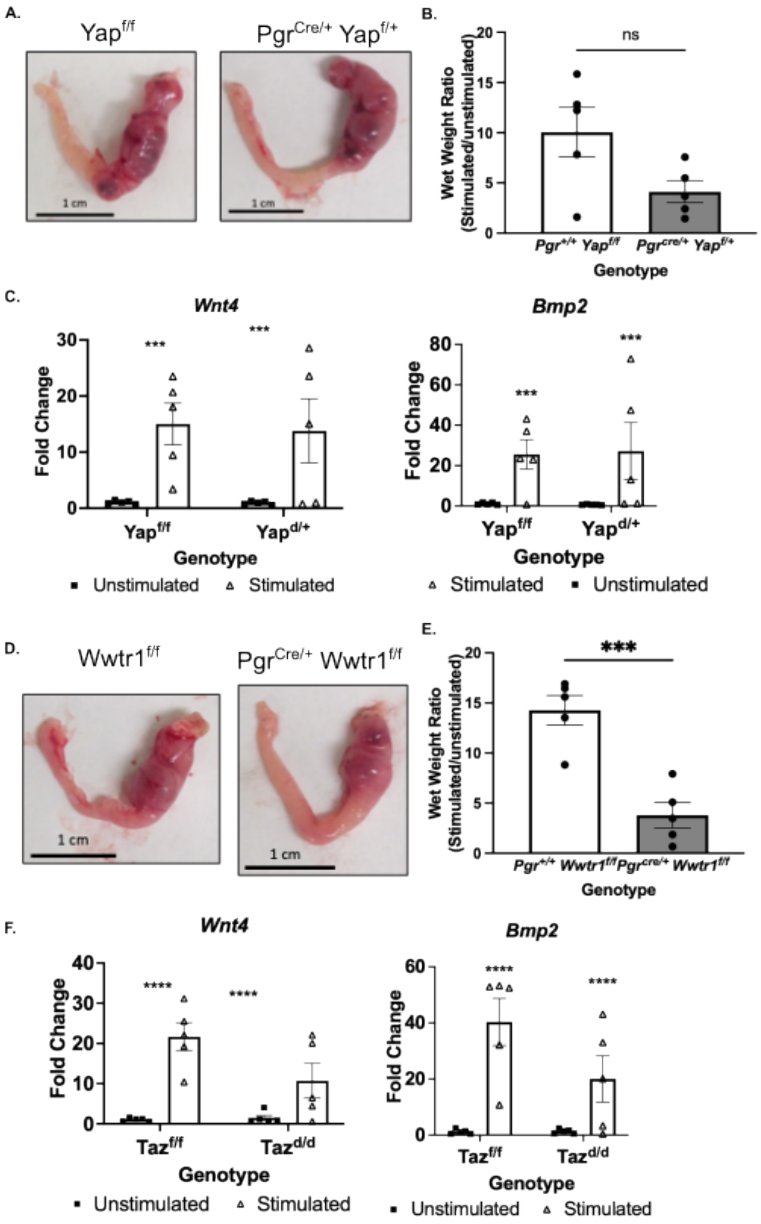

Figure 12. Decidualization response is partially compromised in single knockout females. A. Representative uterine micrographs of unstimulated (left) and stimulated (right) uterine horns after 5 days of artificial decidualization in YKOs. **B.** Uterine wet weight ratio of stimulated over unstimulated horn in YKOs. **C.** Molecular markers of decidualization *Wnt4* and *Bmp2* expression in stimulated and unstimulated horns of YKOs. **D.** Representative uterine micrographs of unstimulated (left) and stimulated (right) uterine horns after 5 days of artificial decidualization in TKOs. **E.** Uterine wet weight ratio of stimulated over unstimulated horn in TKOs. **F.** Molecular markers of decidualization *Wnt4* and *Bmp2* expression in stimulated and unstimulated horns of TKOs.

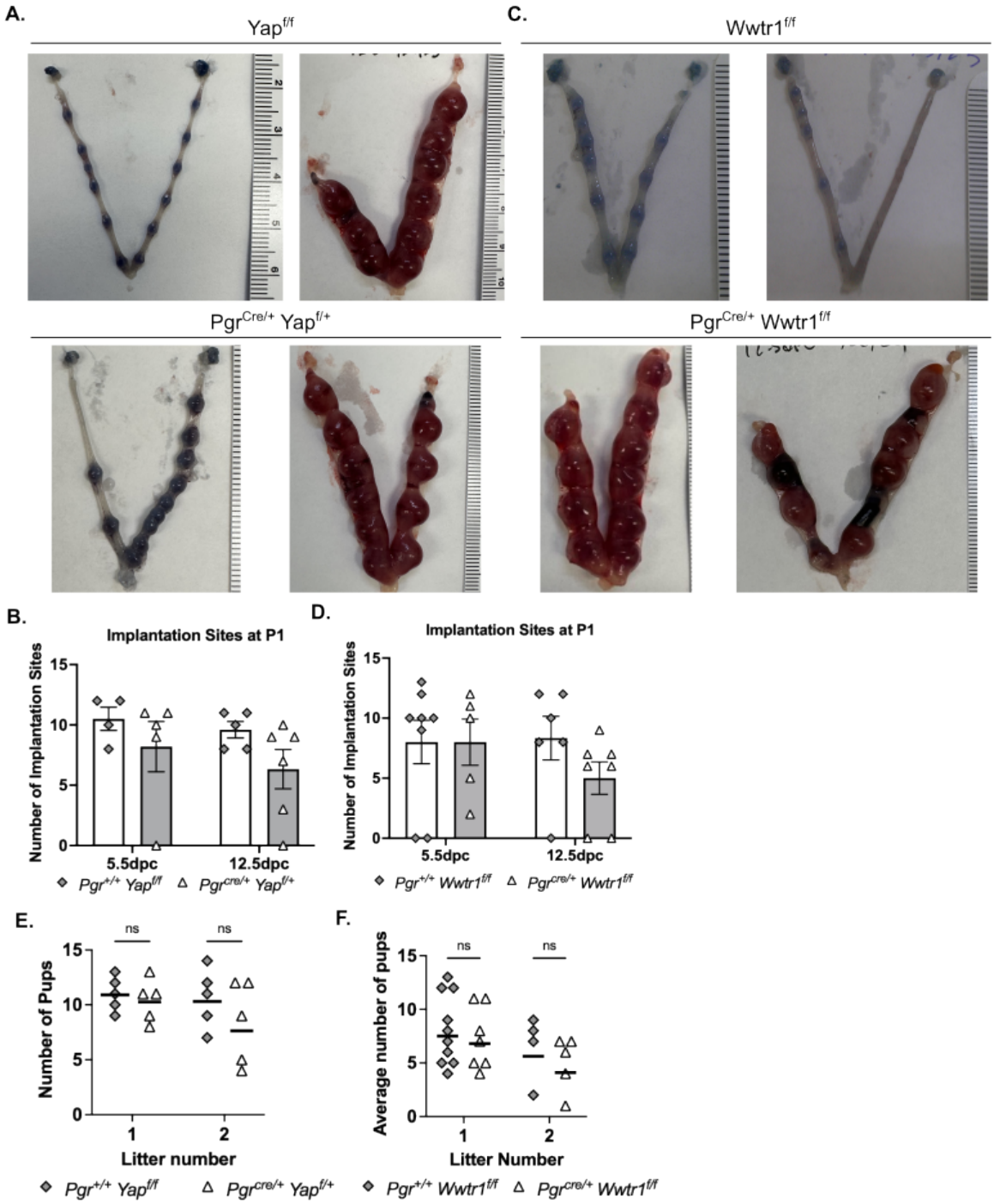

Figure 13. TKO females exhibit increased fetal resorption but comparable first two litter sizes. A. Representative micrographs of uteri in the first pregnancy at 5.5dpc (left) and 12.5dpc (right) in YKOs. **B.** Quantification of implantation sites at 5.5dpc and 12.5dpc of YKOs. **C.** Representative micrographs of uteri in the first pregnancy at 5.5dpc (left) and 12.5dpc (right) of TKOs. **D.** Quantification of implantation sites at 5.5dpc and 12.5dpc of TKOs. **E.** Average number of pups in the first two litters of YKOs and **F.** TKOs.

TKO and YKO females are fertile despite fetal resorption at 12.5dpc

Positive implantation sites were assessed and quantified at two key timepoints in murine pregnancy: 5.5dpc and 12.5dpc (Figure 13). Post-implantation both YKO and TKO gross uterine morphology and positive blue dye injections were apparently normal (Figure 13A and C). At 12.5dpc, post-placentation, both YKOs and TKOs exhibited resorption sites that were visually obvious however not significant quantitatively (Figure 13A and C and not shown). Quantification of positive normal implantation sites in primiparous females indicated comparable quantities between YKOs and TKOs and controls (Figure 13B and D). Indeed, an expanded dataset shows comparable litter sizes in the first two litters for both YKOs and TKOs.

3.4 Discussion

Classically, *Yap1* and *Wwtr1 (Wwtr1)* are assumed to have redundant functions within tissues[64]. Most investigations within specific tissue types have looked at either only *Yap1* or both *Yap1* and *Wwtr1* combined without assessing each gene's independent role. This is because in mammals *Wwtr1* arose from a duplication event of the *Yap1* gene. In invertebrates like *Drosophila sp.*, *Yap1* analogs like Yorkie are present but there is not *Wwtr1*. Structurally *Yap1* and *Wwtr1* as paralogs are very similar and contain all of the same essential binding domains however *Yap1* contains two double tryptophan repeats rather than one that is found in *Wwtr1*[64]. These tryptophan repeats are sites where cofactors can bind to either YAP or WWTR1 and so the idea that YAP and WWTR1 are not functionally distinct is at least plausible based on their structural similarities. However, individual whole-body deletions of *Yap1* and *Wwtr1* induce very different phenotypes. *Yap1* null mice are embryonic lethal at embryonic day 8.5 because of compromised yolk

sac vasculogenesis, chorioallantoic attachment, and embryo elongation[93]. Conversely, *Wwtr1* null mice are viable but exhibit polycystic kidney disease, post-natal death, smaller body size, reduced lifespan, and litters from null mice were reduced compared to controls[94, 95]. These individual null mutants suggest that at least during embryonic development, YAP and WWTR1 play independent roles.

However, the literature is somewhat biased, and this is particularly apparent in conditional knockout models. One positive example within murine cardiac tissue individual *Yap1* knockout induces cardiomyopathy postnatally resulting in death by 20 weeks of age while *Wwtr1* knockout had no effect on cardiac development[67]. Despite these results in the individual knockouts, the authors investigated gene dosage compensation to determine if *Yap1* and *Wwtr1* deletion may have a combinatorial effect. They found that conditional deletion of both *Yap1* and *Wwtr1* lead to postnatal lethality; heterozygous deletion of *Yap1* plus homozygous deletion of *Wwtr1* induced lethality at 33 weeks of age; heterozygous deletion of *Wwtr1* plus homozygous deletion of *Yap* lead to lethality by 10 days[67]. This study was particularly interesting in the context of *Yap/Wwtr1* allelic compensation since individual conditional knockouts displayed completely different phenotypes, but combinatorial deletion of alleles led to varying degrees of severity in cardiomyopathy and lethality suggesting combinatorial and independent roles for *Yap1* and *Wwtr1* in embryonic cardiac development. Another study investigated *Yap1* and *Wwtr1* double deletion in an inducible knockout model in the colonic smooth muscle and found that deletion of these two factors generated a loss in smooth muscle contractility[96]. However, the individual contributions of either YAP or WWTR1 were not investigated in the context raising the question whether one or the other

is contributing to the phenotype. These studies pose interesting questions into the roles and temporality of *Yap1* and *Wwtr1* expression in varying stages of organ development, tissue repair, and even cancer. We postulate that these two paralogs are jointly involved in many of these processes but perhaps serve roles in specific temporal timepoints during these processes which may explain why single knockouts display variance in phenotypes, but double knockouts display more severe or additive phenotypes. Concordant with some of the literature, our study indicates that both YAP and WWTR1 may serve independent roles in the murine uterus.

The lack of complete *Yap1* deletion is unfortunate for the investigation of the independent role of YAP in the murine uterus. The lack of recombination can be attributed to *Progesterone receptor (PR)* and *Yap1*'s proximity on murine chromosome 9 and their Precise location both being 2.46cM (MGI). Due to this closeness of our Cre driver, PR, and its target, *Yap1* it is physically impossible to generate a double *Yap1* knockout. However, the lack of complete *Yap1* knockout allowed an interesting look into gene dosage for *Yap1* and *Wwtr1* in the murine uterus in the context of pregnancy and estrous cyclicity. Our study suggests that there may be both independent as well as combinatorial roles for *Yap1* and *Wwtr1* in the uterus and warrants further investigation of a double knockout model.

CHAPTER IV: YAP1 AND WWTR1 ARE REQUIRED FOR THE MAINTENANCE OF PREGNANCY

4.1 Introduction

Successful reproduction is an impeccably complex process. The coordination of intricate molecular signals with large-scale physiological changes imparts many opportunities for error. An unfortunate statistic is that 20% of couples attempting to reproduce are infertile from either male or female contributions (NICHD). Within mammals, the fertilization of ovulated oocyte(s) is just the beginning, assuming that ovulation is not compromised. Following fertilization and early embryonic development, an embryo implants into a receptive maternal endometrium that is significantly remodeled throughout pregnancy to support gestation[97]. In humans and mice, successful reproduction requires the coordinated efforts of many molecular and cellular signals and the appropriate interplay between systems, including the neuroendocrine, immune, vascular, and female reproductive tract. Humans undergo spontaneous endometrial stromal cell decidualization, a terminal differentiation of the underlying stroma within the endometrium, which is induced by increasing levels of progesterone during the secretory phase of the menstrual cycle[97]. This process is critical to control trophoblast invasion and allow appropriate embryo invasion and occurs spontaneously each cycle in the absence of a conceptus[98, 99]. In mice, decidualization only occurs when an embryo physically attaches to the maternal endometrial epithelium that communicates with the stroma and initiates decidualization[79]. In humans, decidualization prepares the maternal endometrium for implantation while in mice implantation initiates decidualization. In both mice and humans, decidualization controls the level of trophoblast

invasion and is integral to pregnancy establishment. Therefore, understanding the molecular mechanisms that underlie these complex coordinated events is essential to identifying mechanisms that may go awry and contribute to infertility.

Many molecular pathways have been implicated in decidualization and implantation, including WNT, NOTCH, and HIPPO signaling[78]. Of particular interest is the mechanosensing HIPPO pathway. This pathway was first identified in *Drosophila* and so named due to mutations in this pathway leading to increased body size[100]. The Hippo signaling pathway in mammals controls organ size, growth, and proliferation and does so by sensing and responding to changes in the extracellular environment, like the presence and tension of nearby cells, as well as growth factor availability[63]. The Hippo pathway is a kinase cascade whereby external signals like those mentioned above induce the phosphorylation of MST1/2 through a variety of upstream signals. MST1/2 phosphorylates LATS1/2, which then phosphorylates YAP1 and WWTR1, two transcriptional cofactors. YAP1 and WWTR1 are either bound or degraded in the cytoplasm and therefore inactive when the HIPPO signaling pathway is active. Conversely, when the HIPPO signaling pathway is deactivated, YAP1 and WWTR1 translocate to the nucleus and bind their canonical partner transcription factors, the TEADs, where they regulate directly gene transcription of extracellular and cytoplasmic matrix components, cell cycle genes, and indirectly by acting as distal enhancer recruiters[63]. This pathway is well conserved among mammals and has been implicated to play a role in female reproductive function.

In the murine uterus, YAP1 exhibits dynamic expression with the highest levels of mRNA and protein expression at estrus, an estrogen-dominated stage[73]. In addition,

YAP1 is significantly increased and phosphorylated with 17β-estradiol treatment of ovariectomized mice, suggesting YAP1's importance in specific phases of the estrus cycle[73]. Beyond the estrus cycle, YAP1 is expressed throughout the murine endometrium in early pregnancy prior to embryo implantation at embryonic day 0.5 and beyond[101]. Post-implantation *Yap1* and its targets, *Ctgf* and *Ankrd1*, are significantly increased. A similar response is observed in oil-induced decidualization, suggesting a potential role for YAP1 in maternal preparation of pregnancy[101]. In addition, conditional deletion of *Yap1* and its homolog, *Wwtr1* (formerly known as *Taz*), under *Anti-Mullerian hormone receptor type 2* driven *Cre* expression, results in degradation of the oviductal isthmus myosalpinx complicating embryo transport, suggesting an essential role for YAP1 and WWTR1 in structural integrity[68]. Beyond what is known in the mouse, YAP1 and WWTR1 have been independently identified as critical for endometrial stromal cell decidualization *in vitro*. YAP1 expression increases in the first 48 hours of *in vitro* endometrial stromal cell decidualization, and knockdown by shYAP prior to induction of *in vitro* decidualization results in a compromised decidualization response[75]. In addition, WWTR1 increases during in vitro decidualization at day 6, and the knockdown of WWTR1 also compromises the expression of decidualization markers IGFBP1 and dPRL (unpublished)[76]. These studies highlight the roles of YAP1 and WWTR1 in *in vitro* decidualization, but this potential has yet to be explored *in vivo*. In this study, we generated conditional knockout of YAP1 and WWTR1 under the *Progesterone receptor Cre* to explore the potential roles and regulation of these Hippo homologs in pregnancy.

4.2 Materials and Methods

Animal Models

Pgr$^{Cre/+}$[91] mice were crossed to *Yap*$^{fl/fl}$ *Wwtr1*$^{fl/fl}$[67, 92] to generate *Pgr*$^{Cre/+}$ *Yap*$^{fl/+}$ *Wwtr1*$^{fl/fl}$ partial double knockouts (pdKO). The *Pgr*$^{Cre/+}$ mice are a mixed background of 129Sv × C57BL/6, the *Yap*$^{fl/fl}$ *Wwtr1*$^{fl/fl}$ mice are 129SvEv. Animals were housed and maintained in a designated animal care facility at Michigan State University on a 12-hour light/dark cycle with free access to food and water. All animal procedures were approved by the Institutional Animal Care and Use Committee of Michigan State University.

Fertility Evaluation

Females were co-housed with proven fertile wild-type males for a 6-month breeding trial. Males were rotated in or out of cages if females did not produce a live born litter within one-month from time of set up. For timed mating experiments, proven fertile wild-type males were placed in female cages in the evening. Seminal plugs were checked each morning with day of plug designated at 0.5 days post coitus (dpc). Tail vein injection with Chicago blue dye served as a positive identifier for implantation sites at all time points. Following blue dye injection, female mice were sacrificed for collection at a variety of timepoints including 1.5, 3.5, 4.5, 5.5, 7.5, 9.5, and 12.5dpc. Body weight, uterine wet weight, ovarian wet weight, implantation site number, and gross morphology were catalogued. Uterine, oviductal, and ovarian tissues were divided and flash frozen or stored in RNAlater for downstream RNA and protein analyses or fixed in 4% paraformaldehyde for histological analysis. A subset of tissues were fixed in 10% DMSO in methanol for tissue clearing and advanced light sheet microscopy.

Artificial Decidualization

Sexually mature (8 weeks or older) female mice were ovariectomized followed by two weeks of rest. Animals were treated with three daily subcutaneous injections of 100ng

17β-estradiol followed by two days of rest then three daily injections of 1mg progesterone plus 6.7ng 17β-estradiol. Six hours following injection on the third day, an intraluminal scratch was performed surgically on the anti-mesometrial side of the endometrium of one uterine horn utilizing a blunted 25G needle. The unscratched uterine horn served as an unstimulated hormonal control. Decidualization reaction was maintained with daily subcutaneous injection of 1mg progesterone plus 6.7ng 17β-estradiol for 5 total days followed by euthanasia (n=5/genotype). Uterine tissues were collected as described above. Decidual reaction was measured by uterine wet weight ratio of stimulated/unstimulated horn and molecular markers *Wnt4* and *Bmp2* by qPCR of stimulated uterine horn compared to unstimulated horn from the same animal.

Oviductal and Uterine Flushes

Sexually mature female mice (8 weeks or older) were mated to proven fertile wild-type males. Oviductal flushes were performed with phosphate buffered saline (PBS) by inserting a 30G needle into the infundibulum of both oviducts at 1.5dpc (n=6 per genotype). Flushed products were collected, counted, categorized, and imaged. Uterine and oviductal flushes were performed at 3.5dpc with uterine flushes performed by inserting a 30G needle into the uterotubal junction and flushing toward the cervix utilizing PBS. Flushed products were similarly collected, counted, categorized, and imaged.

Immunohistochemistry

Tissues were fixed in 4% paraformaldehyde, dehydrated in ethanol and xylene, and embedded in paraffin. Sections (6 μm) were deparaffinized and rehydrated in a graded alcohol series followed by antigen retrieval (Vector Laboratories, Burlingame, CA) and hydrogen peroxide treatment. Next, sections were blocked and incubated with

antibodies against YAP, WWTR1, ER-alpha, PGR, Ki67, SUSD2 or ASMA overnight at 4°C (see Table A1 for IHC antibody information). On the following day, sections were incubated with biotinylated secondary antibodies followed by incubation with horseradish peroxidase conjugated streptavidin. Immunoreactivity was detected using the DAB substrate kit (Vector Laboratories) and visualized as brown staining by light microscopy. Incubation with secondary antibody only served as a negative control. Alternatively, after dehydration, slides were stained with Masson's Trichrome followed by rehydration in a graded ethanol series then cover slipped and visualized by light microscopy. ImageJ image analysis software (NIH, v2.14.0), was utilized to determine a digital HSCORE for staining intensity of luminal epithelium, glandular epithelium, and stromal compartments of each uterine section or for granulosa cells in ovarian cross-sections.

RNA isolation and real-time quantitative PCR

Total RNA was isolated from frozen mouse tissue using TRIzol reagent (Invitrogen, Waltham, MA). About 1µg of RNA was reverse transcribed to cDNA using a High-Capacity cDNA Reverse Transcription kit according to the manufacturer's instructions (Applied Biosystems, Foster City, CA). Quantitative real-time PCR (qPCR) was performed with SYBR Green PCR Master Mix (Applied Biosystems) using the BioRad CFX Opus 384 qPCR system utilizing primers targeting genes of interest (Table A2). Expression was normalized to the average of *36b4* and *18s* per sample and fold change determined compared to time matched floxed controls ($Pgr^{+/+}$ $Yap^{fl/fl}$ $Wwtr1^{fl/fl}$).

RNA-sequencing and data analysis

Total RNA was isolated from flash frozen mouse uteri utilizing TRIzol reagent as described above. Following isolation, RNA was treated with a RNA Clean and

Concentrator kit (Zymo) followed by DNAse treatment (TURBO DNA-free kit, Invitrogen) and stored in nuclease-free water at -80°C. Concentration was determined utilizing a Qubit RNA BR Assay Kit (Invitrogen). Samples were sent for RNA integrity analysis then subsequently sent to a sequencing facility for library preparation and sequencing (Michigan State University Genomics Core). Libraries were prepped with Illumina Stranded mRNA Library Prep kit (Illumina) and sequenced (paired end 150bp) on a NovaSeq 6000 Instrument (Illumina) to an average depth of 40 million read pairs per sample. Reads were quality trimmed, adapters were removed using TrimGalore (version 0.6.10), and quality-trimmed reads were assessed with MultiQC (version 1.7). Trimmed reads were mapped to Mus Musculus GRCm39.110 and gene counts quantified using STAR (version 2.6.0c). Model-based differential expression analysis was performed using edgeR-robust method (version 3.42.4) [102] in R. Genes with low counts per million (CPM) were removed using the filterByExpr function from edgeR. Multidimensional scaling plots, generated with the plotMDS function of edgeR, were used to verify group separation prior to statistical analysis. DEG were identified as FDR P value less than 0.05. Visualization of DEG was performed utilizing EnhancedVolcano (version 1.18.0) to generate a volcano plot. Counts per million of selected DEG were plotted using the box plot function of ggplot2 (version 3.4.4). Gene set enrichment and visualization was completed using the ShinyGO online tool (version 0.80) [103].

Whole-mount immunofluorescence, 3D uterine imaging, and analysis

Uteri were dissected from 3.5 (n=2) and 5.5dpc (n=8) pdKO and control females. Whole mount immunofluorescent staining was performed as previously described[104]. Briefly, following animal euthanasia, uterine samples were subsequently fixed in

DMSO:methanol (1:4) and stored at -20°C. Then, samples were rehydrated in 1:1, Methanol:PBST (PBS + 1% Triton X-100) for 15 minutes then washed for 15 minutes in 100% PBST. Tissues were then incubated in a blocking solution of PBS, 1% Triton X-100, and 2% powdered milk for 2 hours at room temperature. Samples were stained with primary antibodies for rat anti-CDH1 (M108, Takara Biosciences), rabbit anti-cytokeratin 8 (MA5-14476, Invitrogen) and rabbit anti-FOXA2 (Abcam, ab108422) diluted at 1:500 in blocking solution for 7 nights at 4°C. Uterine samples were then washed in PBST for 15 minutes twice and 45 minutes four times then incubated with fluorescently conjugated Alexa Fluor 555 Donkey anti-Rabbit IgG secondary antibody (A31572, Invitrogen), and 647 Goat anti-Rat secondary antibody (A21247, Invitrogen) and Hoechst (B2261, Sigma Aldrich) at 1:500 for 2 nights at 4°C. Samples were then washed in PBST for 15 minutes twice and 45 minutes four times, dehydrated in methanol then incubated overnight in 3% H2O2 diluted in methanol. Tissues were then washed in 100% methanol for 15 minutes twice then for 60 minutes and cleared overnight using BABB (benzyl alcohol:benzyl benzoate, 1:2). Stained tissue samples were imaged with a Leica TCS SP8 X Confocal Laser Scanning Microscope System (Leica Microsystems) with a white-light laser, using a 10x air objective. For each uterine horn, z-stacks were generated with a 7.0μm increment, and image analysis was carried out using Imaris v9.2.1 (Bitplane, Zurich, Switzerland). Briefly, confocal LIF files were imported into the Surpass mode of Imaris, and Surface module 3D renderings were used to create structures for the oviductal–uterine junctions, embryos, implantation chambers, and horns as described previously[105]. We used the Contour modules for Hoechst and FOXA2 fluorescent signal (embryo), and CDH1 signal (oviduct and implantation chamber). Embryo 3D volume was

assessed using the surface statistics function, while embryo implantation chamber length was calculated using the measurement points module of Imaris software.

Statistical analysis

Data were tested for normality then log transformed in the case of non-normal data and analyzed by unpaired t-tests, one-way ANOVA, Fisher's exact test, or mixed effects analysis as indicated. Data that were not normal were analyzed utilizing Kruskal-Wallis nonparametric tests. Statistical analyses were performed utilizing GraphPad Prism 10 (GraphPad Software) and values were considered significant if $p<0.05$.

Data Availability

Raw FASTQ files were deposited in the NCBI Gene Expression Omnibus as GSE267798.

4.3 Results

Generation of Yap1 and Wwtr1 partial double knockout

Progesterone receptor (Pgr) Cre expressing male mice were crossed to double floxed females (*Yap*$^{f/f}$ *Wwtr1*$^{f/f}$) to generate heterozygous founders. Offspring were then backcrossed to generate *Pgr*$^{Cre/+}$ *Yap*$^{f/f}$ *Wwtr1*$^{f/f}$ females for fertility investigation (Figure 14). The resulting mice were genotyped as *Pgr*$^{Cre/+}$ *Yap*$^{f/+}$ *Wwtr1*$^{f/f}$ (pdKO) or *Pgr*$^{+/+}$ *Yap*$^{f/f}$ *Wwtr1*$^{f/f}$ but never as *Pgr*$^{Cre/+}$ *Yap*$^{f/f}$ *Wwtr1*$^{f/f}$ (Figure 14). Investigation into the Mouse Genome Informatics database revealed that *Progesterone* and *Yap1* are approximately 900kB or effectively 0cM apart, and therefore, it was impossible to generate a fully floxed *Yap* allele with *Pgr Cre* and ultimately not possible to generate a fully homozygous knockout of *Yap1* and *Wwtr1*. The investigation continued into the role of *Yap* and *Wwtr1* in the murine reproductive tract utilizing the partial double knockout model.

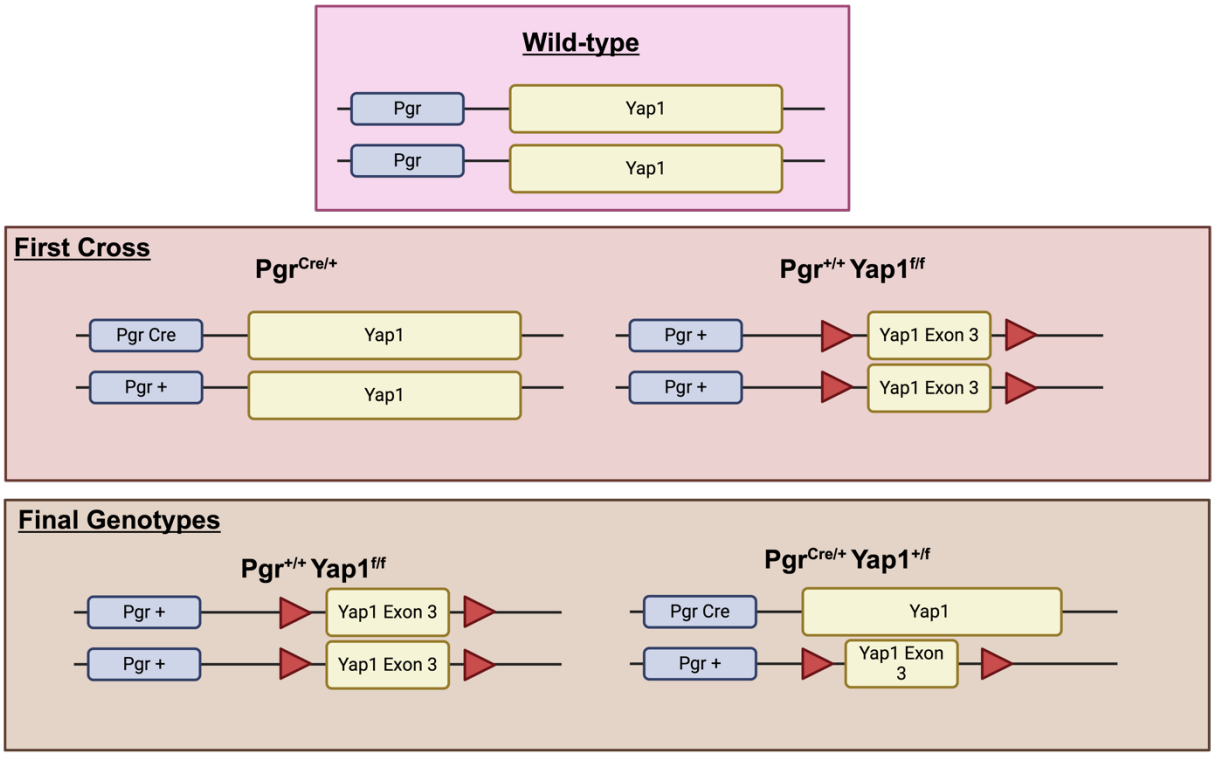

Figure 14. Illustration of alleles to generate floxed animals. Wild-type mice express progesterone receptor and Yap1 less than 900kB apart on chromosome 9. Double *Yap1 floxed* animals were crossed to heterozygous *Pgr Cre* expressing males. Resulting offspring following backcross were either *Yap1 floxed* or *Pgr Cre/+ Yap +/flox*.

Progesterone Cre conditional deletion of Yap1 and Wwtr1 exon 3 does not affect reproductive tract structure

Uteri and ovaries were assessed for Cre-mediated recombination of the *Yap1* and *Wwtr1* alleles (Figure 15). At 3.5dpc, neither *Yap1* nor *Wwtr1* were differentially expressed in uteri utilizing primers that amplify the floxed exon 3, but the target gene *Ccn2* was significantly decreased (unpaired t-test p=0.032, Figure 15A-D). However, at 5.5dpc, *Wwtr1* was significantly decreased in pdKO uteri (unpaired t-test p=0.017, Figure 15B). Immunohistochemical analysis indicated epithelium and stromal compartment-specific expression of YAP1 and WWTR1 in uteri at 3.5dpc, however expression levels were not significantly different between controls and pdKOs (Figure 15E-F). Evidence of

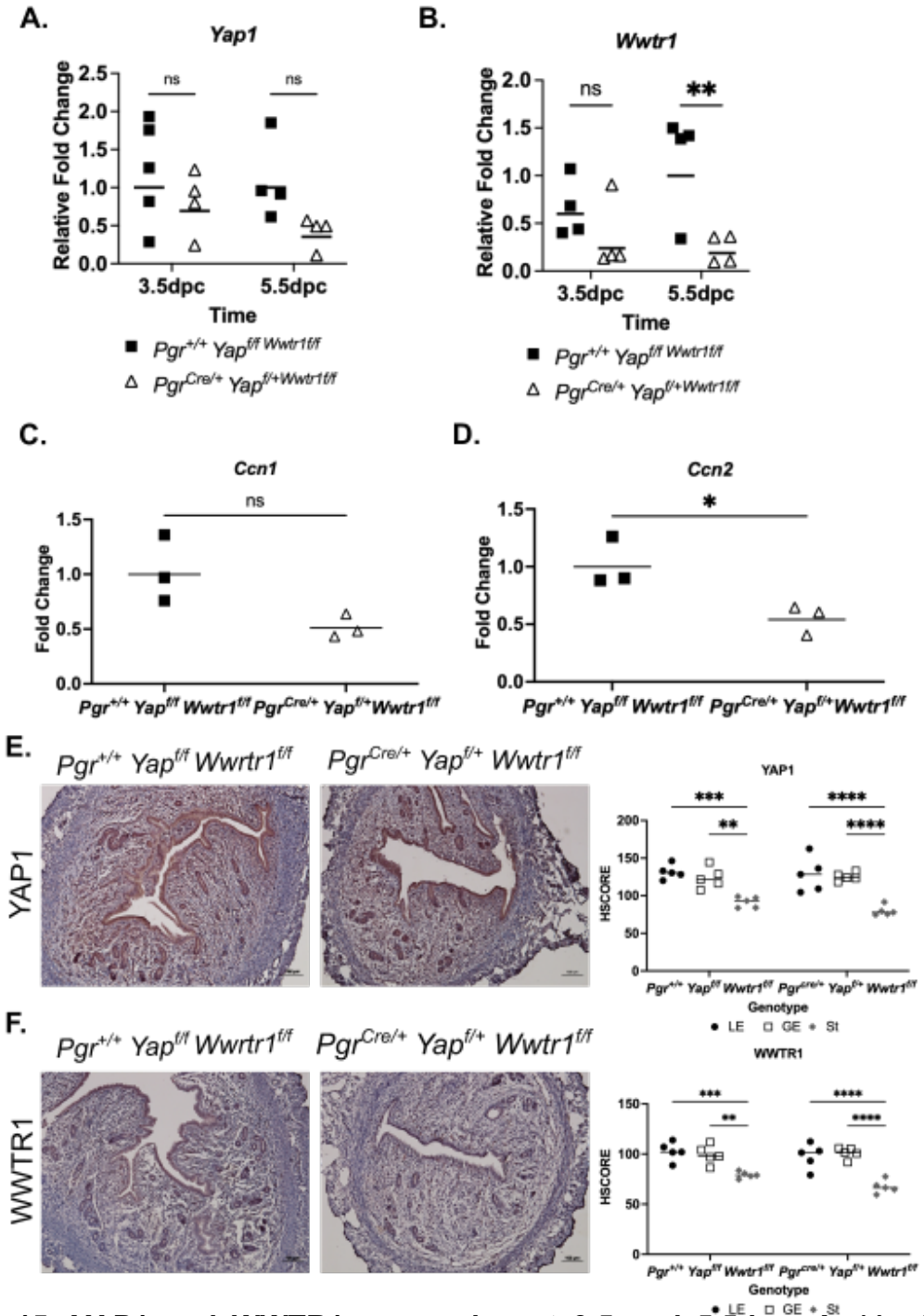

Figure 15. YAP1 and WWTR1 expression at 3.5 and 5.5dpc. A. *Yap1* mRNA expression is not significantly different in pdKOs compared to controls in early pregnancy. **B.** *Wwtr1* mRNA expression is significantly decreased in pdKOs at 5.5dpc but not at 3.5dpc compared to controls. **C.** YAP/WWTR1 target gene *Ccn1* is not differentially expressed at 3.5dpc in pdKOs. **D.** *Ccn2*, a YAP/WWTR1 target gene, is significantly decreased at 3.5dpc in pdKOs. **E.** YAP1 protein expression at 3.5dpc and semi-quantitative HSCORE. **F.** WWTR1 protein expression at 3.5dpc and semi-quantitative HSCORE.

Yap1 and *Wwtr1* and target gene depletion was not evident in whole ovaries (Figure B1A). In addition, both YAP1 and WWTR1 protein expression was not significantly different in granulosa cells of 3.5dpc control and pdKO ovaries (Figure B1B). In addition to these molecular analyses, no structural differences were observed in the ovaries, oviducts, and uteri of virgin females at proestrus or 3.5dpc (Figure B2A-B).

Partial ablation of Yap and Wwtr1 induces subfertility

$Pgr^{Cre/+}$ $Yap^{fl/+}$ $Wwtr1^{fl/fl}$ partial double knockouts (pdKO) produced significantly fewer total pups throughout a 6-month breeding trial (n=4, Mixed-effects analysis factor genotype, p=0.006, Figure 16A). In addition, pdKO females had smaller litter sizes than controls (unpaired t-test p=0.0007, Figure 16B). The pdKO mice bore approximately 50%

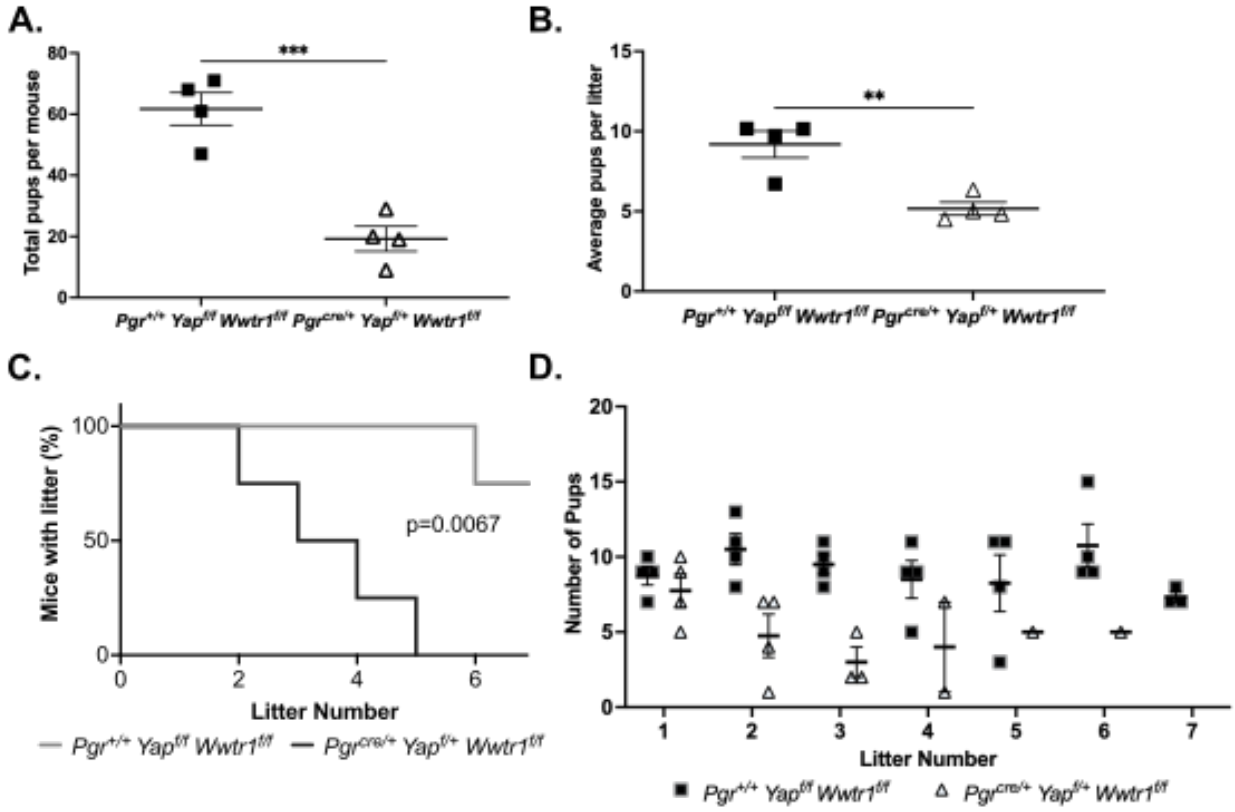

Figure 16. pdKOs are subfertile with smaller litter sizes. A. pdKO females had fewer total pups across a 6-month breeding trial. **B.** pdKO females had smaller litter sizes compared to controls across a 6-month breeding trial. **C.** pdKO females exhibited a reduced capacity to produce pups over time. **D.** pdKO females began to lose the ability to bear live born litters after the second litter.

fewer pups and litters than the floxed controls throughout the breeding trial (Table A5). In addition, the pdKO mice displayed a reduced capacity to produce pups as time progressed (Mantel-Cox test p=0.007, Figure 16C). One individual only produced two live-born litters when placed with multiple fertile males (Figure 16D). In addition to the subfertility shown throughout the breeding trial, pdKO females in an expanded cohort exhibited significantly reduced first and second litter sizes (Mixed effects analysis factor genotype, p=0.0026, Figure B3A). This was also associated with increased inter-litter timing (Mixed effects analysis factor genotype p<0.0001, factor litter number p=0.0032, Figure B3B). Despite increased inter-litter timing, pdKO body weight measured over an 8-week period matched that of the wild types (Figure B3C). At the termination of the 6-month breeding trial, n=3 mice per genotype were collected for analyses. These mice did not display any significant differences in body, uterine, or ovarian weight at the time of

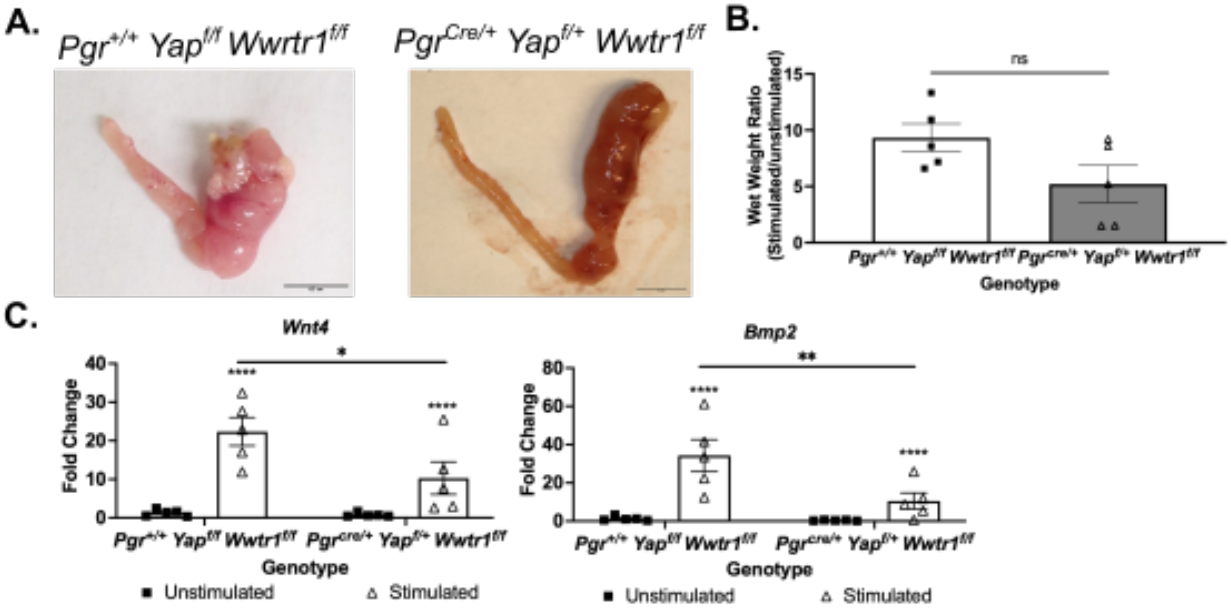

Figure 17. Loss of *Yap1* and *Wwtr1* compromises the decidualization response. **A.** Representative micrographs of unstimulated (left) and stimulated (right) uterine horns 5 days after artificial decidualization induction. **B.** Uterine wet weight ratio of stimulated over unstimulated horn after 5 days of artificial decidualization. **C.** mRNA fold change of decidualization markers *Wnt4* and *Bmp2* 5 days after artificial decidualization induction.

collection (not shown), and no alterations in reproductive tract structure were observed grossly nor with histological analyses (Figure B2C).

Yap1-Wwtr1 partial double knockout females exhibit decreased decidualization response

Artificial decidualization was maintained for 5 days, and then uteri were collected for analysis. Representative images show unstimulated (left) and stimulated (right) horns for floxed controls and pdKOs (Figure 17A). The uterine wet weight ratio of stimulated to unstimulated horn was not different in the pdKO group compared to controls (Figure 17B). However, mRNA expression of decidualization response genes, *Wnt4* and *Bmp2*, indicated a blunted decidualization response in the stimulated uterine horns of pdKOs compared to controls (Two-way ANOVA p=0.04 *Wnt4*, and p=0.006 *Bmp2*, Figure 17C).

Loss of Yap1 and Wwtr1 leads to incomplete pregnancy failure

Pregnancy was assessed in control and pdKO mice at various time points including implantation (4.5dpc, n=6-8), post-implantation (5.5dpc, n=6-10), early pregnancy (7.5dpc, n=5-7), placentation initiation (9.5dpc, n=5-7), and post-placentation (12.5dpc, n=8-10) (Figure 18A-B). The gross morphology of the uteri was normal at all time points except 12.5dpc when pdKO mice exhibited many resorption sites (Figure 18A). Quantification of normal implantation sites, when assessed by blue dye reaction, revealed variance in phenotype. At 4.5dpc, the time of implantation, pdKO females were split with 50% of mice with positive implantation sites with blue dye injection and 50% of mice without positive implantation sites (Figure 18B). However, by 5.5dpc, most pdKO females had positive implantation sites with numbers comparable to controls (Figure 18B). At 7.5dpc and 9.5dpc, the number of mice with positive implantation sites decreased to ~40%, with ~60% not having positive implantation sites at 9.5dpc (Figure 18B). At

12.5dpc, embryonic loss was evident with visually identifiable resorption sites (Figure 18B). In addition, across all time points measured, pdKO females exhibited a higher likelihood of being not pregnant compared to controls (33% of individuals, Fisher's exact test $p<0.0001$, Figure 18C).

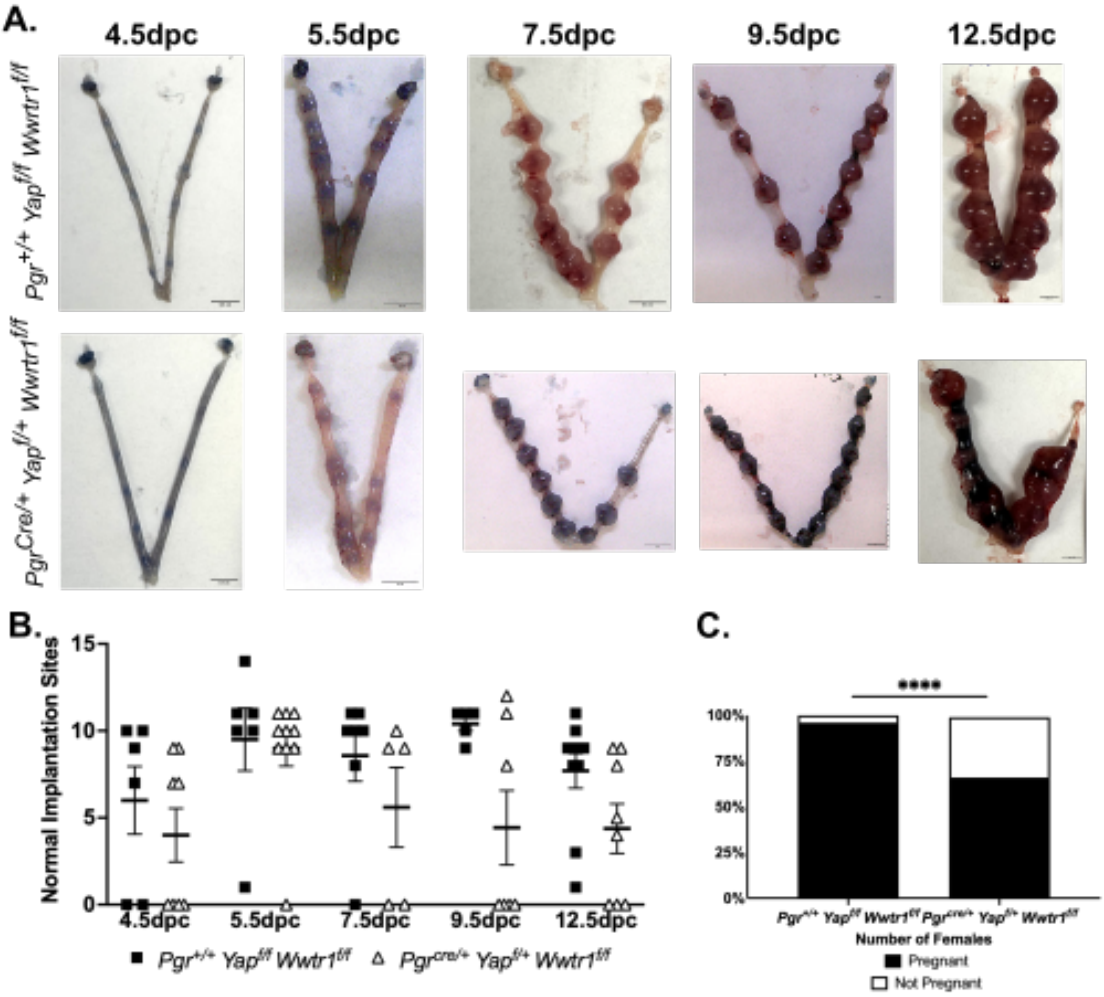

Figure 18. pdKOs exhibit fetal loss at 12.5dpc. A. Representative micrographs of control (top panel) and pdKO (bottom panel) uteri at various stages of pregnancy. Scale bars = 0.5cm. **B.** Quantification of normal implantation sites across pregnancy in both control and pdKO mice (Mixed-effects model comparison genotype $p=0.0154$). **C.** pdKO females exhibit a higher rate of nonpregnancy compared to controls across all timepoints collected (Fisher's Exact Test, $p=0.0058$).

pdKOs display modest interruptions in embryo transport

Determination of the cause of pregnancy failure prompted the investigation into ovulation and fertilization rates and embryo transport. Post-fertilization at 1.5dpc, when

all ovulated oocytes should be in the oviducts, we noted comparable numbers of unfertilized oocytes (UFO) and 2-cell embryos in pdKOs and controls (Figure 19A). However, at 3.5dpc, the time of embryo entry into the uterus, we noted the emergence of two mutually exclusive groups: pdKO females with embryos found only within the oviducts and pdKO females with embryos found only within the uterus (Figure 19B-C). The total

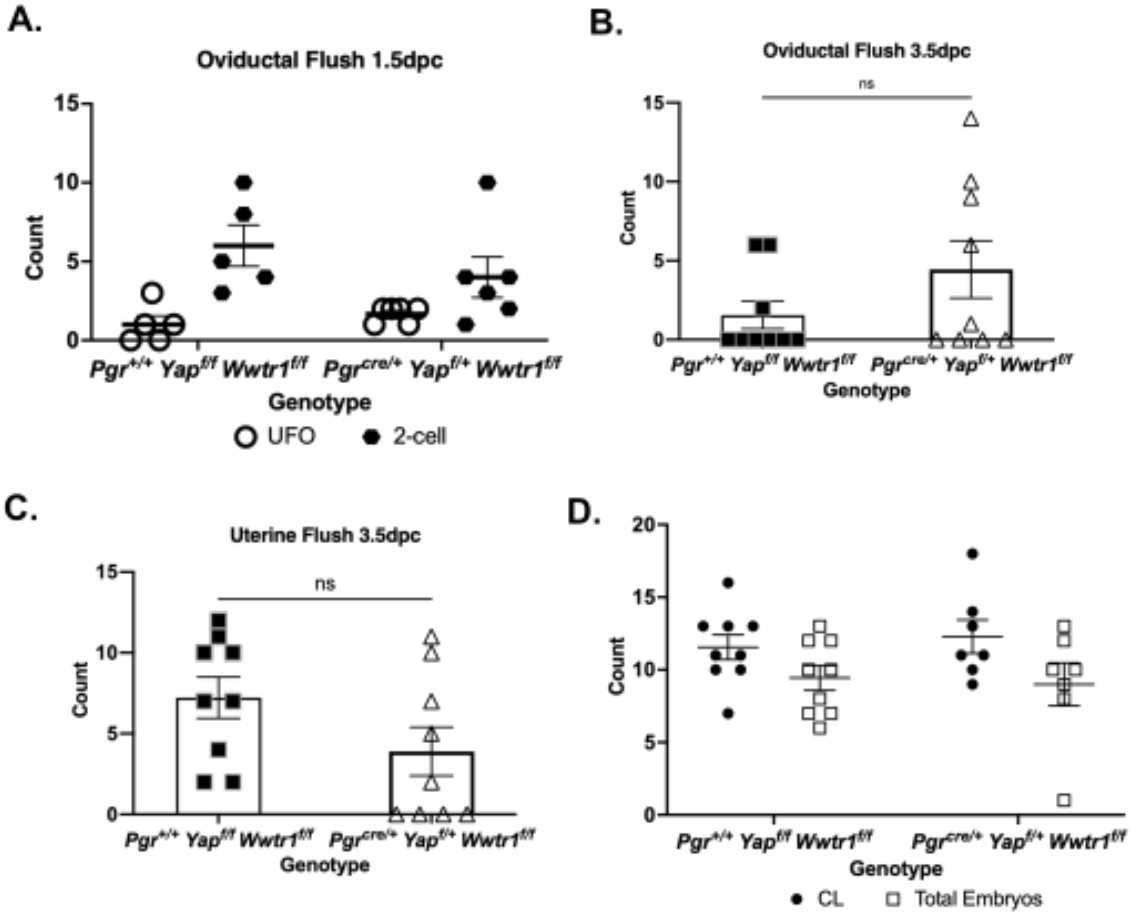

Figure 19. pdKOs females have delayed uterine embryo entry. A. Quantity of unfertilized oocytes (UFO) and 2-cell embryos flushed from oviducts at 1.5dpc from floxed controls and pdKOs. **B.** Total embryos flushed from oviducts of floxed controls and pdKOs at 3.5dpc. **C.** Total embryos flushed from uteri of floxed controls and pdKOs at 3.5dpc. **D.** Total corpus lutea (CL) and embryos flushed at 3.5dpc.

number of visual corpus lutea did not differ between pdKOs and controls, nor did the total number of embryos flushed at 3.5dpc (Figure 19D). In addition, visualization of oviducts indicated appropriate folding patterns (Figure B4A)[106]. Individual uteri were imaged utilizing tissue clearing to allow visualization of embryos using the whole-mount

immunofluorescent protocol. Embryos found within pdKO uteri at 3.5dpc were 50% of the quantity found within control uteri (Figure B4B and B4C).

pdKOs exhibit altered maternal endometrial receptivity

To disseminate the cause of delayed embryo entry into the maternal endometrium combined with partially delayed implantation and to rationalize delayed embryonic development, we investigated endometrial receptivity at 3.5dpc (Figure 20). The

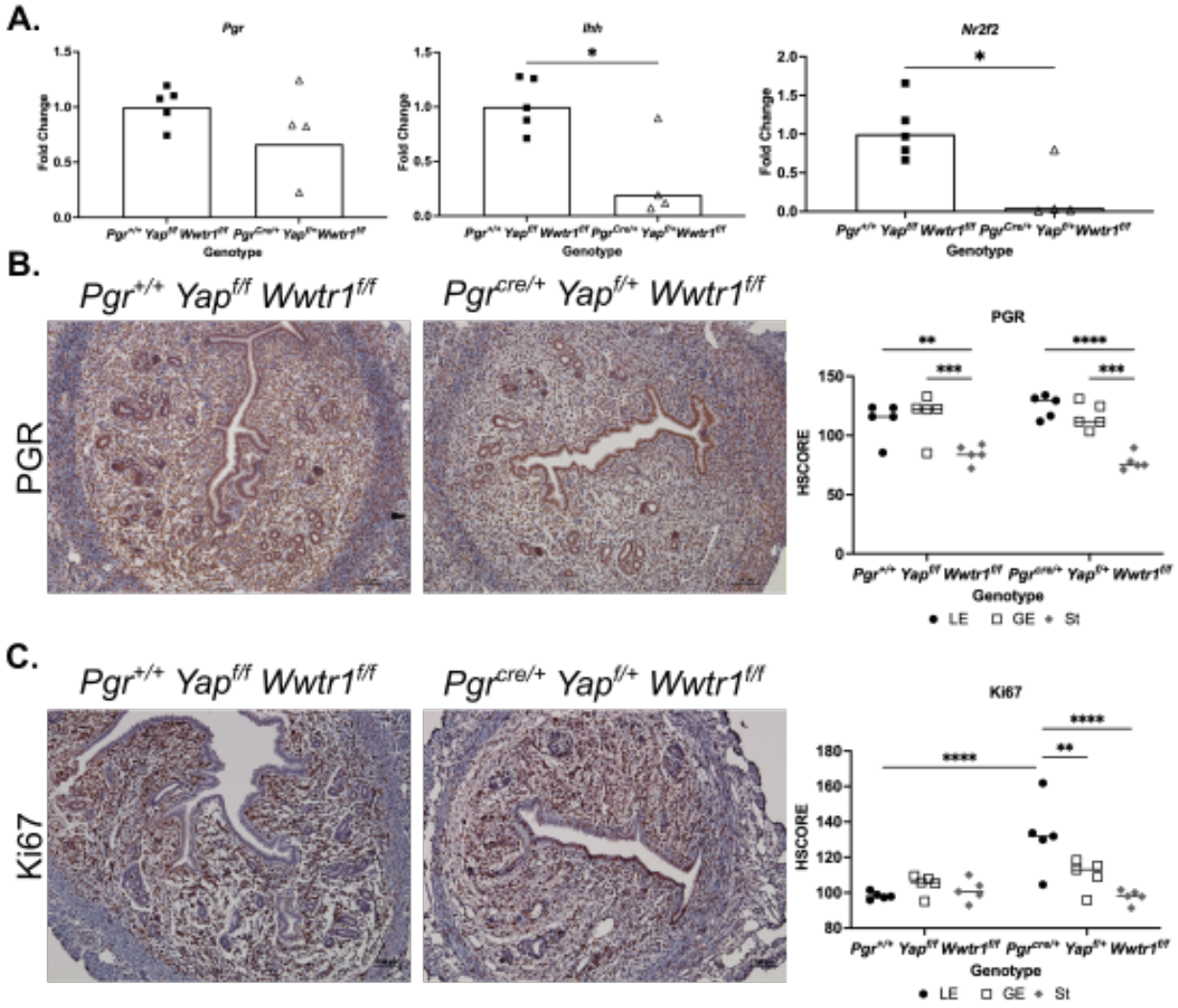

Figure 20. *Yap1* and *Wwtr1* are required for appropriate endometrial receptivity. **A.** mRNA relative fold change of *Pgr* and two target genes *Ihh* and *Nr2f2* at 3.5dpc in whole uteri of controls and pdKOs. **B.** Immunohistochemical staining for PGR and semi-quantitative H-CORE of DAB signal in control and pdKO uteri at 3.5dpc. **C.** Immunohistochemical staining for Ki67 and semiquantitative HSCORE of DAB signal at 3.5dpc in control and pdKO uteri.

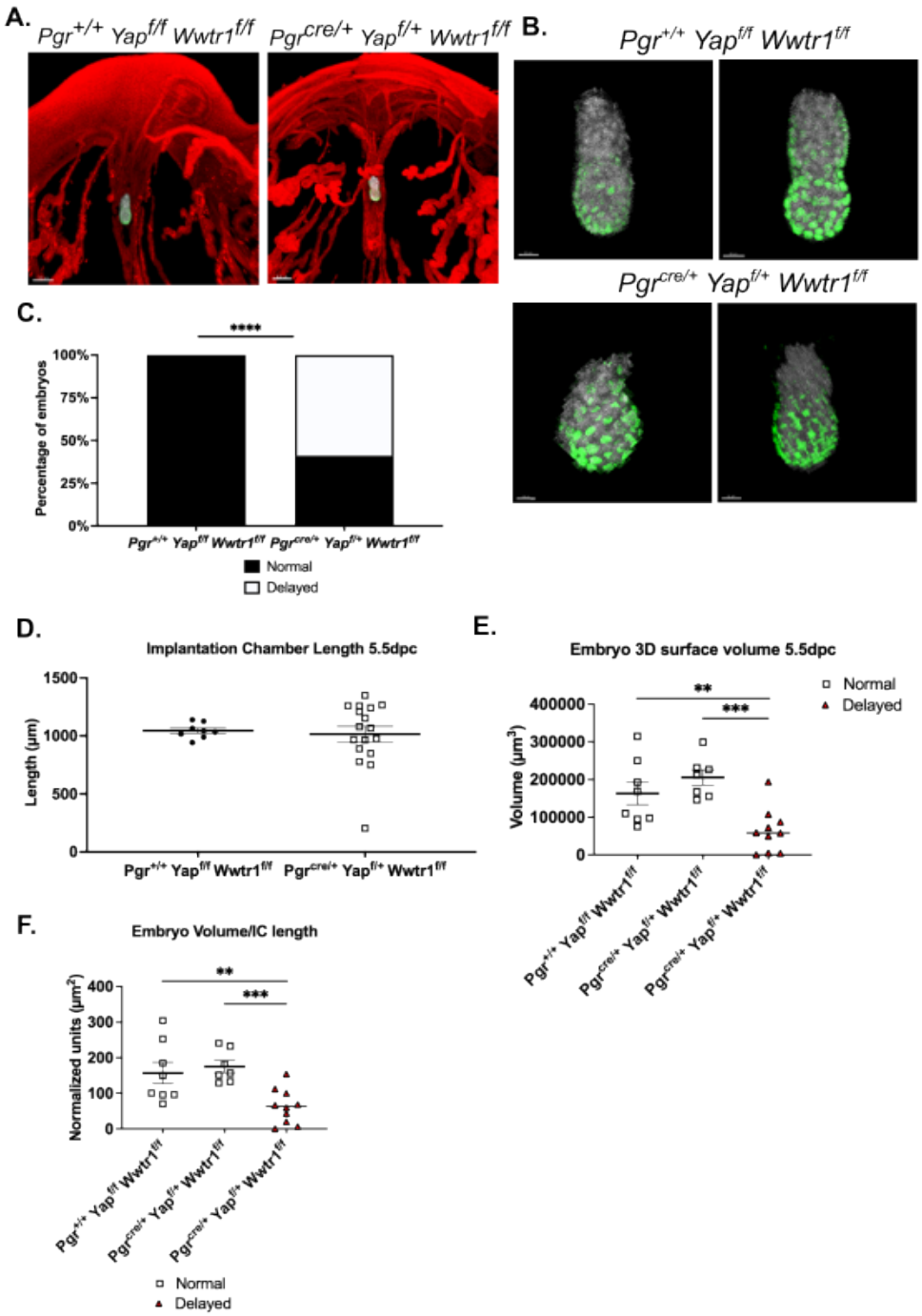

Figure 21. Loss of *Yap1* and *Wwtr1* in maternal endometrium induces delayed embryonic development. A. Representative micrographs of whole mount uterine imaging of individual implantation chambers and embryos at 5.5dpc (red=E-cadherin, white=Hoechst, Green=FOXA2). **B.** Representative embryos from controls and pdKOs at 5.5dpc (white=Hoechst, Green=FOXA2). **C.** Quantification of normal and delayed embryos imaged at 5.5dpc. **D.** Plotted implantation chamber length for controls and pdKOs at 5.5dpc. **E.** 3D embryo surface volume of normal and delayed embryos at 5.5dpc. **F.** Ratio of embryo volume to respective implantation chamber length for normal and delayed embryos at 5.5dpc.

progesterone receptor expression by both mRNA and protein was not altered in pdKO uteri at 3.5dpc (Figure 20A and B). However, we noted significantly decreased target gene expression, *Ihh,* and *Nr2f2*, in 3.5dpc uteri (unpaired t-test, $p<0.01$, Figure 20A). In addition, luminal epithelial expression of proliferation marker Ki67 was maintained in pdKO uteri (Figure 20C). Interestingly, estrogen receptor signaling decreased in pdKOs compared to controls at 3.5dpc (Unpaired t-test, $p<0.03$, Figure B5).

pdKO uteri contain embryos exhibiting delayed development

Implantation chamber morphology was notably normal when visualized with whole uterine imaging at 5.5dpc (Figure 21A). However, pdKO uteri contained embryos that morphologically appeared delayed with decreased elongation compared to controls at 5.5dpc (Figure 21B). Most embryos visualized (59%) within pdKO uteri were delayed (Figure 21C). Overall, implantation chamber length was not affected despite delayed embryos being found in most implantation sites within pdKOs visualized (Figure 21D). Delayed embryos with decreased elongated morphology had 3D surface volumes significantly lower compared to normal elongated embryos found within both control and pdKO implantation sites (unpaired t-test, $p=0.01$ compared to normal control embryos and $p=0.001$ compared to normal pdKO embryos Figure 21E). Additionally, the ratio of embryo volume to implantation chamber length of those embryos that were identified as delayed was significantly decreased (unpaired t-test, $p<0.01$, Figure 21F). This finding necessitates further investigation of the factors contributing to delayed embryo development and implantation in our mouse model.

pdKOs have a unique transcriptional profile

Whole uterine cross-sections at 7.5dpc from pdKO (n=3) and floxed controls (n=4) were subjected to bulk mRNA sequencing to elucidate the transcriptional repercussions associated with the loss of Yap1 and Wwtr1 in the pregnant uterus. Samples were separated on an MDS plot based on genotype (Figure 22A). We identified 16,674 total genes after filtering and 1,785 differentially expressed genes (DEG), with 884 genes upregulated and 901 downregulated in the knockouts compared to controls (Figure 22B).

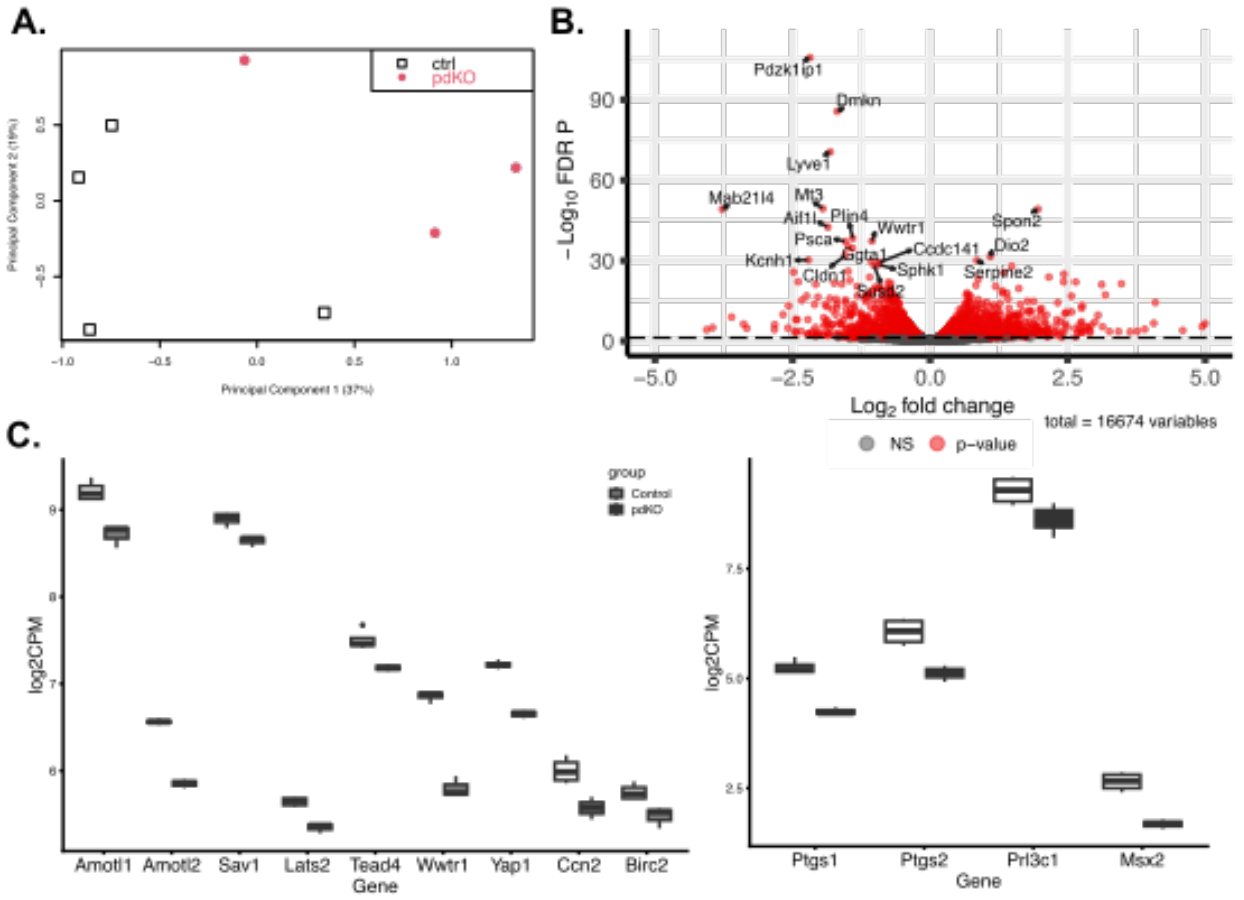

Figure 22. Transcriptional changes associated with *Yap1* and *Wwtr1* function during pregnancy. A. MDS plot of all uteri samples sequenced at 7.5dpc for controls and pdKOs. **B.** Volcano plot of all genes identified with significantly differentially expressed genes shown in red. **C.** Log2CPM values of significantly differentially expressed Hippo signaling genes and decidualization associated genes in pdKO uteri compared to controls. **D.** Normalized exon 3 (floxed or excised exon) counts for *Yap1* and *Wwtr1* in control and pdKO uteri. **E.** GO cellular component enrichment for all DEG. **F.** Enrichment of upregulated DEG for Disease RGD terms.

Figure 22 (cont'd)

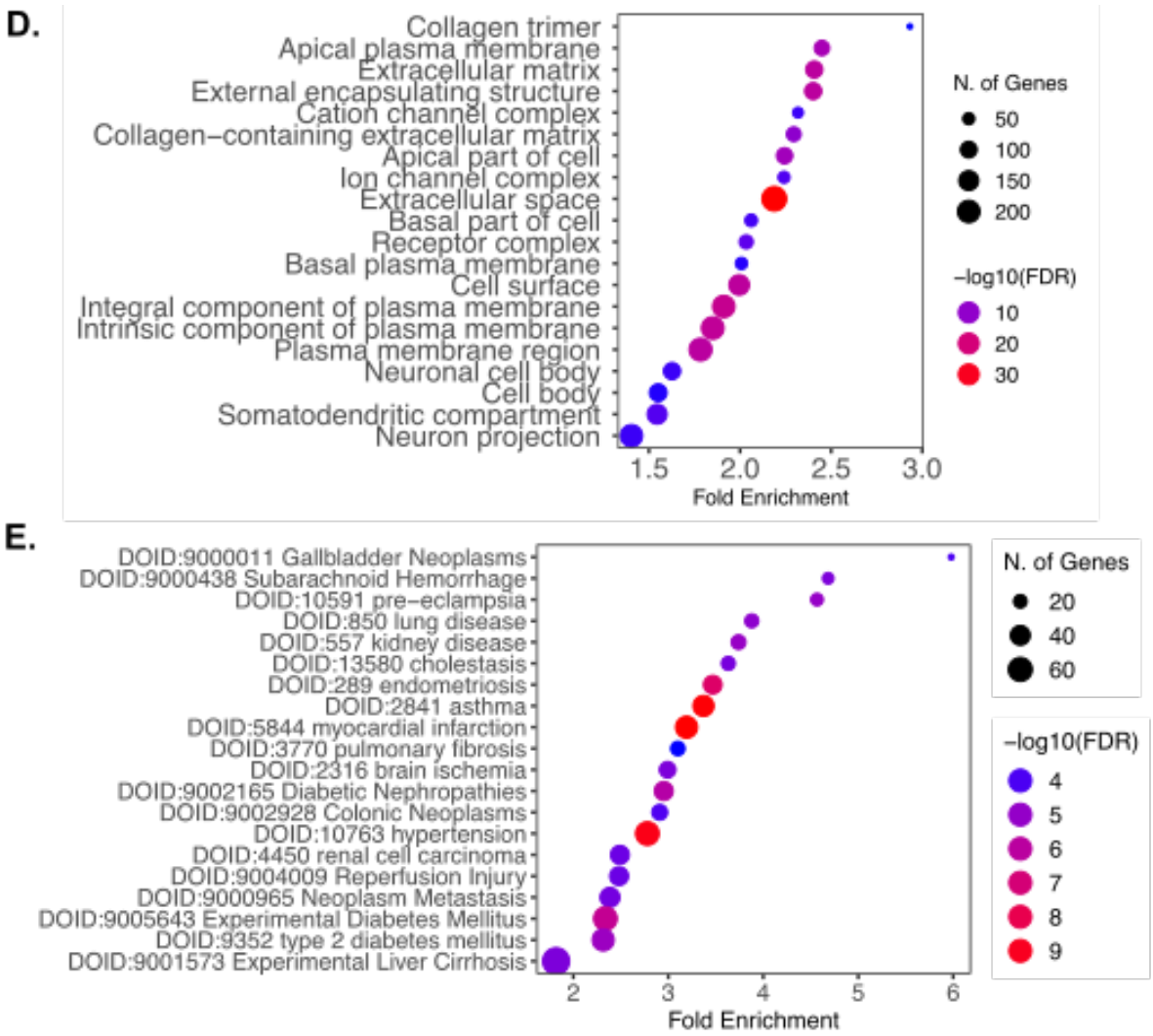

Differentially expressed genes (DEG) included eight genes from the Hippo signaling pathway including upstream regulators (Amotl1 and Amotl2), kinases (Sav1 and Lats2), transcription factor (Tead4), transcriptional effectors (Yap1 and Wwtr1), and target genes (Ccn2 and Birc5) (Figure 22C). Decreased differentially expressed genes also included four decidualization response genes (Figure 22D). DEG contributed to Gene Ontology Cellular Component terms like extracellular matrix, collagen trimer, and collagen-containing extracellular matrix, indicating that loss of Yap1 and Wwtr1 affected genes involved in cellular structure (Figure 22E). In addition, upregulated genes were enriched

for Rat Genome Database (RGD) disease terms like pre-eclampsia, endometriosis, liver cirrhosis, and pulmonary fibrosis, indicating that pdKO uteri were enriched for genes connected with reproductive diseases associated with pregnancy loss and fibrosis, which has classically been associated with Hippo signaling (Figure 22F).

4.4 Discussion

The deficient uterine receptivity and dysregulation of hormonal signals within the pdKO females is interesting (Figure 23). However, the interplay between the Hippo signaling pathway and the hormonal response has been observed before. The functional kinases of the Hippo kinase cascade, serine/threonine kinase 3 and 4 (Stk3/4), have been shown to be differentially expressed throughout the murine estrous cycle primarily under the control of estrogen signaling[107]. Indeed, YAP1 expression is also differentially regulated throughout the murine estrous cycle, with its level being highest during estrous and diestrus[73]. Importantly, estrus in female mice is when ovulation occurs, and 3 days later is when the window of receptivity begins suggesting that YAP1 is present and may play a role in hormone response during this period. In addition to the cyclical presence of YAP1 as well as activation of the Hippo signaling pathway, the function of this pathway has also been associated with hormonal action. In disease states like breast cancer and endometriosis, YAP1 bound to TEAD transcription factors can induce transcription of *ESR1,* or alternatively, in endometriosis, YAP1 can regulate upstream factors that influence *PGR* expression [108, 109]. These reports support an indirect method of hormonal control and interpretation of the signal, but it is possible within the canonical function of YAP1/WWTR1 as transcriptional coactivators that they could play a direct role in hormone receptor function. In one study, YAP/TEAD complexes bound to ESR1

enhancer regions and estrogen response elements [110]. We propose that within our model, it is possible that the loss of *Yap1/Wwtr1* and subsequent binding to TEADs, prevents the acquisition and activation of distal estrogen and progesterone receptor response elements and enhancer recruiters. This would explain why the loss of *Yap1/Wwtr1* during the receptive window leads to a failure of PGR and ESR1-regulated genes to be activated despite appropriate expression of receptor levels during this time (Figure 23). The mechanistic aspect of this hypothesis remains to be tested but opens a path for novel roles of YAP1/WWTR1 function within the murine uterus.

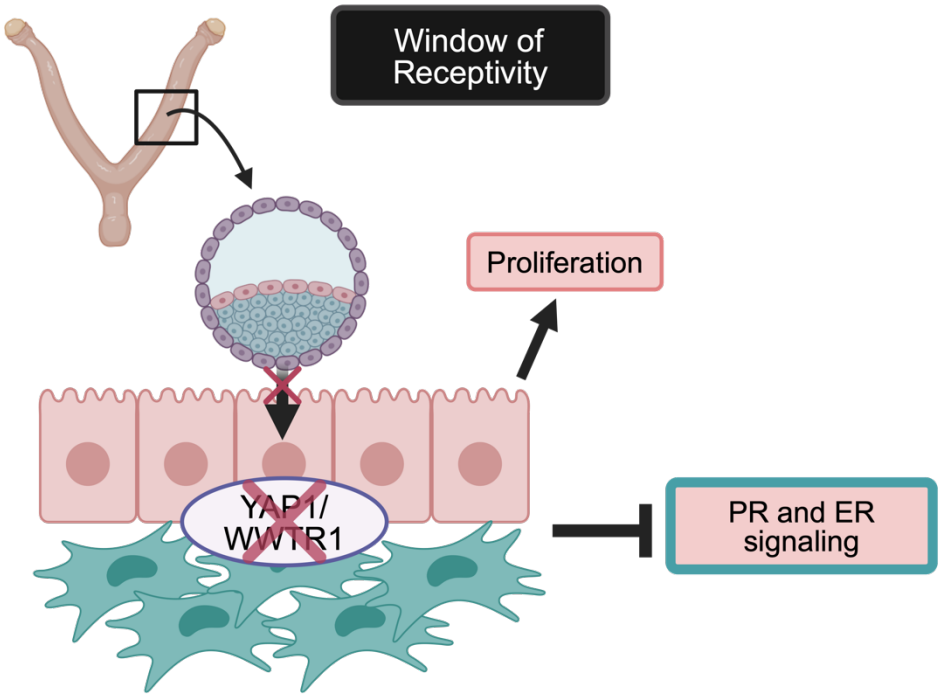

Figure 23. Summary Figure. YAP and WWTR1 are required for Progesterone and Estrogen receptor (PR and ER) signaling during the window of receptivity. Blastocyst attachment is delayed likely due to maintained proliferation in the luminal epithelium. In addition, loss of YAP1 and WWTR1 in both the endometrial epithelium and stroma leads to suppressed ER and PR signaling compromising pregnancy initiation.

We showed that depletion of *Yap1* and *Wwtr1* led to a lack of decidualization response and maternal remodeling. YAP1 and WWTR1 are classically noted to respond to extracellular changes in stiffness transduced through the Hippo signaling pathway and

decidualization and pregnancy processes, which rely on appropriate extracellular changes to alter the maternal endometrial environment[63]. They also classically regulate the transcription of extracellular and structural component genes in addition to cell cycle regulatory genes[63]. Unsurprisingly, the loss of Yap1/Wwtr1 led to the enrichment of DEG in GO Cellular Component terms like plasma membrane, collagen-containing matrix, and extracellular matrix (Table A8). Within the upregulated and downregulated DEG of the bulk mRNA sequencing, specific classes of genes included extracellular matrix genes such as collagens, CCNs, laminins, and extracellular remodeling genes like matrix metalloproteases (Tables A8 and A9). However, differential gene expression analysis of whole tissue makes it difficult to determine whether altered wound healing or fibrosis occurs in the pdKO females. Given the phenotypic data that show a progressive loss of fertility in the pdKO females, it is likely that either aberrant wound repair mechanisms or increased scarring and associated fibrosis are occurring. Both wound healing and fibrosis-associated markers were found within the DEG at 7.5dpc, including the decrease of angiogenic markers *Vegfc*, *Vegfb*, increased *Pdgfrb*, and increased expression of *Il13ra1* and *Il4ra1*. Angiogenesis is associated with wound healing but is negatively associated with fibrosis[111]. These results suggest that loss of *Yap1*/*Wwtr1* leads to decreased wound healing during pregnancy through the downregulation of proangiogenic factors. However, vasculature responds to a lack of angiogenic signal by upregulating receptor expression on the vascular smooth muscle[111]. In addition, IL13RA1 forms a heteromeric complex with IL4RA and activation of this receptor complex is widely considered pro-fibrotic, supporting that the pdKO uteri may be exhibiting increased fibrosis[111]. Indeed, pathway enrichment for upregulated DEG in Disease

RGD included disease terms for fibrotic diseases like pulmonary fibrosis and liver cirrhosis (Figure 22E and Tables A6 and A7). It is likely that loss of *Yap1/Wwtr1* contributes to both a lack of wound healing and increased fibrosis within the murine uterus during pregnancy and this contributes to the repetitive pregnancy loss seen within the pdKO females.

The incomplete penetrance of phenotype in the pdKO females can be attributed to a lack of recombination of one *Yap1* allele. Both *Progesterone receptor* and *Yap1* are located on chromosome 9 in mice with *Pgr* being located at 8899834-8968612 bp on the sense strand and *Yap1* being located at 7932000-8004597 bp on the antisense strand (Mgi). Both *Pgr* and *Yap1* are located at 2.46cM and due to the basics of recombination efficiency, the likelihood of recombination for these two genes is nearly 0%. Unfortunately, this contributes to the only possible genotype being *Pgr Cre* on the sense strand and one deleted allele of *Yap1* on the antisense strand within any given *Pgr* expressing cell within the murine uterus. The proximity of these genes led to the partiality of the double knockout and the lack of complete phenotype. Despite the incomplete penetrance of phenotype, we observed significant differences in pdKO females compared to controls, which compromised fertility. It is likely that complete conditional uterine knockout of *Yap1* combined with *Wwtr1* would lead to a much more severe effect, including fully compromised decidualization and fertility due to a lack of maternal remodeling. Currently, we are working to generate cell type-specific knockouts to determine the endometrial compartmental contributions of total *Yap1* and *Wwtr1* knockout.

CHAPTER V: DISCUSSION AND FUTURE DIRECTIONS

5.1 Coordinate roles of NOTCH and HIPPO signaling beyond female reproduction

Molecular mechanisms governing female fertility are varied but include several ubiquitous pathways like NOTCH and HIPPO signaling. NOTCH signaling, as previously shown, is involved in maternal preparation of pregnancy during decidualization and implantation (reviewed in [82]). Separately, the HIPPO signaling pathway is also implicated in decidualization and we show its involvement in preparing the endometrium for pregnancy [75, 76, 112]. These two pathways not only are involved in similar reproductive functions but serve coordinating roles in other tissues. For example, in stem cells, YAP/WWTR1 and Notch signaling activation are required to maintain colonic stem cell crypts through a shared upstream regulator, Claudin-7[113]. In addition to serving coordinate roles in a variety of tissues, there are also reports of crosstalk between the NOTCH and HIPPO signaling pathways. During liver development, YAP was shown to transcriptionally regulate *Notch2* expression and NOTCH signaling was separately shown as a potential target of YAP in hepatocytes[114, 115]. In another report, YAP and NICD bind cooperatively to RBPJ and TEAD bound DNA to induce transcription of target genes, specifically the NOTCH ligand *Jagged2*, in neural crest cells[116]. Furthermore, in the adult liver, YAP/WWTR1 activation is directly correlated with positive feedback of NOTCH signaling activation contributing to hepatocellular carcinoma pathogenesis[117]. These studies offer insights into the potential crosstalk of these two pathways in the uterus and provide an avenue of future investigation.

In addition, both the NOTCH and HIPPO signaling pathways are known to communicate with immune signaling. In fact, conditional knockout of *Rbpj* in the female

murine reproductive tract led to recurrent pregnancy failure caused by a dysregulated immune environment in the uterus[59]. Specifically, nodules were evident in multiparous *Rbpj* knockout females indicating lack of uterine repair. The investigators noted that these knockout females had failed postpartum repair due to increased macrophage recruitment and activation by IFNγ[59]. In addition to uterine specific mechanisms, NOTCH signaling is also implicated in immune cell development in the spleen and thymus[118]. The ubiquitous nature of this pathway makes it both interesting and complicated to investigate and particularly challenging when generating mouse models. Another ubiquitous pathway, the HIPPO signaling pathway, has been connected to regulation of macrophage recruitment and activation in cardiac tissue following myocardial injury[119]. Similarly to the NOTCH signaling pathway, the HIPPO signaling pathway is also implicated in lymphocyte differentiation and regulation[120]. A novel avenue within the murine reproductive tract would be to investigate the regulation of immune response, particularly in post-partum repair and pregnancy establishment, by the NOTCH and HIPPO signaling pathways. Utilizing previously published models, RNA sequencing combined with immune flow cytometry panels could easily be accomplished to understand the molecular and functional repercussions of loss of NOTCH and/or HIPPO signaling factors.

While our studies did not indicate direct interaction of HIPPO and NOTCH signaling in the endometrium, we think this would be an innovative area for future studies. Both HIPPO and NOTCH signaling have been shown to regulate processes critical to female fertility, are present during similar temporal windows during pregnancy establishment, and serve to regulate similar processes like proliferation and differentiation. In addition, both pathways significantly affect hormonal signaling, which has the potential to have profound

effects on fertility. Finally, further investigation into how alterations in the YAP/WWTR1 and the HIPPO signaling pathway leads to infertility or contributes to infertility in diseases such as like endometriosis is another timely investigation that warrants further effort. We propose these two pathways as a major nexus in female fertility and suggest future studies into their roles and potential for therapeutic intervention to combat infertility.

Specific future directions include investigating the crosstalk and potential regulation of the HIPPO and NOTCH signaling pathways within the female reproductive tract. Utilizing the models that have already been published in coordinated experiments would help to uncover some of these potential roles. Specifically, generating a stromal knockout of *Yap1*, *Wwtr1*, and *Notch1* or *Rbpj* in combination followed by phenotypic characterization would help determine if there are cooperative roles of these pathways in decidualization. Unfortunately, a good stromal *Cre* has not been generated but many researchers are working toward this goal. Following the characterization of these models, molecular analyses including chromatin immunoprecipitation and fluorescent in situ hybridization of uteri could help determine if there are direct regulatory roles of either the HIPPO signaling pathway on the NOTCH signaling pathway and the reverse. These connections, if uncovered, would help inform women's health through identifying basic reproductive mechanisms. In addition, investigation into whether the HIPPO signaling pathway contributes to disease pathogenesis in fertility impairing gynecologic maladies like endometriosis, adenomyosis, or recurrent pregnancy failure is another possible direction. Given that the NOTCH signaling pathway contributes to endometriosis pathology, this would be another potential area of investigation of crosstalk amongst these two pathways in a diseased state.

The NOTCH and HIPPO signaling pathways are ubiquitous throughout mammalian systems, tissues, and cells. These pathways likely play key roles in many different tissues including within the female reproductive tract even beyond what has been investigated to date. These pathways offer many molecules to be investigated in the context of reproductive function including interplay amongst the two pathways.

5.2 Mechanical transduction of female reproductive events

The female reproductive tract and in particular the uterus is structurally very flexible. This is required to adapt to changing abdominal pressure and of course to internal changes within the uterus itself. Some of these changes throughout the menstrual and estrous cycles include changes in fluid accumulation and entry and exit of internal objects like ovulated oocytes within the oviductal ampulla, or an implanting and growing embryo in the maternal endometrium and uterine lumen. At a cellular level, the cells in the reproductive tract must adapt to these changes in tension from either external or internal sources to keep the tissue itself intact. Evidence of mechanical alterations in the uterus in response to a variety of factors is overwhelming. Studies from our laboratory and many others have investigated the plasticity and specific molecular effects of mechanical modulation within the endometrium.

Specific changes within the endometrial extracellular and intracellular matrix have been associated with pregnancy initiation and specifically endometrial stromal cell decidualization. Alpha Smooth muscle actin was noted to appear at the time of implantation within the stromal layers during early pregnancy in a baboon model[121]. While ASMA was present during pregnancy, Smooth muscle myosin was shown to increase in response to estrogen and progesterone treatment concordant with the luteal

phase specifically in glandular epithelium or in the luminal epithelium in non-implantation sites in early pregnancy. These results were particularly interesting because both ASMA and SMM are considered myofibroblast markers, but they were present in decidualized epithelioid-like cells and in the epithelium, neither of which are considered myofibroblasts. The expression of these factors is likely related to transitory changes in cellular structure and identity that are associated with preparation and change of the maternal endometrium. Studies have also shown that alterations in intracellular tension and extracellular matrix has significant effects on decidualization. Baboon stromal cells were isolated and cultured then treated with cytoskeleton disrupting chemicals to investigate whether actin or microtubule structure were required for endometrial stromal cell decidualization *in vitro*[122]. Disruption of microtubules did not sufficiently affect decidualization response. However, treatment with Cytochalasin D, an inhibitor of actin polymerization, combined with cAMP induced significant levels of IGFBP1 secretion[122]. Classically, cAMP is not sufficient to induce decidualization on its own suggesting that alteration of the stromal cell cytoskeleton was sufficient to induce decidualization response. Indeed, our laboratory has recently replicated these results independent of cAMP signaling in primary human endometrial stromal cells indicating that altering the actin structure is sufficient to induce decidualization (unpublished). In addition, a regulator of actin, Cofilin, was shown to be differentially localized throughout the baboon menstrual cycle[123]. They showed that during the proliferative phase under estrogen dominance, Cofilin localized to the apical pole of the luminal epithelium where it is phosphorylated and inactive while during the progesterone dominated secretory phase, it is localized basally where it potentially regulates actin dynamics to prepare for implantation[123].

These studies highlight the importance of matrix remodeling in the context of endometrial stromal cell decidualization but molecular mechanisms that regulate these changes are not well understood. We suggest a future investigation into mechanotransduction pathways, like the HIPPO signaling pathway, as one potential area.

The HIPPO signaling pathway is known to regulate many extracellular matrix and plasma membrane specific genes like CCN1, CCN2, AMOTs and AMOTLs, ADAMTS, and LMNB, amongst others. In addition to regulating these structural and cell identity related genes, the HIPPO signaling pathway acts as a mechanosensory such that it senses and responds to changes in the tension of the extracellular matrix environment that are transduced into the cell and leads to changes in the actomyosin complexes internally[124]. Our individual and partial double knockout models of *Yap1* and *Wwtr1* showcase the importance of mechanotransduction in reproductive tract function. Previous models showed that deletion of these two factors lead to degeneration of tissue and structural components such as in the oviductal muscular layer as well as the colonic smooth muscle[68, 96]. While we did not directly observe alterations in reproductive tract structure with a *Progesterone Cre* mediated knockout, we did note alterations in processes that are related to changes in cell identity, such as decidualization, and contractility, and interruptions in embryonic transport[112]. These data related to the known roles of YAP and WWTR1 in tissue suggest that they are required for appropriate structural interpretations in the female reproductive tract such as responding to changes in tension and possibly uterine repair. Interestingly, many of the differentially expressed genes from our RNAseq point to the plasma membrane, extracellular matrix, and extracellular space and contain genes that are considered structural in nature. A recent

report also noted that YAP is a critical mediator of endometrial repair following mechanical injury[125]. This report nicely supports the recurrent pregnancy loss phenotype in our model where some individuals were only able to produce 2 litters in a 6-month breeding trial and suggests that YAP loss compromises uterine repair post-parturition. Another study indirectly showed that following injury from an NSAID, ibuprofen, YAP upregulation promoted PTGS2-PGE2 signaling and resulted in increased proliferation of endometrial cells promoting pro-repair mechanisms suggesting that YAP can be helpful for repairing or preventing damage within the uterus[126]. Indeed, in other tissues, overexpression of YAP and WWTR1 have been directly associated with pro-repair immunomodulatory mechanisms such as in cardiac tissue following myocardial infarction[119, 127]. The role of the HIPPO signaling effectors, YAP and WWTR1, in endometrial regeneration is a clear next step following our research. Previous studies point to possible immune modulation as well as regulation of proliferation and differentiation, all of which are required for post-partum repair.

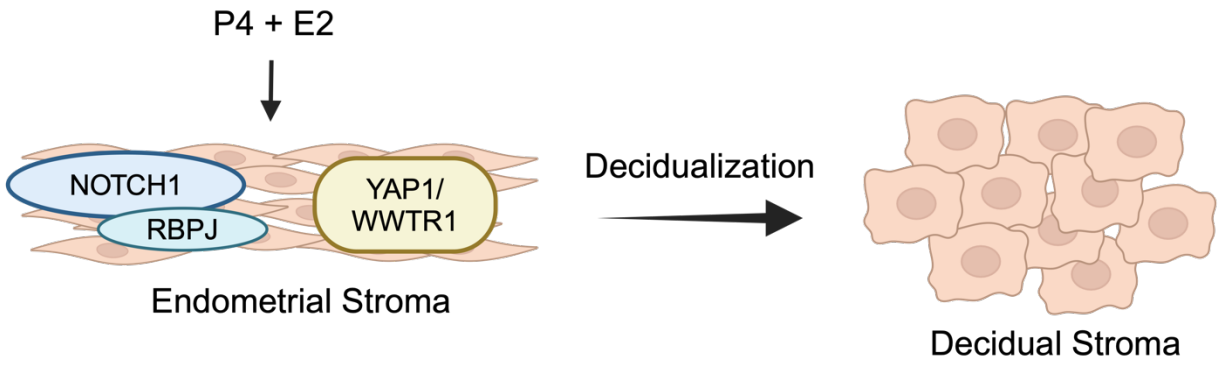

Figure 24. NOTCH1 signaling and the HIPPO effectors, YAP1 and WWTR1 are required for endometrial stromal cell decidualization initiation. Progesterone (P4) and 17β-Estradiol (E2) administration cyclically or *in vitro* initiates endometrial stromal cell decidualization mediated in part by NOTCH1, RBPJ, YAP1, and WWTR1 activation.

The work outlined within this dissertation provides insight into molecular pathways, specifically the NOTCH and HIPPO signaling pathways, contributing to endometrial

stromal cell decidualization. Principally, our work indicated that the NOTCH signaling activation through its transcriptional effector, RBPJ, is required for endometrial stromal cell decidualization initiation *in vivo* but is not required for decidualization maintenance (Figure 24). Secondly, we showed that YAP1 and WWTR1 likely serve both individual and redundant roles in decidualization as well as successful pregnancy (Figure 24). These key discoveries have enlightened basic reproductive biology and have posed an opportunity to investigate whether signaling in these pathways goes awry in patients experiencing infertility. While this research has uncovered the basic mechanisms that contribute to decidualization, many questions related to the specific molecular intricacies that guide these responses remain undiscovered. For example, the upstream regulators of the NOTCH signaling pathway in the context of decidualization remain an important unanswered question. In addition, how the HIPPO signaling pathway contributes to the decidualization response beyond potential transcriptional regulation of hormone response also remains unanswered. In addition, how the individual factors within each of these pathways, ligands, receptors, transcriptional effectors, contribute canonically and noncanonically to decidualization remain open avenues for future investigations.

REFERENCES

1. Jones, R.E. and K.H. Lopez, *Human reproductive biology*. 2014, Elsevier/AP, Academic Press is an imprint of Elsevier,: Amsterdam ; Boston. p. xi, 381 pages.

2. Croy, B.A., et al., *The guide to investigation of mouse pregnancy*. 2014, Elsevier/Academic Press,: Amsterdam. p. xx, 808 pages.

3. Masuda, H., et al., *A novel marker of human endometrial mesenchymal stem-like cells.* Cell Transplant, 2012. **21**(10): p. 2201-14.

4. Kopan, R., *Notch signaling.* Cold Spring Harb Perspect Biol, 2012. **4**(10).

5. Yu, F.X. and K.L. Guan, *The Hippo pathway: regulators and regulations.* Genes Dev, 2013. **27**(4): p. 355-71.

6. D'Souza, B., L. Meloty-Kapella, and G. Weinmaster, *Canonical and Non-Canonical Notch Ligands*, in *Notch Signaling*. 2010. p. 73-129.

7. Aster, J.C., W.S. Pear, and S.C. Blacklow, *The Varied Roles of Notch in Cancer.* Annu Rev Pathol, 2017. **12**: p. 245-275.

8. McIntyre, B., T. Asahara, and C. Alev, *Overview of Basic Mechanisms of Notch Signaling in Development and Disease.* Adv Exp Med Biol, 2020. **1227**: p. 9-27.

9. Su, R.W. and A.T. Fazleabas, *Implantation and Establishment of Pregnancy in Human and Nonhuman Primates.* Adv Anat Embryol Cell Biol, 2015. **216**: p. 189-213.

10. Murta, D., et al., *Dynamics of Notch signalling in the mouse oviduct and uterus during the oestrous cycle.* Reprod Fertil Dev, 2015.

11. Afshar, Y., L. Miele, and A.T. Fazleabas, *Notch1 is regulated by chorionic gonadotropin and progesterone in endometrial stromal cells and modulates decidualization in primates.* Endocrinology, 2012. **153**(6): p. 2884-96.

12. Fazleabas, A.T., et al., *Modulation of the baboon (Papio anubis) uterine endometrium by chorionic gonadotrophin during the period of uterine receptivity.* Proc Natl Acad Sci U S A, 1999. **96**(5): p. 2543-8.

13. Strug, M.R., et al., *Intrauterine human chorionic gonadotropin infusion in oocyte donors promotes endometrial synchrony and induction of early decidual markers for stromal survival: a randomized clinical trial.* Hum Reprod, 2016. **31**(7): p. 1552-61.

14. Caliceti, C., et al., *17beta-estradiol enhances signalling mediated by VEGF-A-delta-like ligand 4-notch1 axis in human endothelial cells.* PLoS One, 2013. **8**(8): p. e71440.

15. Rizzo, P., et al., *Targeting Notch signaling cross-talk with estrogen receptor and ErbB-2 in breast cancer.* Adv Enzyme Regul, 2009. **49**(1): p. 134-41.

16. Hao, L., et al., *Notch-1 activates estrogen receptor-alpha-dependent transcription via IKKalpha in breast cancer cells.* Oncogene, 2010. **29**(2): p. 201-13.

17. Wei, Y., et al., *Nuclear estrogen receptor-mediated Notch signaling and GPR30-mediated PI3K/AKT signaling in the regulation of endometrial cancer cell proliferation.* Oncol Rep, 2012. **27**(2): p. 504-10.

18. Chang, Y.H., D.C. Ding, and T.Y. Chu, *Estradiol and Progesterone Induced Differentiation and Increased Stemness Gene Expression of Human Fallopian Tube Epithelial Cells.* J Cancer, 2019. **10**(13): p. 3028-3036.

19. Cobellis, L., et al., *The pattern of expression of Notch protein members in normal and pathological endometrium.* J Anat, 2008. **213**(4): p. 464-72.

20. Vanorny, D.A. and K.E. Mayo, *The role of Notch signaling in the mammalian ovary.* Reproduction, 2017. **153**(6): p. R187-R204.

21. Vanorny, D.A., et al., *Notch signaling regulates ovarian follicle formation and coordinates follicular growth.* Mol Endocrinol, 2014. **28**(4): p. 499-511.

22. Prasasya, R.D. and K.E. Mayo, *Notch Signaling Regulates Differentiation and Steroidogenesis in Female Mouse Ovarian Granulosa Cells.* Endocrinology, 2018. **159**(1): p. 184-198.

23. Terauchi, K.J., et al., *Role of Notch signaling in granulosa cell proliferation and polyovular follicle induction during folliculogenesis in mouse ovary.* Cell Tissue Res, 2016. **365**(1): p. 197-208.

24. Rochette, M.J. and M.P. Murphy, *Gamma-secretase: substrates and inhibitors.* Mol Neurobiol, 2002. **26**(1): p. 81-95.

25. Hubbard, N., R.D. Prasasya, and K.E. Mayo, *Activation of Notch Signaling by Oocytes and Jag1 in Mouse Ovarian Granulosa Cells.* Endocrinology, 2019. **160**(12): p. 2863-2876.

26. Afshar, Y., et al., *Notch1 mediates uterine stromal differentiation and is critical for complete decidualization in the mouse.* FASEB J, 2012. **26**(1): p. 282-94.

27. Su, R.W., et al., *Decreased Notch pathway signaling in the endometrium of women with endometriosis impairs decidualization.* J Clin Endocrinol Metab, 2015. **100**(3): p. E433-42.

28. Wu, Y., et al., *Notch1 is crucial for decidualization and maintaining the first pregnancy in the mouse.* Biol Reprod, 2021. **104**(3): p. 539-547.

29. Su, R.W., et al., *Aberrant activation of canonical Notch1 signaling in the mouse uterus decreases progesterone receptor by hypermethylation and leads to infertility.* Proc Natl Acad Sci U S A, 2016. **113**(8): p. 2300-5.

30. Strug, M.R., et al., *The Notch Family Transcription Factor, RBPJkappa, Modulates Glucose Transporter and Ovarian Steroid Hormone Receptor Expression During Decidualization.* Reprod Sci, 2018: p. 1933719118799209.

31. Otti, G.R., et al., *Notch2 controls prolactin and insulin-like growth factor binding protein-1 expression in decidualizing human stromal cells of early pregnancy.* PLoS One, 2014. **9**(11): p. e112723.

32. Yang, Y., et al., *poFUT1 promotes endometrial decidualization by enhancing the O-fucosylation of Notch1.* EBioMedicine, 2019. **44**: p. 563-573.

33. Shawber, C.J., et al., *Vascular Notch proteins and Notch signaling in the peri-implantation mouse uterus.* Vasc Cell, 2015. **7**: p. 9.

34. Marchetto, N.M., et al., *Endothelial Jagged1 Antagonizes Dll4/Notch Signaling in Decidual Angiogenesis during Early Mouse Pregnancy.* Int J Mol Sci, 2020. **21**(18).

35. Cuman, C., et al., *Fetal-maternal communication: the role of Notch signalling in embryo implantation.* Reproduction, 2014. **147**(3): p. R75-86.

36. Cuman, C., et al., *Preimplantation human blastocysts release factors that differentially alter human endometrial epithelial cell adhesion and gene expression relative to IVF success.* Hum Reprod, 2013. **28**(5): p. 1161-71.

37. Zhang, S., et al., *Uterine Rbpj is required for embryonic-uterine orientation and decidual remodeling via Notch pathway-independent and -dependent mechanisms.* Cell Res, 2014. **24**(8): p. 925-42.

38. Levin, H.I., et al., *Dynamic maternal and fetal Notch activity and expression in placentation.* Placenta, 2017. **55**: p. 5-12.

39. Haider, S., J. Pollheimer, and M. Knofler, *Notch signalling in placental development and gestational diseases.* Placenta, 2017. **56**: p. 65-72.

40. Lu, J., et al., *Spatiotemporal coordination of trophoblast and allantoic Rbpj signaling directs normal placental morphogenesis.* Cell Death Dis, 2019. **10**(6): p. 438.

41. Escobar-Morreale, H.F., *Polycystic ovary syndrome: definition, aetiology, diagnosis and treatment.* Nat Rev Endocrinol, 2018. **14**(5): p. 270-284.

42. Amjadi, F., et al., *Comparative evaluation of NOTCH signaling molecules in the endometrium of women with various gynecological diseases during the window of implantation.* Iran J Basic Med Sci, 2019. **22**(4): p. 426-431.

43. Yang, D., et al., *Identification of Potential Biomarkers of Polycystic Ovary Syndrome via Integrated Bioinformatics Analysis.* Reprod Sci, 2020.

44. Giudice, L.C. and L.C. Kao, *Endometriosis.* Lancet, 2004. **364**(9447): p. 1789-99.

45. Buzzio, O.L., et al., *FOXO1A differentially regulates genes of decidualization.* Endocrinology, 2006. **147**(8): p. 3870-6.

46. Kim, J.J., et al., *Role of FOXO1A in the regulation of insulin-like growth factor-binding protein-1 in human endometrial cells: interaction with progesterone receptor.* Biol Reprod, 2005. **73**(4): p. 833-9.

47. Kim, J.J. and A.T. Fazleabas, *Uterine receptivity and implantation: the regulation and action of insulin-like growth factor binding protein-1 (IGFBP-1), HOXA10 and forkhead transcription factor-1 (FOXO-1) in the baboon endometrium.* Reprod Biol Endocrinol, 2004. **2**: p. 34.

48. Park, Y., et al., *Cis-Regulatory Evolution of Forkhead Box O1 (FOXO1), a Terminal Selector Gene for Decidual Stromal Cell Identity.* Mol Biol Evol, 2016. **33**(12): p. 3161-3169.

49. Van Sinderen, M., et al., *Localisation of the Notch family in the human endometrium of fertile and infertile women.* J Mol Histol, 2014. **45**(6): p. 697-706.

50. Korbel, C., et al., *Notch signaling controls sprouting angiogenesis of endometriotic lesions.* Angiogenesis, 2018. **21**(1): p. 37-46.

51. Brown, D.M., et al., *Notch-1 Signaling Activation and Progesterone Receptor Expression in Ectopic Lesions of Women With Endometriosis.* J Endocr Soc, 2018. **2**(7): p. 765-778.

52. Gonzalez-Foruria, I., et al., *Dysregulation of the ADAM17/Notch signalling pathways in endometriosis: from oxidative stress to fibrosis.* Mol Hum Reprod, 2017. **23**(7): p. 488-499.

53. Song, Y., et al., *Interleukin-6 (IL-6) Activates the NOTCH1 Signaling Pathway Through E-Proteins in Endometriotic Lesions.* J Clin Endocrinol Metab, 2020. **105**(5).

54. Taran, F.A., E.A. Stewart, and S. Brucker, *Adenomyosis: Epidemiology, Risk Factors, Clinical Phenotype and Surgical and Interventional Alternatives to Hysterectomy.* Geburtshilfe Frauenheilkd, 2013. **73**(9): p. 924-931.

55. Qi, S., et al., *Aberrant expression of Notch1/numb/snail signaling, an epithelial mesenchymal transition related pathway, in adenomyosis.* Reprod Biol Endocrinol, 2015. **13**: p. 96.

56. Steegers, E.A., et al., *Pre-eclampsia.* Lancet, 2010. **376**(9741): p. 631-44.

57. Cobellis, L., et al., *Distribution of Notch protein members in normal and preeclampsia-complicated placentas.* Cell Tissue Res, 2007. **330**(3): p. 527-34.

58. Hunkapiller, N.M., et al., *A role for Notch signaling in trophoblast endovascular invasion and in the pathogenesis of pre-eclampsia.* Development, 2011. **138**(14): p. 2987-98.

59. Strug, M.R., et al., *RBPJ mediates uterine repair in the mouse and is reduced in women with recurrent pregnancy loss.* FASEB J, 2018. **32**(5): p. 2452-2466.

60. Jonusiene, V. and A. Sasnauskiene, *Notch and Endometrial Cancer.* Adv Exp Med Biol, 2021. **1287**: p. 47-57.

61. Suzuki, T., et al., *Imbalanced expression of TAN-1 and human Notch4 in endometrial cancers.* Int J Oncol, 2000. **17**(6): p. 1131-9.

62. Pillidge, Z. and S.J. Bray, *SWI/SNF chromatin remodeling controls Notch-responsive enhancer accessibility.* EMBO Rep, 2019. **20**(5).

63. Totaro, A., T. Panciera, and S. Piccolo, *YAP/TAZ upstream signals and downstream responses.* Nat Cell Biol, 2018. **20**(8): p. 888-899.

64. Piccolo, S., S. Dupont, and M. Cordenonsi, *The biology of YAP/TAZ: hippo signaling and beyond.* Physiol Rev, 2014. **94**(4): p. 1287-312.

65. Lau, L.F. and S.C. Lam, *The CCN family of angiogenic regulators: the integrin connection.* Exp Cell Res, 1999. **248**(1): p. 44-57.

66. Lv, X., et al., *Timely expression and activation of YAP1 in granulosa cells is essential for ovarian follicle development.* FASEB J, 2019. **33**(9): p. 10049-10064.

67. Xin, M., et al., *Hippo pathway effector Yap promotes cardiac regeneration.* Proc Natl Acad Sci U S A, 2013. **110**(34): p. 13839-44.

68. Godin, P., et al., *YAP and TAZ are required for the postnatal development and the maintenance of the structural integrity of the oviduct.* Reproduction, 2020. **160**(2): p. 307-318.

69. Sun, T., M.E. Pepling, and F.J. Diaz, *Lats1 Deletion Causes Increased Germ Cell Apoptosis and Follicular Cysts in Mouse Ovaries.* Biol Reprod, 2015. **93**(1): p. 22.

70. Jamin, S.P., et al., *Requirement of Bmpr1a for Mullerian duct regression during male sexual development.* Nat Genet, 2002. **32**(3): p. 408-10.

71. Jorgez, C.J., et al., *Granulosa cell-specific inactivation of follistatin causes female fertility defects.* Mol Endocrinol, 2004. **18**(4): p. 953-67.

72. St-Jean, G., et al., *Lats1 and Lats2 are required for the maintenance of multipotency in the Mullerian duct mesenchyme.* Development, 2019. **146**(20).

73. Moon, S., et al., *Estrogen Regulates the Expression and Localization of YAP in the Uterus of Mice.* Int J Mol Sci, 2022. **23**(17).

74. Golal, E., et al., *The investigation of hippo signaling pathway in mouse uterus during peri-implantation period.* Arch Gynecol Obstet, 2023. **307**(6): p. 1795-1809.

75. Chen, H., et al., *YAP mediates human decidualization of the uterine endometrial stromal cells.* Placenta, 2017. **53**: p. 30-35.

76. Strakova, Z., J. Reed, and I. Ihnatovych, *Human transcriptional coactivator with PDZ-binding motif (TAZ) is downregulated during decidualization.* Biol Reprod, 2010. **82**(6): p. 1112-8.

77. Ochoa-Bernal, M.A. and A.T. Fazleabas, *Physiologic Events of Embryo Implantation and Decidualization in Human and Non-Human Primates.* Int J Mol Sci, 2020. **21**(6).

78. Gellersen, B. and J.J. Brosens, *Cyclic decidualization of the human endometrium in reproductive health and failure.* Endocr Rev, 2014. **35**(6): p. 851-905.

79. Ramathal, C.Y., et al., *Endometrial decidualization: of mice and men.* Semin Reprod Med, 2010. **28**(1): p. 17-26.

80. Miele, L., *Notch signaling.* Clin Cancer Res, 2006. **12**(4): p. 1074-9.

81. Kopan, R. and M.X. Ilagan, *The canonical Notch signaling pathway: unfolding the activation mechanism.* Cell, 2009. **137**(2): p. 216-33.

82. Moldovan, G.E., L. Miele, and A.T. Fazleabas, *Notch signaling in reproduction.* Trends Endocrinol Metab, 2021.

83. Strakova, Z., et al., *Multipotent properties of myofibroblast cells derived from human placenta.* Cell Tissue Res, 2008. **332**(3): p. 479-88.

84. Daikoku, T., et al., *Lactoferrin-iCre: a new mouse line to study uterine epithelial gene function.* Endocrinology, 2014. **155**(7): p. 2718-24.

85. Dickson, M.J., et al., *Inserting Cre recombinase into the Prolactin 8a2 gene for decidua-specific recombination in mice.* Genesis, 2022. **60**(4-5): p. e23473.

86. Han, H., et al., *Inducible gene knockout of transcription factor recombination signal binding protein-J reveals its essential role in T versus B lineage decision.* Int Immunol, 2002. **14**(6): p. 637-45.

87. Alam, S.M., T. Konno, and M.J. Soares, *Identification of target genes for a prolactin family paralog in mouse decidua.* Reproduction, 2015. **149**(6): p. 625-32.

88. Afshar, Y.R., *The of Notch1 in Endometrial Receptivity and Decidualization*, in *Physiology and Biophysics*. 2012, University of Illinois at Chicago: Chicago, Illinois. p. 282.

89. Dickson, M.J., et al., *Inserting Cre Recombinase into the Prolactin 8a2 gene for Decidua-Specific recombination in Mice.* bioRxiv, 2022: p. 2022.01.28.478238.

90. Marquardt, R.M., et al., *Progesterone and Estrogen Signaling in the Endometrium: What Goes Wrong in Endometriosis?* Int J Mol Sci, 2019. **20**(15).

91. Soyal, S.M., et al., *Cre-mediated recombination in cell lineages that express the progesterone receptor.* Genesis, 2005. **41**(2): p. 58-66.

92. Xin, M., et al., *Regulation of insulin-like growth factor signaling by Yap governs cardiomyocyte proliferation and embryonic heart size.* Sci Signal, 2011. **4**(196): p. ra70.

93. Morin-Kensicki, E.M., et al., *Defects in yolk sac vasculogenesis, chorioallantoic fusion, and embryonic axis elongation in mice with targeted disruption of Yap65.* Mol Cell Biol, 2006. **26**(1): p. 77-87.

94. Hossain, Z., et al., *Glomerulocystic kidney disease in mice with a targeted inactivation of Wwtr1.* Proc Natl Acad Sci U S A, 2007. **104**(5): p. 1631-6.

95. Tian, Y., et al., *TAZ promotes PC2 degradation through a SCFbeta-Trcp E3 ligase complex.* Mol Cell Biol, 2007. **27**(18): p. 6383-95.

96. Daoud, F., et al., *Inducible Deletion of YAP and TAZ in Adult Mouse Smooth Muscle Causes Rapid and Lethal Colonic Pseudo-Obstruction.* Cell Mol Gastroenterol Hepatol, 2021. **11**(2): p. 623-637.

97. Cha, J., X. Sun, and S.K. Dey, *Mechanisms of implantation: strategies for successful pregnancy.* Nat Med, 2012. **18**(12): p. 1754-67.

98. Sternberg, A.K., et al., *How Mechanical Forces Change the Human Endometrium during the Menstrual Cycle in Preparation for Embryo Implantation.* Cells, 2021. **10**(8).

99. Gellersen, B., et al., *Invasiveness of human endometrial stromal cells is promoted by decidualization and by trophoblast-derived signals.* Hum Reprod, 2010. **25**(4): p. 862-73.

100. Meng, Z., T. Moroishi, and K.L. Guan, *Mechanisms of Hippo pathway regulation.* Genes Dev, 2016. **30**(1): p. 1-17.

101. Zhang, T., et al., *Endometrial extracellular matrix rigidity and IFNtau ensure the establishment of early pregnancy through activation of YAP.* Cell Prolif, 2021. **54**(2): p. e12976.

102. Zhou, X., H. Lindsay, and M.D. Robinson, *Robustly detecting differential expression in RNA sequencing data using observation weights.* Nucleic Acids Res, 2014. **42**(11): p. e91.

103. Ge, S.X., D. Jung, and R. Yao, *ShinyGO: a graphical gene-set enrichment tool for animals and plants.* Bioinformatics, 2020. **36**(8): p. 2628-2629.

104. Arora, R., et al., *Insights from imaging the implanting embryo and the uterine environment in three dimensions.* Development, 2016. **143**(24): p. 4749-4754.

105. Valero-Pacheco, N., et al., *Maternal IL-33 critically regulates tissue remodeling and type 2 immune responses in the uterus during early pregnancy in mice.* Proc Natl Acad Sci U S A, 2022. **119**(35): p. e2123267119.

106. Harwalkar, K., et al., *Anatomical and cellular heterogeneity in the mouse oviduct-its potential roles in reproduction and preimplantation developmentdagger.* Biol Reprod, 2021. **104**(6): p. 1249-1261.

107. Moon, S., et al., *STK3/4 Expression Is Regulated in Uterine Endometrial Cells during the Estrous Cycle.* Cells, 2019. **8**(12).

108. Ma, S., et al., *Transcriptional repression of estrogen receptor alpha by YAP reveals the Hippo pathway as therapeutic target for ER(+) breast cancer.* Nat Commun, 2022. **13**(1): p. 1061.

109. Lin, S.C., et al., *Targeting YAP1 ameliorates progesterone resistance in endometriosis.* Hum Reprod, 2023. **38**(6): p. 1124-1134.

110. Zhu, C., et al., *A Non-canonical Role of YAP/TEAD Is Required for Activation of Estrogen-Regulated Enhancers in Breast Cancer.* Mol Cell, 2019. **75**(4): p. 791-806 e8.

111. Wynn, T.A., *Cellular and molecular mechanisms of fibrosis.* J Pathol, 2008. **214**(2): p. 199-210.

112. Moldovan, G.E., et al., *Yes Associated Transcriptional Regulator 1 (YAP1) and WW Domain Containing Transcription Regulator (WWTR1) are required for murine pregnancy initiation.* bioRxiv, 2024.

113. Naser, A.N., et al., *Colonic crypt stem cell functions are controlled by tight junction protein claudin-7 through Notch/Hippo signaling.* Ann N Y Acad Sci, 2024.

114. Wu, N., et al., *The Hippo signaling functions through the Notch signaling to regulate intrahepatic bile duct development in mammals.* Lab Invest, 2017. **97**(7): p. 843-853.

115. Yimlamai, D., et al., *Hippo pathway activity influences liver cell fate.* Cell, 2014. **157**(6): p. 1324-1338.

116. Manderfield, L.J., et al., *Hippo signaling is required for Notch-dependent smooth muscle differentiation of neural crest.* Development, 2015. **142**(17): p. 2962-71.

117. Kim, W., et al., *Hippo signaling interactions with Wnt/beta-catenin and Notch signaling repress liver tumorigenesis.* J Clin Invest, 2017. **127**(1): p. 137-152.

118. Radtke, F., N. Fasnacht, and H.R. Macdonald, *Notch signaling in the immune system.* Immunity, 2010. **32**(1): p. 14-27.

119. Mia, M.M., et al., *YAP/TAZ deficiency reprograms macrophage phenotype and improves infarct healing and cardiac function after myocardial infarction.* PLoS Biol, 2020. **18**(12): p. e3000941.

120. Ueda, Y., N. Kondo, and T. Kinashi, *MST1/2 Balance Immune Activation and Tolerance by Orchestrating Adhesion, Transcription, and Organelle Dynamics in Lymphocytes.* Front Immunol, 2020. **11**: p. 733.

121. Christensen, S., et al., *Smooth muscle myosin II and alpha smooth muscle actin expression in the baboon (Papio anubis) uterus is associated with glandular secretory activity and stromal cell transformation.* Biol Reprod, 1995. **53**(3): p. 598-608.

122. Kim, J.J., R.C. Jaffe, and A.T. Fazleabas, *Insulin-like growth factor binding protein-1 expression in baboon endometrial stromal cells: regulation by filamentous actin and requirement for de novo protein synthesis.* Endocrinology, 1999. **140**(2): p. 997-1004.

123. Morris, K., et al., *Cofilin and slingshot localization in the epithelium of uterine endometrium changes during the menstrual cycle and in endometriosis.* Reprod Sci, 2011. **18**(10): p. 1014-24.

124. Dupont, S., et al., *Role of YAP/TAZ in mechanotransduction.* Nature, 2011. **474**(7350): p. 179-83.

125. Zhang, T., et al., *Extracellular matrix stiffness mediates uterine repair via the Rap1a/ARHGAP35/RhoA/F-actin/YAP axis.* Cell Commun Signal, 2023. **21**(1): p. 22.

126. Wang, Q., et al., *TT-10 may elevate YAP and repair mouse uterine damage resulting from the inhibition effect of ibuprofen on COX2-PGE2 and YAP.* Toxicol Lett, 2023. **383**: p. 215-226.

127. Ramjee, V., et al., *Epicardial YAP/TAZ orchestrate an immunosuppressive response following myocardial infarction.* J Clin Invest, 2017. **127**(3): p. 899-911.

APPENDIX A: ADDITIONAL TABLES

Table A1. Antibodies used in all studies.

Antibody	Manufacturer	Catalog Number	Host Species
ESR1	Vector Laboratories	VP-E613	Mouse
P-ESR1	Abcam	Ab31477	Rabbit
Ki67	BD Biosciences	550609	Mouse
RPSUH (RBPJ)	Cell Signaling Technologies	5313	Rabbit
Anti-Rabbit IgG Biotinylated	Vector Laboratories	BA-1000	Goat
Anti-Mouse IgG Biotinylated	Vector Laboratories	BA-9200	Goat
YAP1	Cell Signaling Technology	14074	Rabbit
TAZ (WWTR1)	Cell Signaling Technology	72804	Rabbit
ER	Invitrogen	MA5-13304	Mouse
PGR	Invitrogen	MA5-14505	Rabbit
Ki67	BD Pharmigen	BD550609	Mouse
ASMA	Cell Signaling Technology	19245	Rabbit

Table A2. Primers and primer sequences used in all studies.

Gene Symbol	Species	Application	Forward	Reverse
Rpl19	Mouse	Taqman	Mm01606037_g1	
Rbpj	Mouse	Taqman	Mm01217627_g1	
Prl8A2	Mouse	qPCR	CTCATCCTGCTTGGAAAGTCCT	GGAGTGCCCCTGAGAAGTGA
18S	Mouse	qPCR	GTAACCCGTTGAACCCCATT	CCATCCAATCGGTAGTAGCG
Rplp0	Mouse	qPCR	CATCACCACGAAAATCTCCA	TTGTCAAACACCTGCTGGAT
eGFP	Eimeria acervulina	qPCR	AAGCTGACCCTGAAGTTCATCTGC	CTTGTAGTTGCCGTCGTCCTTGAA
36b4	Mouse	qPCR	CAT CAC CAC GAA AAT CTC CA	TTG TCA AAC ACC TGC TGG AT
18s	Mouse	qPCR	GTA ACC CGT TGA ACC CCA TT	CCA TCC AAT CGG TAG TAG CG
Wnt4	Mouse	qPCR	AGT GCC AAT ACC AGT TCC G	CAC ACT TCT CCA GTT CTC CAC
Bmp2	Mouse	qPCR	CGC AGC TTC CAT CAC GAA	GCT TCC TGT ATC TGT TCC CG
Ccn1	Mouse	qPCR	CCA GTG TAC AGC AGC CTA AA	CTG GAG CAT CCT GCA TAA GTA A
Areg	Mouse	qPCR	CTG AGG ACA ATG CAG GGT AAA	ATC TGG AAC CAT CCG AAA GC
Prl3c1	Mouse	qPCR	GCC ACA CGA TAT GAC CGG AA	TTT GCT CCC TCC AGA ACG AC
Yap1	Mouse	qPCR	GAA AGG GCT CTA GTG GGT AAA G	AAA TCA GGC TAA GGG AAG TAA GG
Wwtr1	Mouse	qPCR	CCA ATG CAC TGA CCA CTC A	CTC CTC TTG ACG CAT CCT AAT C
Pgr	Mouse	qPCR	TGT CAC TAT GGC GTG CTT AC	CTC CTT CAT CCT CTG CTC ATT T
Esr1	Mouse	qPCR	AAC CGC CCA TGA TCT ATT CTG	AGA TTC AAG TCC CCA AAG CC
Ccn2	Mouse	qPCR	GGG CCT CTT CTG CGA TTT C	ATC CAG GCA AGT GCA TTG GTA
Muc1	Mouse	qPCR	GCT GGT GCT GGT CTG TAT TT	CCA CAG CTG GGT TGG TAT AAG
Muc4	Mouse	qPCR	AAT GTT CCT GCC TAT ACT GCC	TTG TAT GGT TCC TGG GTC AC
Ltf	Mouse	qPCR	ATC TCT GTG CCC TGT GTA TTG	ACA TTT CCT GCC TTC TCA GC
C3	Mouse	qPCR	GTG GTC ACT CAG GGA TCT AAT G	GCT CCA ATC AGG GTG TAG TAA G
Ihh	Mouse	qPCR	CAT CTT CAA GGA CGA GGA GAA C	CGC CAG CAG TCC ATA CTT ATT
Nr2f2	Mouse	qPCR	AGG AGA GAG AGA GAG AGA GAG A	GGA AGC TGA GGG TCA GAT AAA G

Table A3. 6-month Fertility assessment of YKO females.

Genotype	n	Total Number of litters	Number of pups	Mean pups per litter	Mean litter per mouse	Mean pups per litter ± SEM	Mean litter per mouse ± SEM
$Pgr^{+/+}$ $Yap^{F/F}$	4	17	197	11.6	4.25	11.6±0.20	4.25±0.70
$Pgr^{Cre/+}$ $Yap^{F/+}$	4	12	79	6.6	3	6.6±0.0.29	3.0±1.0

Table A4. 6-month Fertility assessment of TKO females.

Genotype	n	Total Number of litters	Number of pups	Mean pups per litter	Mean litter per mouse	Mean pups per litter ± SEM	Mean litter per mouse ± SEM
$Pgr^{+/+}$ $Taz^{F/F}$	4	23	242	10.5	5.75	10.5±0.20	5.75±0.60
$Pgr^{Cre/+}$ $Taz^{F/F}$	4	13	88	6.8	3.3	6.8±0.29	3.3±0.61

Table A5. 6-month Fertility assessment of pdKO females.

Genotype	n	Total Number of litters	Number of pups	Mean pups per litter	Mean litter per mouse	Mean pups per litter ± SEM	Mean litter per mouse ± SEM
$Pgr^{+/+}$ $Yap^{F/F}$ $Taz^{F/F}$	4	27	247	9.1	6.75	9.1±0.15	6.75±0.1
$Pgr^{Cre/+}$ $Yap^{F/+}$ $Taz^{F/F}$	4	15	77	5.1	3.8	5.1±0.32	3.8±0.44

Table A6. Gene Ontology Biological Process term enrichment for upregulated DEG.

Enrichment FDR	nGenes	Pathway Genes	Fold Enrichment	Pathway
7.31456971702305e-08	50	388	2.749318562	GO:0001655 urogenital system development
5.34888089469474e-06	42	345	2.585960993	GO:0072001 renal system development
5.7949819813431e-07	56	596	2.405002098	GO:0010817 reg. of hormone levels
1.01809213452179e-09	109	1264	2.067553345	GO:0060429 epithelium development
4.17047935339575e-08	93	1063	2.031402358	GO:0009887 animal organ morphogenesis
7.97012608799304e-07	83	986	1.976343691	GO:0033993 response to lipid
5.44162346305777e-06	77	921	1.932647629	GO:0009725 response to hormone
1.93448274583305e-09	122	1444	1.931018888	GO:0007155 cell adhesion
7.40902715597227e-08	102	1136	1.923269588	GO:0035295 tube development
7.97012608799304e-07	92	1096	1.898401485	GO:0051241 negative reg. of multicellular organismal proc.
1.76047828205931e-08	122	1454	1.850944739	GO:0051094 positive reg. of developmental proc.
1.31739974190693e-08	131	1623	1.816554128	GO:0051240 positive reg. of multicellular organismal proc.
1.8295819386673e-06	113	1534	1.728180983	GO:0007267 cell-cell signaling
4.22966561210842e-07	125	1652	1.725805919	GO:0009719 response to endogenous stimulus
3.68077315894188e-07	127	1708	1.723403085	GO:0045595 reg. of cell differentiation
5.40416192746001e-06	110	1604	1.70283262	GO:0006811 ion transport
7.97012608799304e-07	128	1765	1.685284713	GO:0042127 reg. of cell population proliferation
1.66679994467691e-06	135	1913	1.635932102	GO:0040011 locomotion
2.65495056101494e-06	132	1807	1.631798276	GO:0022008 neurogenesis
5.34888089469474e-06	131	1776	1.61419188	GO:0010647 positive reg. of cell communication

Table A7. Gene Ontology Biological Process term enrichment for downregulated DEG.

Enrichment FDR	nGenes	Pathway Genes	Fold Enrichment	Pathway
0.013078838	11	77	3.467256044	GO:0044304 main axon
0.03625576	10	79	3.152050949	GO:0008076 voltage-gated potassium channel complex
0.001002348	24	222	2.725251504	GO:0034703 cation channel complex
0.004298753	22	186	2.467495099	GO:0031256 leading edge membrane
0.001211308	27	295	2.431582161	GO:0034702 ion channel complex
0.031730229	21	183	2.15685284	GO:0001726 ruffle
0.00110041	37	407	2.113844168	GO:0016324 apical plasma membrane
0.03625576	23	254	2.021555753	GO:0016323 basolateral plasma membrane
0.00110041	44	503	1.981289168	GO:0031012 extracellular matrix
0.00110041	44	505	1.976421136	GO:0030312 external encapsulating structure
0.03625576	26	304	1.916650335	GO:0045178 basal part of cell
0.003382197	41	503	1.90243075	GO:0045177 apical part of cell
0.017290194	32	363	1.899417715	GO:0031253 cell projection membrane
4.55E-05	76	992	1.845184672	GO:0009986 cell surface
0.033449674	31	373	1.834106021	GO:0062023 collagen-containing extracellular matrix
0.03625576	31	395	1.816470387	GO:0043235 receptor complex
6.18E-06	102	1714	1.762526788	GO:0005615 extracellular space
9.10E-05	99	1362	1.648367627	GO:0098590 plasma membrane region
0.001002348	85	1525	1.608655402	GO:0005887 integral component of plasma membrane
0.00291086	86	1609	1.529419274	GO:0031226 intrinsic component of plasma membrane

Table A8. Gene Ontology Cellular Component term enrichment for upregulated DEG.

Enrichment FDR	nGenes	Pathway Genes	Fold Enrichment	Pathway
1.24E-11	61	503	2.851455409	GO:0031012 extracellular matrix
1.24E-11	61	505	2.844466548	GO:0030312 external encapsulating structure
8.57E-09	47	407	2.803098336	GO:0016324 apical plasma membrane
2.83E-08	45	373	2.770672493	GO:0062023 collagen-containing extracellular matrix
5.21E-26	147	1714	2.635925367	GO:0005615 extracellular space
6.53E-09	54	503	2.607526295	GO:0045177 apical part of cell
0.003000982	21	172	2.497068584	GO:0042383 sarcolemma
0.000125196	37	395	2.256203605	GO:0043235 receptor complex
5.90E-14	113	1525	2.223223519	GO:0005887 integral component of plasma membrane
0.001583732	29	304	2.215796181	GO:0045178 basal part of cell
5.90E-14	118	1609	2.181713863	GO:0031226 intrinsic component of plasma membrane
1.10E-09	85	992	2.150464333	GO:0009986 cell surface
1.81E-05	62	725	1.940078349	GO:0043025 neuronal cell body
9.96E-10	111	1362	1.923321106	GO:0098590 plasma membrane region
1.52E-05	68	810	1.885888255	GO:0044297 cell body
2.92E-06	86	1086	1.805932078	GO:0036477 somatodendritic compartment
0.000371318	61	783	1.769119438	GO:0097447 dendritic tree
0.000621971	60	781	1.74543894	GO:0030425 dendrite
0.000123389	107	1596	1.546888629	GO:0043005 neuron projection
0.001282092	99	1500	1.484242049	GO:0045202 synapse

Table A9. Gene Ontology Cellular Component term enrichment for downregulated DEG.

Enrichment FDR	nGenes	Pathway Genes	Fold Enrichment	Pathway
0.002597182	13	65	4.24401146	GO:0006940 reg. of smooth muscle contraction
0.001968066	25	205	2.72052016	GO:0072330 monocarboxylic acid biosynthetic proc.
0.002597182	31	301	2.3614115	GO:0046394 carboxylic acid biosynthetic proc.
0.002912305	31	303	2.34189571	GO:0016053 organic acid biosynthetic proc.
0.000186667	56	541	2.07664533	GO:0001525 angiogenesis
2.87976402932549e-05	76	763	2.00205196	GO:0001944 vasculature development
0.000186667	63	637	1.97219078	GO:0048514 blood vessel morphogenesis
0.000119538	71	732	1.95778971	GO:0001568 blood vessel development
0.001968066	50	574	1.95319396	GO:0044283 small molecule biosynthetic proc.
0.001968066	52	651	1.92052236	GO:0032787 monocarboxylic acid metabolic proc.
0.001888098	69	911	1.75689525	GO:0030001 metal ion transport
0.000186667	90	1202	1.73929238	GO:0006812 cation transport
0.002597182	67	893	1.73251344	GO:0098655 cation transmembrane transport
0.000797202	79	1037	1.72966437	GO:0044255 cellular lipid metabolic proc.
0.001968066	75	954	1.69068084	GO:0032101 reg. of response to external stimulus
0.000248153	95	1160	1.68619425	GO:0072359 circulatory system development
0.001968066	76	905	1.68619425	GO:0035239 tube morphogenesis
0.000186667	104	1436	1.6766465	GO:0006629 lipid metabolic proc.
0.000839856	91	1136	1.64881317	GO:0035295 tube development
0.000619542	107	1604	1.59167032	GO:0006811 ion transport

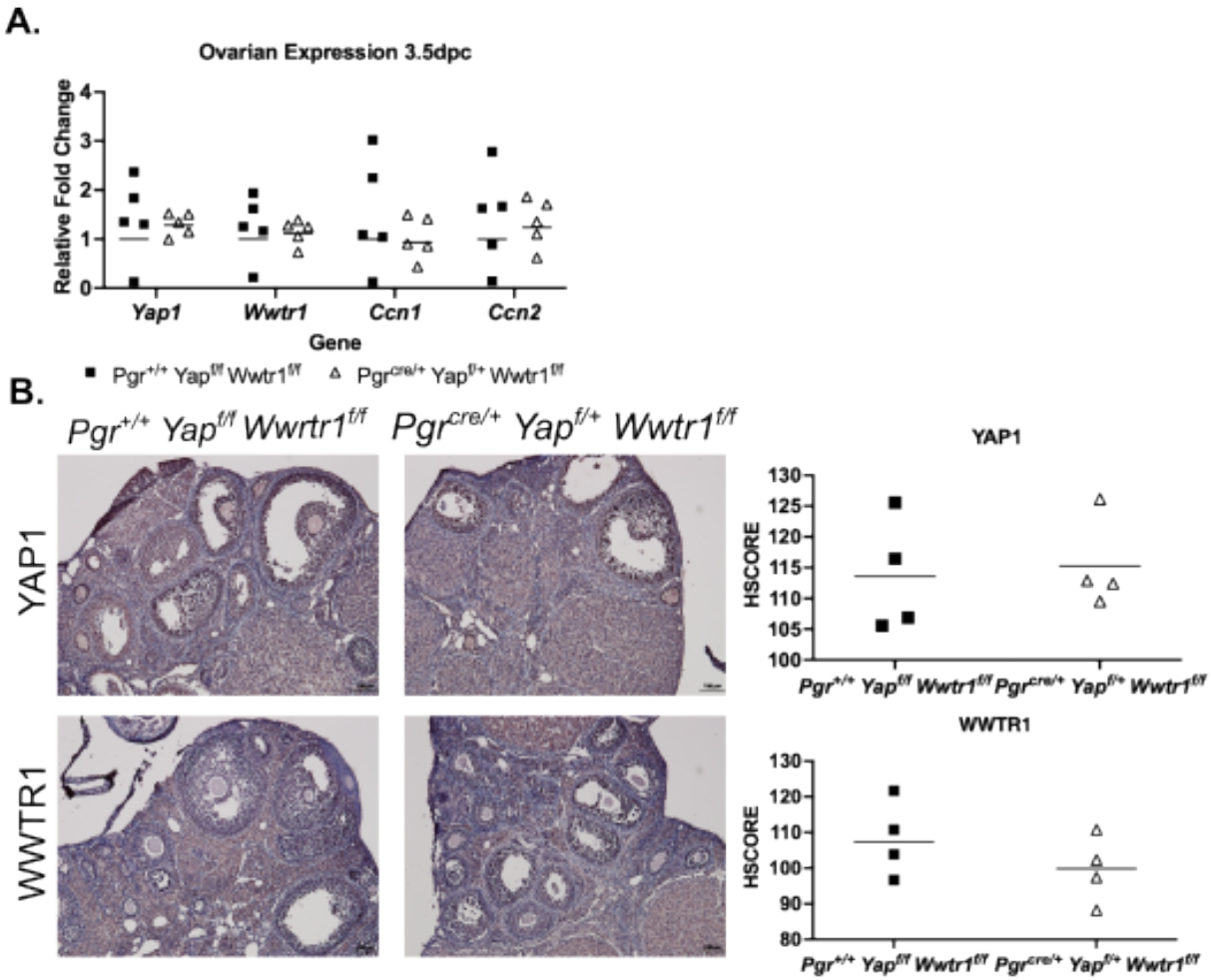

Figure B1. Analysis of ovaries from pdKO mice A. mRNA analysis of *Yap1, Wwtr1, Ccn1,* and *Ccn2* of whole ovaries collected at 3.5dpc. **B.** DNA expression of floxed alleles in pdKO and control ovaries at 3.5dpc. **C.** Immunohistochemical analysis of YAP1 and WWTR1 in ovaries at 3.5dpc and semiquantitative HSCORE.

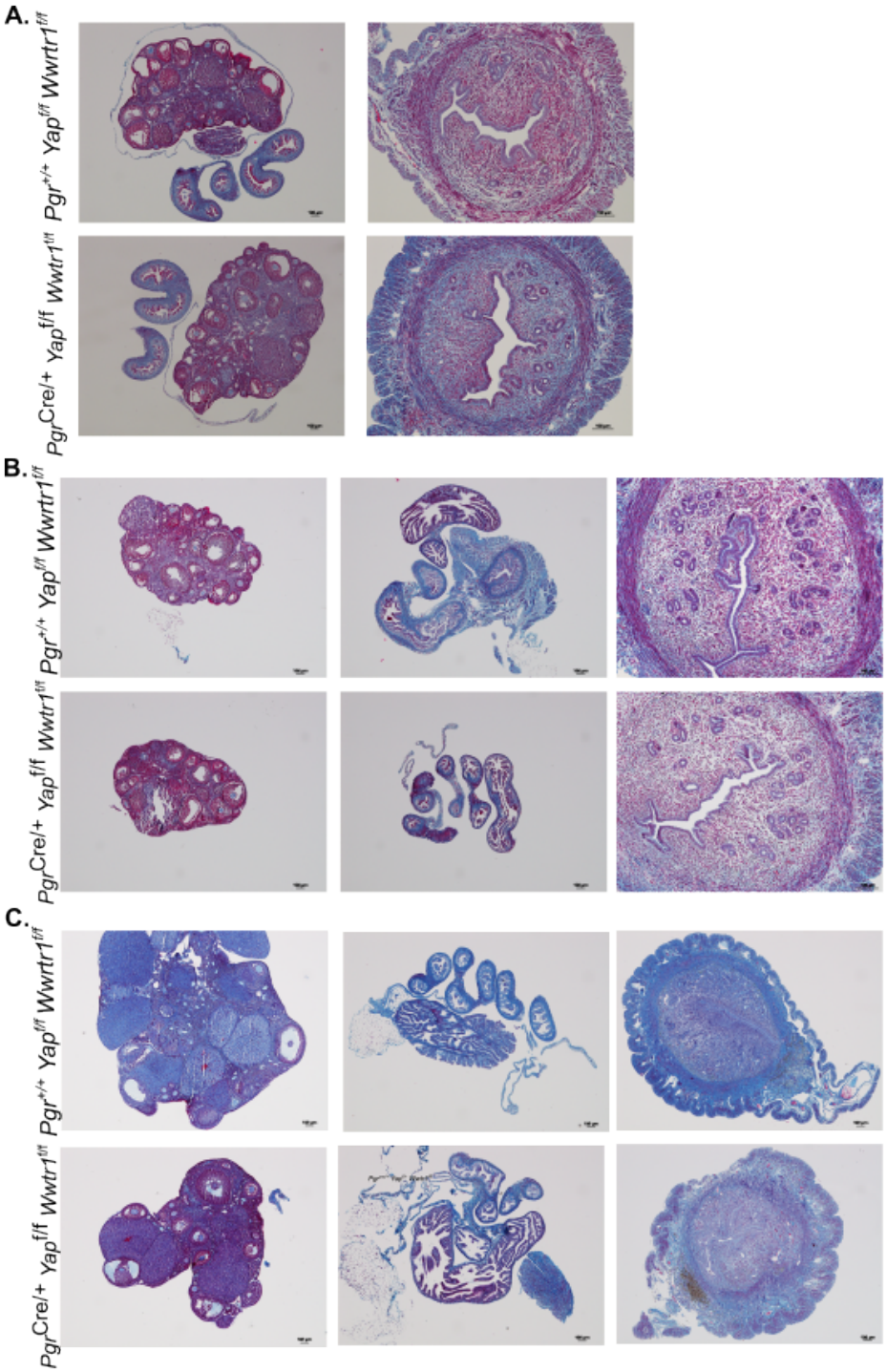

Figure B2. pdKO histoarchitechture is comparable to controls in primigravid and multigravida females. A. Representative micrographs of trichrome staining of ovaries, oviducts, and uteri of virgin females at proestrus (8 weeks of age). **B.** Representative trichrome micrographs of ovaries, oviducts, and uteri at 3.5dpc in primigravid females (8-12 weeks of age). **C.** Representative micrographs of trichrome staining of ovaries (left panel), oviducts (center panel), and uteri (right panel) from multigravida breeding trial females (8 months of age).

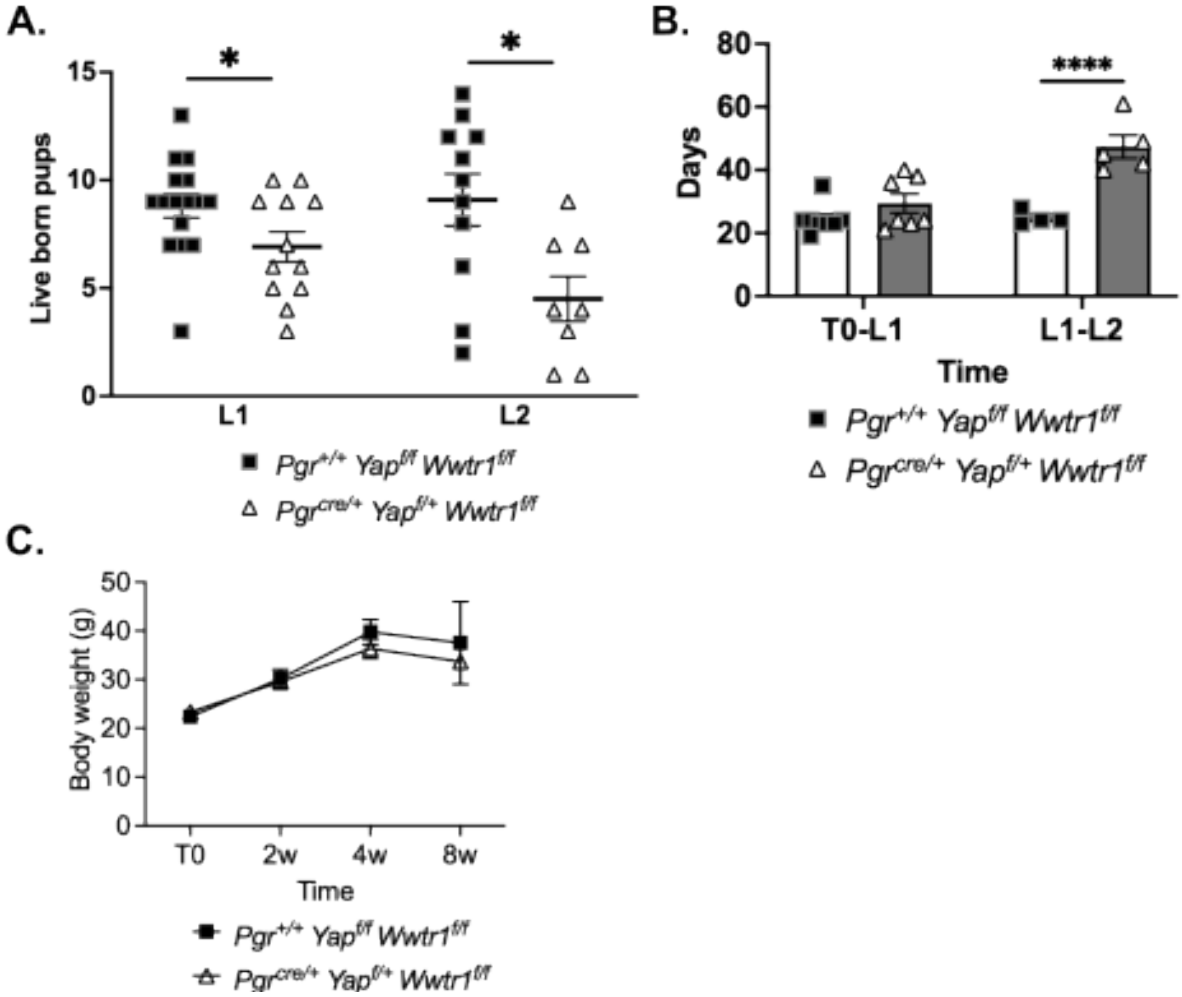

Figure B3. pdKOs exhibit increased inter-litter timing and smaller litter sizes. A. Expanded dataset showing decreased pups per litter in pdKOs compared to controls. **B.** pdKOs exhibit increased inter-litter timing. **C.** pdKOs exhibit a proportional body weight increase to controls over an 8-week period.

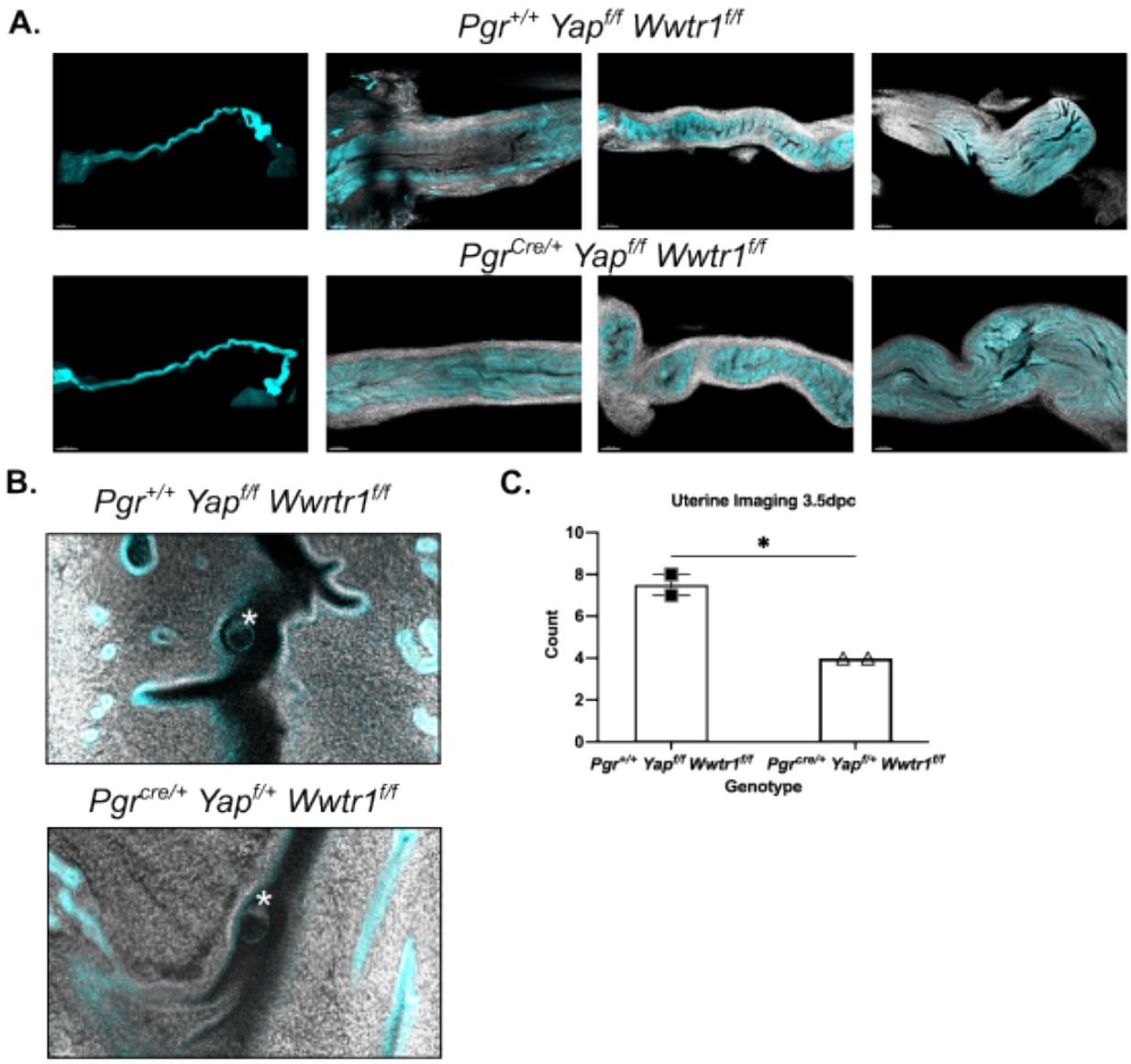

Figure B4. 3D imaging reveals normal oviductal fold patterning in pdKOs. A. Representative micrographs of fluorescent whole mount imaging of oviducts of floxed controls (top panel) and pdKOs (bottom panel) at 3.5dpc in primigravid females. Images are whole oviduct (left), longitudinal folds (left middle), transverse folds (right middle), and continuous longitudinal folds (right) (white=Hoechst, blue=E-Cadherin, n=4).**B.** Representative micrographs of fluorescent imaging of embryos (marked with adjacent asterisk) within uteri at 3.5dpc (white=Hoechst, E-cadherin=blue). **C.** Embryos counted in uterine horns at 3.5dpc with whole mount fluorescent uterine imaging (n=2 females/genotype).

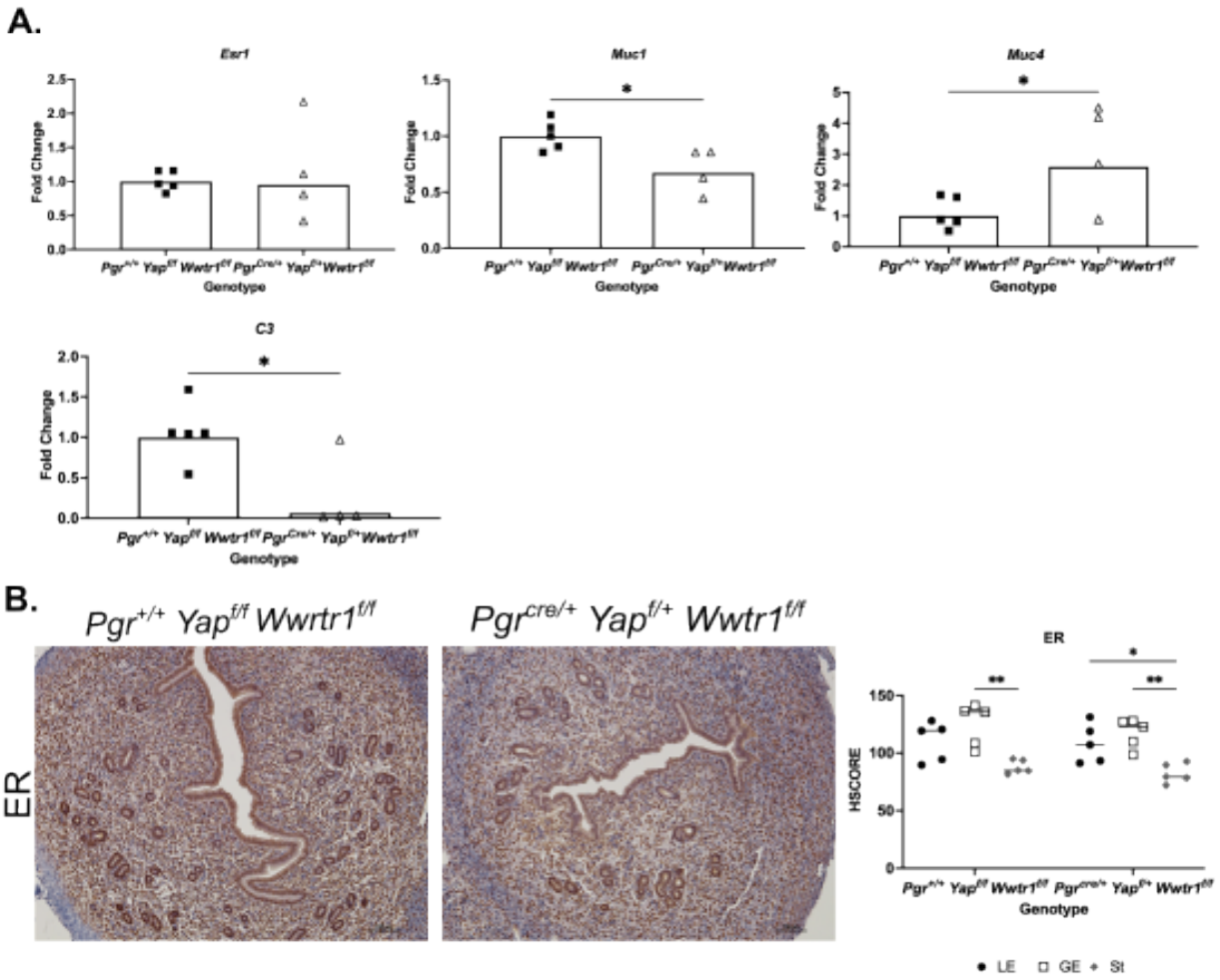

Figure B5. Estrogen receptor signaling is not aberrant in pdKOs. A. *Esr1* and target genes, *Muc1, C3, Muc4* mRNA expression in 3.5dpc uteri. **B.** Immunohistochemical analysis of Estrogen receptor expression and semiquantitative HSCORE of positive DAB stain in 3.5dpc uteri.